# Regulation of nitrous oxide production in low oxygen waters off the coast of Peru

Claudia Frey[1,2,*], Hermann W. Bange[2], Eric P. Achterberg[3], Amal Jayakumar[1], Carolin R. Löscher[4], Damian L. Arévalo-Martínez[2], Elizabeth León-Palmero[5], Mingshuang Sun[2], Xin Sun[1], Ruifang C. Xie[3], Sergey Oleynik[1], Bess B. Ward[1]

[1]*Department of Geoscience, Princeton University, Princeton, Guyot Hall, 08544 Princeton, USA*

[2] *Helmholtz Centre for Ocean Research Kiel, Düsternbrooker Weg 20, 24105 Kiel, Germany*

[3] *Helmholtz Centre for Ocean Research Kiel, Wischhofstr. 1-3, 24149 Kiel, Germany*

[4] *Department of Biology, Nordcee, Danish Institute for Advanced Study, University of Southern Denmark,*

[5] *Departamento de Ecología, Facultad de Ciencias, Universidad de Granada, 18071, Granada, Spain*

*current address: Department of Environmental Science, University of Basel, Bernoullistrasse 30, 4056 Basel, Switzerland

**Keywords:** ETSP, ODZ, denitrification, nitrification, $N_2O$ production, $^{15}N$ tracer incubations

**Abstract.** Oxygen deficient zones (ODZs) are major sites of net natural nitrous oxide ($N_2O$) production and emissions. In order to understand changes in the magnitude of $N_2O$ production in response to global change, knowledge on the individual contributions of the major microbial pathways (nitrification and denitrification) to $N_2O$ production and their regulation is needed. In the ODZ in the coastal area off Peru, the sensitivity of $N_2O$ production to oxygen and organic matter was investigated using $^{15}N$-tracer experiments in combination with qPCR and microarray analysis of total and active functional genes targeting archaeal *amoA* and *nirS* as marker genes for nitrification and denitrification, respectively. Denitrification was responsible for the highest $N_2O$ production with a mean of 8.7 nmol $L^{-1}$ $d^{-1}$ but up to 118 ± 27.8 nmol $L^{-1}$ $d^{-1}$ just below the oxic-anoxic interface. Highest $N_2O$ production from ammonium oxidation (AO) of 0.16 ± 0.003 nmol $L^{-1}$ $d^{-1}$ occurred in the upper oxycline at $O_2$ concentrations of 10 - 30 µmol $L^{-1}$ which coincided with highest archaeal *amoA* transcripts/genes. ~~During AO, $N_2O$ can be produced from two $^{15}N$ labeled $NH_4^+$ (double labelled) or from only one $^{15}N$ labelled $NH_4^+$ and one unlabeled nitrogen source (single labelled $N_2O$). Single labelled $N_2O$, representing Hybrid~~ $N_2O$ formation~~,~~ (i.e. $N_2O$ ~~getting~~with one N atom from $NH_4^+$ and the other from other substrates such as $NO_2^-$) was the dominant species, comprising 70 – 85 % of total produced $N_2O$ from $NH_4^+$, regardless of the ammonium oxidation rate or $O_2$ concentrations. Oxygen responses of $N_2O$ production varied with substrate, but production and yields were generally highest below 10 µmol $L^{-1}$ $O_2$. Particulate organic matter additions increased $N_2O$ production by denitrification up to 5-fold suggesting increased $N_2O$ production during times of high particulate organic matter export. High $N_2O$ yields of 2.1% from AO were measured, but the overall contribution by AO to $N_2O$ production was still an order of magnitude lower than that of denitrification. Hence, these findings show that denitrification is the most important $N_2O$ production process in low oxygen conditions fueled by organic carbon supply, which implies a positive feedback of the total oceanic $N_2O$ sources in response to increasing oceanic deoxygenation.



**Formatiert:** Hochgestellt

**Formatiert:** Schriftart: (Standard) Times New Roman, Nicht Fett, Englisch (USA)

**Formatiert:** Schriftart: (Standard) Times New Roman, Nicht Fett, Englisch (USA), Tiefgestellt

**Formatiert:** Schriftart: (Standard) Times New Roman, Nicht Fett, Englisch (USA)

**Formatiert:** Schriftart: (Standard) Times New Roman, Nicht Fett, Englisch (USA), Hochgestellt

**Formatiert:** Schriftart: (Standard) Times New Roman, Nicht Fett, Englisch (USA)

**Formatiert:** Schriftart: (Standard) Times New Roman, Nicht Fett, Englisch (USA), Tiefgestellt

**Formatiert:** Schriftart: (Standard) Times New Roman, Nicht Fett, Englisch (USA)

**Formatiert:** Schriftart: (Standard) Times New Roman, Nicht Fett, Englisch (USA)

**Formatiert:** Schriftart: (Standard) Times New Roman, Nicht Fett, Englisch (USA), Hochgestellt

**Formatiert:** Schriftart: (Standard) Times New Roman, Nicht Fett, Englisch (USA)

**Formatiert:** Schriftart: (Standard) Times New Roman, Nicht Fett, Englisch (USA), Tiefgestellt

**Formatiert:** Schriftart: (Standard) Times New Roman, Nicht Fett, Englisch (USA)

**Formatiert:** Schriftart: (Standard) Times New Roman, Nicht Fett, Englisch (USA)

**Formatiert:** Schriftart: (Standard) Times New Roman, Nicht Fett, Englisch (USA), Tiefgestellt

**Formatiert:** Schriftart: (Standard) Times New Roman, Nicht Fett, Englisch (USA)

**Formatiert:** Schriftart: (Standard) Times New Roman, Nicht Fett, Englisch (USA)

**Formatiert:** Schriftart: (Standard) Times New Roman, Nicht Fett, Englisch (USA)

**Formatiert:** Schriftart: (Standard) Times New Roman, Nicht Fett, Englisch (USA)

**Formatiert:** Schriftart: (Standard) Times New Roman, Nicht Fett, Englisch (USA), Tiefgestellt

**Formatiert:** Schriftart: (Standard) Times New Roman, Nicht Fett, Englisch (USA)

**Formatiert:** Schriftart: Nicht Fett

## Introduction

Nitrous oxide ($N_2O$) is a potent greenhouse gas (IPCC 2013) and precursor for nitric oxide (NO) radicals, which can catalyze the destruction of ozone in the stratosphere (Crutzen 1970, Johnston 1971), and is now the single most important ozone-depleting emission (Ravishankara et al. 2009). The ocean is a significant $N_2O$ source, accounting for up to one third of all- natural emissions (IPCC 2013) and this source may increase substantially as a result of eutrophication, warming, and ocean acidification (see e.g. Capone and Hutchins 2013, Breider et al. 2019). Major sites of oceanic $N_2O$ emissions are regions with steep oxygen ($O_2$) gradients (oxycline), which are usually associated with coastal upwelling regions with high primary production at the surface. There, high microbial respiratory activity during organic matter decomposition leads to the formation of anoxic waters also called oxygen deficient zones (ODZs), in which $O_2$ may decline to functionally anoxic conditions ($O_2$ <10 nmol $kg^{-1}$, Tiano et al. 2014). The most intense ODZs are found in the eastern tropical North Pacific (ETNP), the eastern tropical South Pacific (ETSP) and the northwestern Indian Ocean (Arabian Sea). The anoxic waters are surrounded by large volumes of hypoxic waters (below 20 µmol $L^{-1}$ $O_2$) which are strong net $N_2O$ sources (Codispoti 2010; Babbin et al. 2015). Latest estimates of global, marine $N_2O$ fluxes (Buitenhuis et al. 2018, Ji et al. 2018) agree well with the 3.8 Tg N $y^{-1}$ (1.8 – 9.4 Tg N $y^{-1}$) reported by the IPCC (2013), but have large variability in the resolution on the regional scale, particularly along coasts where $N_2O$ cycling is more dynamic. The expansion of ODZs is predicted in global change scenarios and has already been documented in recent decades (Stramma et al. 2008, Schmidtko et al. 2017). This might lead to further intensification of marine $N_2O$ emissions, which will constitute a positive feedback on global warming (Battaglia and Joos, 2018). However, decreasing $N_2O$ emissions have also been predicted based on reduced nitrification rates due to reduced primary and export production (Martinez-Rey et al. 2015, Landolfi et al. 2017) and ocean acidification (Beman et al. 2011, Breider et al. 2019). The parametrization of $N_2O$ production and consumption in global ocean models is crucial for realistic future predictions, and therefore better understanding of their controlling mechanisms is needed.

$N_2O$ can be produced by both nitrification and denitrification. Nitrification is a two-step process, comprising the oxidation of ammonia ($NH_3$) to nitrite ($NO_2^-$) (ammonia oxidation, AO) and $NO_2^-$ to nitrate ($NO_3^-$) ($NO_2^-$ oxidation). The relative contributions to AO by autotrophic ammonia-oxidizing archaea (AOA) and ammonia-oxidizing bacteria (AOB) have been inferred, based on the abundance of the archaeal and bacterial *amoA* genes, which encode subunit A of the key enzyme ammonia monooxygenase (e.g. (Francis et al. 2005, Mincer et al. 2007, Santoro et al. 2010, Wuchter et al. 2006)). These studies consistently revealed the dominance of archaeal over bacterial ammonia oxidizers, particularly in marine settings (Francis et al. 2005, Wuchter et al. 2006, Newell et al. 2011). In oxic conditions, AO by AOB and AOA forms $N_2O$ as a by-product (Anderson 1964; Vajrala et al. 2013; Stein 2019) and AOA contribute significantly to $N_2O$ production in the ocean (Santoro et al. 2011; Löscher et al. 2012). While hydroxylamine ($NH_2OH$) was long thought to be the only obligate intermediate in AO, NO has recently been identified as an obligate intermediate for AOB (Caranto and Lancaster 2017) and presumably AOA (Carini et al. 2018). Both intermediates are present in and around ODZs and correlated with nitrification activity (Lutterbeck et al. 2018, Korth et al. 2019). Specific details about the precursor of NO to form $N_2O$ in AOA remains controversial. Stiegelmeier et al. (2014) concluded that NO is derived from $NO_2^-$ reduction to form $N_2O$, while Carini et al. (2018) hypothesized that NO is derived from $NH_2OH$ oxidation, which can then form $N_2O$. A hybrid $N_2O$ production mechanism in AOA has been suggested, where NO from $NO_2^-$ reacts with $NH_2OH$ from $NH_4^+$, which is thought to be abiotic, i.e., non-enzymatic (Koslovski et al. 2016). Abiotic $N_2O$ production, also known as chemodenitrification, from intermediates like $NH_2OH$, NO or $NO_2^-$ can occur under acidic conditions (Frame et

al. 2017), or in the presence of reduced metals like Fe or Mn and catalyzing surfaces (Zhu-Barker et al. 2015), but the evidence of abiotic $N_2O$ production/chemodenitrification in ODZs is still lacking.

When $O_2$ concentrations fall below 20 µmol $L^{-1}$, nitrifiers produce $N_2O$ from $NO_2^-$, a process referred to as nitrifier - denitrification (Frame & Casciotti 2010), which has been observed in cultures of AOB (Frame & Casciotti 2010) and AOA (Santoro et al. 2011). During nitrifier-denitrificaaction (and denitrification), two $NO_2^-$ molecules form one $N_2O$, which thus differentiates this process from hybrid $N_2O$ production. It has also been suggested that high concentration of organic particles create high $NO_2^-$ and low-$O_2$ microenvironments enhancing nitrifier-denitrification (Charpentier et al. 2007). Overall, the yield of $N_2O$ per $NO_2^-$ generated from AO is lower in AOA then AOB (Hink et al. 2017a, 2017b) but it should be noted that the degree to which $N_2O$ yield increases with decreasing $O_2$ concentrations is variablevaries with cell densities in cultures orand among field sites, which favors higher $N_2O$ production by nitrification in hypoxic waters (Cohen & Gordon 1978; Yoshida 1988; Goreau et al. 1980; Frame & Casciotti 2010, Santoro et al. 2011, Löscher et al. 2012, Ji et al. 2015a, 2018a).

The anaerobic oxidation of ammonia by $NO_2^-$ (anammox) to form $N_2$ is strictly anaerobic and important in the removal of fixed N from the system, but it is not known to contribute to $N_2O$ production (Kartal et al. 2007, van der Star et al. 2008, Hu et al. 2019). In suboxic and $O_2$ free environments, oxidized nitrogen is respired by bacterial denitrification, which is the stepwise reduction of $NO_3^-$ nitrate to elemental $N_2$ via $NO_2^-$, NO and $N_2O$. $N_2O$ as an intermediate can be consumed or produced, but at the core of the ODZ $N_2O$ consumption through denitrification is enhanced, leading to an under saturation in this zone (Bange 2008, Kock et al. 2016). Reducing enzymes are highly regulated by $O_2$ concentrations and of the enzymes in the denitrification sequence, $N_2O$ reductase is the most sensitive to $O_2$ (Zumft 1997), which can lead to the accumulation of $N_2O$ along the upper and lower ODZ boundaries (Kock et al. 2016). $N_2O$ accumulation during denitrification is mostly linked to $O_2$ inhibiting the $N_2O$ reductase, but other factors such as sulfide accumulation (Dalsgaard et al. 2014), pH (Blum et al. 2018), high $NO_3^-$ or $NO_2^-$ concentrations (Ji et al. 2018), or copper limitation (Granger and Ward 2003) may also be relevant. Recent studies contrast the view of nitrification vs. denitrification as the main $N_2O$ source in ODZs (Nicholls et al. 2007, Babbin et al. 2015, Ji et al. 2015a, Yang et al. 2017). They show the importance of denitrification in $N_2O$ production in the ETNP from model outputs (Babbin et al. 2015) and in the ETSP from tracer incubation experiments (Dalsgaard et al. 2012, Ji et al. 2015a), based on natural abundance isotopes in $N_2O$ (Casciotti et al. 2018) or from water mass analysis of apparent $N_2O$ production (ΔN2O) and $O_2$ utilization (AOU) (Carrasco et al. 2017).[45,46] $N_2O$ production from the addition of $^{15}N$-labeled $NH_4^+$, $NO_2^-$ and/or $NO_3^-$ revealed nitrification as a source of $N_2O$ within the oxic-anoxic interface, but overall denitrification dominated $N_2O$ production with higher rates at the interface and in anoxic waters (Ji et al. 2015a, 2018a). Denitrification is driven by organic matter exported from the photic zone and fuels blooms of denitrifiers leading to high $N_2$ production (Dalsgaard et al. 2012, Jayakumar et al. 2009, Babbin et al. 2014). Denitrification to $N_2$ is enhanced by organic matter additions and the degree of stimulation varies with quality and quantity of organic matter (Babbin et al. 2014). Because $N_2O$ is an intermediate in denitrification, we hypothesize that its production should also be stimulated by organic matter, possibly leading to episodic and variable $N_2O$ fluxes.

$N_2O$ concentration profiles around ODZs appear to be at steady state (Babbin et al. 2015), but are much more variable in regions of intense coastal upwelling where high $N_2O$ emissions can occur (Arévalo-Martínez et al. 2015). The contributions of and controls on the two $N_2O$ production pathways under different conditions of $O_2$ and organic matter supply, are not well understood and may contribute to this variability. Hence, the goal of this study is to understand the factors regulating $N_2O$ production around ODZs in order to better constrain how future

Formatiert: Tiefgestellt

Feldfunktion geändert

Formatiert: Schriftart: (Standard) +Textkörper (Calibri)

changes in $O_2$ concentration and carbon export will impact production, distribution and emissions of oceanic $N_2O$. Our goal was to determine the impact of $O_2$ and particulate organic matter on $N_2O$ production rates using $^{15}N$ tracer experiments in combination with qPCR and functional gene microarray analysis of the marker genes, *nirS* for denitrification and *amoA* for AO by archaea, to assess how the abundance and structure of the community impacts $N_2O$ production rates from the different pathways. $^{15}N$-labelled $NH_4^+$ and $NO_2^-$ was used to trace the production of single- ($^{45}N_2O$) and double- labelled ($^{46}N_2O$) $N_2O$ to investigate the importance of hybrid $N_2O$ production during AO along an $O_2$ gradient.

## 2 Materials and Methods

### 2.1 Sampling sites, sample collection and incubation experiments

Seawater was collected from 9 stations in the upwelling area off the coast of Peru in June 2017 onboard R/V Meteor (Figure 1). Water samples were collected from 10 L Niskin bottles on a rosette with a conductivity-temperature-depth profiler (CTD, seabird electronics 9plus system). In-situ $O_2$ concentrations (detection limit 2 µmol $L^{-1}$ $O_2$), temperature, pressure and salinity were recorded during each CTD cast. $NO_2^-$ and $NO_3^-$ concentrations were measured on board by standard spectrophotometric methods (Hydes et al. 2010) using a QuAAtro autoanalyzer (SEAL Analytical GmbH, Germany). $NH_4^+$ concentrations were determined fluorometrically using ortho- phthaldialdehyde according to Holmes et al. (1999). For $N_2O$, bubble-free triplicate samples were immediately sealed with butyl stoppers and aluminum crimps and fixed with 50 µL of ~~a~~ saturated mercuric chloride ($HgCl_2$). A 10 mL He headspace was created and after an equilibration period of at least 2 hours the headspace sample was measured with a gas chromatograph equipped with an electron capture detector (GC/ECD) according to Kock et al. (2016). The detection limit for $N_2O$ concentration is 2nM ± 0.7nM. At all experimental depths nucleic acid samples were collected by filtering up to 5 L of seawater onto 0.2 µm pore size Sterivex-GP capsule filters (Millipore, Inc., Bedford, MA, USA). Immediately after collection filters were flash frozen in liquid nitrogen and kept at -80°C until extraction.

Three different experiments were carried out at coastal stations, continental slope and offshore stations. Experiments 1 and 2 aimed to investigate the influence of $O_2$ concentration along a natural and artificial $O_2$ gradient and experiment 3 targeted the impact of large particles (>50 µm) on $N_2O$ production. Serum bottles were filled from the Niskin bottles with Tygon tubing after overflowing three times to minimize $O_2$ contamination. Bottles were sealed bubble free with grey butyl rubber septa (National Scientific) and crimped with aluminum seals immediately after filling. The grey butyl rubber septa were boiled in MilliQ for 30min to degas and kept in a He atmosphere until usage. A 3 mL helium (He) headspace was created and samples from anoxic ($O_2$ < below detection) water depths were He purged for 15min. He purging removed dissolved oxygen contamination which is likely introduced during sampling and the headspace prevents possible oxygen leakage from the rubber seals (DeBrabandere et al. 2012). Natural abundance 2000 ppb $N_2O$ carrier gas (1000 µL in He) was injected to trap the produced labeled $N_2O$ and to ensure a sufficient mass for isotope analysis. For all experiments, $^{15}N$-$NO_2^-$,$^{15}N$-$NO_3^-$, and $^{15}N$-$NH_4^+$ tracer ($^{15}N/(^{14}N+^{15}N)$ = 99 atom-%) were injected into five bottles each from the same depth to a final concentration of 0.5 µmol $L^{-1}$, except for the $NO_3^-$ incubations where 2 µmol $L^{-1}$ final concentration were anticipated to obtain 10 % label of the $NO_3^-$ pool. The fraction labeled of the substrate pools was 0.76 – 0.99 for $NH_4^+$, 0.11 – 0.99 for $NO_2^-$ , 0.055 – 0.11 for $NO_3^-$. In the $^{15}N$-$NO_3^-$ treatment, $^{14}N$-$NO_2^-$ was added to trap the

Formatiert: Tiefgestellt

Formatiert: Tiefgestellt

Formatiert: Tiefgestellt

label in the product pool for $NO_3^-$ ~~nitrate~~ reduction rates and in the $^{15}N\text{-}NH_4^+$ treatment, $^{14}N\text{-}NO_2^-$ was added to a final concentration of 0.5 µmol $L^{-1}$ to trap the label in the product pool for AO rates.

For the $O_2$ manipulation experiments, all serum bottles were He purged and after the addition of different amounts of air saturated site water a final headspace volume of 3 mL was achieved. ~~headspace volume was adjusted depending on the amount of site water added and all samples were He purged.~~ Site water from the incubation depth was shaken and exposed to air to reach full $O_2$ saturation. Then 0, 0.2, 0.5, 2 and 5mL $O_2$ saturated seawater was added into serum bottles and to reach final measured $O_2$ concentration of 0 ± 0.18 µM, 0.4 ± 0.24 µM, 1.6 ± 0.12 µM, 5.2 ± 0.96 µM and 11.7 ± 1.09 µM in seawater. For the $^{15}N\text{-}NO_3^-$ incubations two more $O_2$ treatments with 21.5 ± 2.8 and 30.2 ± 3.35 µM $O_2$ were carried out to extend the range of a previous study in which $N_2O$ production from $^{15}NO_3^-$ did not decrease in the presence of up to 7 µM $O_2$ (Ji et al. 2018). ~~For the $^{15}N\text{-}NO_3^-$ incubations two more $O_2$ treatments with 21.5 ± 2.8 and 30.2 ± 3.35 µM $O_2$ were carried out.~~ The $O_2$ concentration was monitored with an $O_2$ sensor spot in one serum bottle per treatment using an $O_2$ probe and meter (FireSting, PyroScience, Aachen, Germany; Figure S1). The sensor spots are highly sensitive in the nanomolar range and prepared according to Larsen et al. (2016).

**Formatiert:** Nicht Hervorheben

For the organic matter additions, concentrated particles > 50 µm from 3 different depths were collected with a Challenger stand-alone pump system (SAPS *in situ* pumps, Liu et al. 2005), autoclaved and He purged, ~~before~~ 200µL of POC solution were added to each serum bottle before $^{15}N\text{-}NO_3^-$ or $^{14}N\text{-}NO_2^-$ tracer injection. The final particle concentrations and C/N ratios varied between 0.18 – 1.37 µM C and 8.1 – 15.4, respectively (Table 2). The concentration and C/N ratio of PON and POC of the stock solutions were analyzed by mass spectrometry using GV Isoprime mass spectrometer.

A set of five bottles was incubated per time course. One bottle was sacrificed at $t_0$, two bottles at $t_1$ and two at $t_2$ to determine a single rate. Total incubation times were adjusted to prevent bottle effects, which become significant after 20 h based on respiration rate measurements (Tiano et al. 2014). Hence, ~~for each~~ experiments ~~varied~~ lasted from 12 hours (at the shelf stations) to 24 hours (at the slope stations). Incubation was terminated by adding 0.1 mL saturated mercuric chloride ($HgCl_2$). All samples were stored at room temperature in the dark and shipped back to the lab.

**2.2 Isotope measurement and rate determination**

The total $N_2O$ in each incubation bottle was extracted with a purge-trap system according to Ji et al. (2015). Briefly, serum bottles were flushed with He for 35 min (38 ml $min^{-1}$), $N_2O$ was trapped by liquid nitrogen, $H_2O$ removed with an ethanol trap, a Nafion® trap and a $Mg(ClO_4)_2$ trap and $CO_2$ removed with an Ascarited $CO_2$-Adsorbance column and afterwards mass 44, 45, 46 and isotope ratios 45/44, 46/44 were detected with a GC-IRMS system (Delta V Plus, Thermo). Every two to three samples, a 20 mL glass vial with a known amount of $N_2O$ gas was measured to calibrate for the $N_2O$ concentration (linear correlation between $N_2O$ peak size and concentration, $r^2$= 0.99). The isotopic composition of the reference $N_2O$ was $\delta^{15}N$= 1.75 ± 0.10 ‰ and $\delta^{18}O$= 1.9 ± 0.19 ‰ present in $^{15}N^{14}N^{16}O$ or $^{14}N^{15}N^{16}O$ for $^{45}N_2O$ and the less abundant $^{15}N^{15}N^{16}O$ for $^{46}N_2O$. To evaluate the analyses of $^{15}N$-enriched $N_2O$ samples, internal isotope standards for $^{15}N_2O$ were prepared by mixing natural abundance $KNO_3$ of known $\delta^{15}N$ values with 99% $Na^{15}NO_3$ (Cambridge Isotope Laboratories) and converted to $N_2O$ using the denitrifier method (Sigman et al. 2001, Weigand et al. 2016). Measured and expected values were compared based on a binominal distribution of $^{15}N$ and $^{14}N$ within the $N_2O$ pool (Frame et al. 2017).

After $N_2O$ analysis, samples incubated with $^{15}NH_4^+$ and $^{15}NO_3^-$ were analyzed for $^{15}NO_2^-$ to determine rates of $NH_4^+$ oxidation and $NO_3^-$ reduction, respectively. The individual sample size, adjusted to contain 20 nmol of $N_2O$, was transferred into 20 mL glass vials and He purged for 10 min. $NO_2^-$ was converted to $N_2O$ using sodium azide in acetic acid (McIlvin and Altabet, 2005) and the nitrogen isotope ratio was measured on a Delta V Plus (Thermo).

For each serum bottle, total $N_2O$ concentration (moles) and $^{45}N_2O/^{44}N_2O$ and $^{46}N_2O/^{44}N_2O$ ratios were converted to moles of $^{44}N_2O$, $^{45}N_2O$ and $^{46}N_2O$. $N_2O$ production rates were calculated from the slope of the increase in mass 44, 45 and 46 over time (Figure S2). To quantify the pathways for $N_2O$ production, rates were calculated based on the equations for $N_2$ production for denitrification and anammox (Thamdrup and Dalsgaard, 2002). In incubations with $^{15}NH_4^+$ and unlabeled $NO_2^-$, it is assumed that AO produces $^{46}N_2O$ from two labeled $NH_4^+$ (equation 1) and some $^{45}N_2O$-labeled $N_2O$ based on binomial distribution (equation 2). If more single labelled $N_2O$ is produced than ~~what is~~ expected (equation 2 and 3), ~~than~~ a hybrid formation of one nitrogen atom from $NH_4^+$ and one from $NO_2^-$ (equation 4) is assumed to be taking place as found in archaeal ammonia oxidizers (Kozlowski et al. 2016). In incubations with $^{15}NO_2^-$, we assume that $^{46}N_2O$ comes from nitrifier-denitrification or denitrification, which cannot be distinguished (equation 1). Hence, any production of $^{45}N_2O$ not attributed to denitrification stems from hybrid $N_2O$ formation by archaeal nitrifiers (equation 4). In incubations with $^{15}NO_3^-$, denitrification produces $^{46}N_2O$ and was the only process considered and hence was calculated based on equation (1). Rates (R) are calculated as nmol $N_2O$ $L^{-1}$ $d^{-1}$ (Trimmer et al. 2016):

(1) $R_{external} = slope^{46}N_2O \times (f_N)^{-2}$

(2) $R_{expected} = slope^{46}N_2O \times 2 \times (1 - f_N) \times (f_N)^{-1}$

(3) $R_{above} = slope^{45}N_2O - p^{45}N_2O_{expected}$

(4) $R_{hybrid} = (f_N)^{-1} \times \left(slope^{45}N_2O + 2 \times slope^{46}N_2O \times \left(1 - {f_N}^{-1}\right)\right)$

(5) $R_{total} = pN_2O_{external} + pN_2O_{hybrid}$

where $f_N$ is the fraction of $^{15}N$ in the substrate pool ($NH_4^+$, $NO_2^-$ or $NO_3^-$), which is assumed to be constant over the incubation time. Hence, changing $f_N$ due to any other concurrent N-consumption or production process during the incubation is neglected. Nevertheless, ~~this assumption~~the assumption of constant $f_N$ ~~brings some initial considerations which need to be accounted for~~has implications that may affect the results. There is a potential for overestimating hybrid $N_2O$ production in $^{15}NO_2^-$ incubations by 5% in samples with high $NO_2^-$ reduction rates. But in incubations from anoxic depths with high $NO_3^-$ ~~NO3-~~ reduction rates, no hybrid $N_2O$ production ~~is~~was found at all. For example, accounting for a decrease in $f_N$ of the $NO_3^-$ ~~nitrate~~ pool by active $NO_2^-$ oxidation, the process with highest rates (Sun et al. 2017), had an effect of only ± 0.2% on the final rate estimate. The presence of DNRA complicates $^{15}N$-labelling incubations because it can change $f_N$ ~~f~~ in all three tracer experiments. In $^{15}NO_3^-$ incubations, active DNRA produces $^{15}NO_2^-$ and $^{15}NH_4^+$ from $^{15}NO_3^-$, which can contribute to $^{46}N_2O$ production by AO. Even ~~when~~if a maximum DNRA rate (20 nM $d^{-1}$ ~~in~~ Lam et al. 2009) is assumed to produce 0.02 nM $^{15}NH_4^+$ during the 24 h incubations and all of it is oxidized (maximum $N_2O$ production from AO 0.16 nM $d^{-1}$, this study) its contribution to $^{46}N_2O$ production is likely minor and within the standard error of the high $N_2O$ production rates from $NO_3^-$. ~~H~~Hence an overestimation of the $N_2O$ production rates is unlikely. The same applies in incubations with $^{15}N$-$NO_2^-$ when DNRA produces $^{15}NH_4^+$, additional $^{46}N_2O$ can be produced with a hybrid mechanism by AO. In $^{15}NO_2^-$ incubations with high starting $f_N$ ~~f~~ (>0.7) the production of $^{14}NO_2^-$ by $NO_3^-$ reduction (which decreases



Formatiert: Nicht Hervorheben

Formatiert: Schriftart: Nicht Fett
Formatiert: Schriftart: Nicht Fett, Tiefgestellt
Formatiert: Schriftart: Nicht Fett
Formatiert: Schriftart: Nicht Fett, Hochgestellt
Formatiert: Schriftart: Nicht Fett
Formatiert: Schriftart: Nicht Fett, Tiefgestellt
Formatiert: Schriftart: Nicht Fett, Hochgestellt
Formatiert: Schriftart: Nicht Fett
Formatiert: Schriftart: Nicht Fett, Tiefgestellt
Formatiert: Schriftart: Nicht Fett, Hochgestellt
Formatiert: Schriftart: Nicht Fett
Formatiert: Schriftart: Nicht Fett
Formatiert: Schriftart: Nicht Fett, Tiefgestellt
Formatiert: Schriftart: Nicht Fett
Formatiert: Schriftart: Nicht Fett
Formatiert: Schriftart: Nicht Fett
Formatiert: Schriftart: Nicht Fett
Formatiert: Schriftart: Nicht Fett
Formatiert: Schriftart: Nicht Fett
Formatiert: Schriftart: Nicht Fett
Formatiert: Schriftart: Nicht Fett
Formatiert: Schriftart: Nicht Fett
Formatiert: Tiefgestellt
Formatiert: Schriftart: Nicht Fett
Formatiert: Schriftart: Nicht Fett, Tiefgestellt
Formatiert: Schriftart: Nicht Fett
Formatiert: Schriftart: Nicht Fett
Formatiert: Schriftart: Nicht Fett
Formatiert: Schriftart: Nicht Fett, Tiefgestellt
Formatiert: Schriftart: Nicht Fett
Formatiert: Schriftart: Nicht Fett

$f_N$f) leads to an underestimation by ~~max.~~upto 9%, whereas in incubations with a low $f_N$f (<0.3) the effect is less ~~with max.~~(upto 3% underestimation of $N_2O$ production rates). In $^{15}NH_4^+$ incubations ($f_N$ f>0.9), maximum ~~a~~ DNRA rate would lead to an underestimation of 3.5%. Slope of $^{46}N_2O$ and slope of $^{45}N_2O$ represent the $^{46}N_2O$ and $^{45}N_2O$ production rates, which were tested for significance based on a linear regression (n=5, student t-test, $R^2 > 0.80$, $p<0.05$). Linear regressions that were not significantly different from zero were reported as 0. The error for each $N_2O$ production rate was calculated as the standard error of the slope. Detection limits were 0.002 nmol $L^{-1}$ $d^{-1}$ for $N_2O$ production from AO and 0.1 nmol $L^{-1}$ $d^{-1}$ for $N_2O$ production from denitrification based on the average measured standard error for rates (Dalsgaard et al. 2012). The curve-fitting tool of Sigma Plot was used for the $O_2$ sensitivity experiments. A one-way ANOVA was performed on the $N_2O$ production rates to determine if rates were significantly different between POM treatments.

The rates (R) of $NH_4^+$ oxidation to $NO_2^-$ and $NO_3^-$ reduction to $NO_2^-$ were calculated based on the slope of the linear regression of $^{15}NO_2^-$ enrichment over time (n = 5) (equation 6).

$$(6)\quad R = f_N^{-1} \times slope\,\delta\ ^{15}NO_2^- \qquad (6)$$

where $f_N$ is the fraction of $^{15}N$ in the substrate pool ($NH_4^+$ or $NO_3^-$).

Yield (%) of $N_2O$ production during $NH_4^+$ oxidation was defined as the ratio of the production rates (equation 7).

$$(7)\quad Yield_{NH4} = \frac{N-N_2O\ (\frac{nM}{d})}{N-NO_2^-(\frac{nM}{d})} \times 100\% \qquad (7)$$

Yields of $N_2O$ production during denitrification were calculated based on the fact that $N_2O$ is not a side product during $NO_3^-$ ~~nitrate~~ reduction to $NO_2^-$ but rather the next intermediate during denitrification (equation 8).

$$(8)\quad Yield_{NO3} = \frac{N-N_2O\ (\frac{nM}{d})}{N-NO_2^-(\frac{nM}{d}) + N-N_2O\ (\frac{nM}{d})} \times 100\% \qquad (8)$$

All rates, yields and errors are reported in Table S3.

*2.3 Molecular Analysis – qPCR, Microarrays*

DNA and RNA were extracted using the DNA/RNA ALLPrep Mini Kit (Qiagen) followed by immediate cDNA Synthesis from purified and DNA-cleaned RNA using a SuperScript III First Strand Synthesis System (Invitrogen). The PicoGreen dsDNA Quantification Kit (Invitrogen) was used for DNA quantification and Quant-iT OliGreen ssDNA Quantification Kit (life technologies) was used for cDNA quantification.

The abundances of total and active *nirS* and archaeal *amoA* communities were determined by quantitative PCR (qPCR) with assays based on SYBR Green staining according to methods described previously (Jayakumar et al. 2013, Peng et al. 2013). Primers nirS1F and nirS3R (Braker et al. 1998) were used to amplify a 260-bp conserved region within the *nirS* gene. The *nirS* p~~P~~rimers are not specific for epsilon-proteobacteria (Murdock et al. 2017), but in previous metagenomes from the ETSP epsilon-proteobacteria where below 3-4 % of the reads or not found, except in very sulfidic, coastal stations (Stewart et al. 2011, Wright et al. 2012, Ganesh et al. 2012, Schunck et al. 2013, Kavelage et al. 2015). Primers Arch-amoAF and Arch- amoAR (Francis et al. 2005) were used to quantify archaeal *amoA* abundance. A standard curve containing 6 serial dilutions of a plasmid with either an archaeal *amoA* fragment or a *nirS* fragment was used on respective assay plates. Assays were performed in a StratageneMx3000P qPCR cycler (Agilent Technologies) in triplicates of 20- 25ng DNA or cDNA, along with a no primer control and a no template control. Cycle thresholds (Ct values) were determined automatically and used

Formatiert: Schriftart: Nicht Fett
Formatiert: Schriftart: Nicht Fett
Formatiert: Schriftart: Nicht Fett
Formatiert: Schriftart: Nicht Fett
Formatiert: Schriftart: Nicht Fett
Formatiert: Schriftart: Nicht Fett, Hochgestellt
Formatiert: Schriftart: Nicht Fett
Formatiert: Schriftart: Nicht Fett, Tiefgestellt
Formatiert: Schriftart: Nicht Fett, Hochgestellt
Formatiert: Schriftart: Nicht Fett
Formatiert: Schriftart: Nicht Fett
Formatiert: Schriftart: Nicht Fett
Formatiert: Hochgestellt
Formatiert: Schriftart: Kursiv

to calculate the number of *nirS* or archaeal *amoA* copies in each reaction, which was then normalized to copies per milliliter of seawater (assuming 100% recovery). The detection limit was around 15 copies $mL^{-1}$ based on the Ct values of the no template control.

Microarray experiments were carried out to describe the community composition of the total and active *nirS* and archaeal *amoA* groups using the DNA and cDNA qPCR products. Pooled qPCR triplicates were purified and cleaned using the QIAquick PCR Purification Kit (Qiagen). Microarray targets were prepared according to Ward and Bouskill (2011). Briefly, dUaa was incorporated into DNA and cDNA targets during linear amplification with random octomers and a Klenow polymerse using the BioPrime kit (Invitrogen) and then labeled with Cy3, purified and quantified. Each probe is a 90-mer oligonucleotide consisting of a 70-mer archetype sequence combined with a 20-mer reference oligo as a control region bound to the glass slide. Each archetype probe represents a group of related sequences with 87 ± 3% sequence identity of the 70-mer sequence. Microarray targets were hybridized in duplicates on a microarray slide, washed and scanned using a laser scanner 4200 (Agilent Technologies) and analyzed with GenePix Pro 6.0. The resulting fluorescence ratio (FR) of each archaeal *amoA* or *nirS* probe was divided by the FR of the maximum archaeal *amoA* or *nirS* FR on the same microarray to calculate the normalized FR (nFR). nFR represents the relative abundance of each archetype and was used for further analyses.

Two different arrays were used, BCO16 which contains 99 archaeal *amoA* archetype probes representing ~8000 archaeal *amoA* sequences (Biller et al. 2012) and BCO15 which contains 167 *nirS* archetype probes representing ~2000 sequences (collected from NCBI in 2009). A total of 74 assays were performed with 21 *nirS* cDNA targets, 21 *nirS* DNA targets, 16 *amoA* cDNA targets and 16 *amoA* DNA samples. The original microarray data from BCO15 and BC016 are available via GEO (Gene Expression Omnibus; http://www.ncbi.nlm.nih.gov/geo/) at NCBI (National Center for Biotechnology Information) under GEO Accession No GSE142806~~XXXX~~.

**2.4. Data analysis**

Spearman Rank correlation was performed from all $N_2O$ production rates, AO and $NO_3^-$ ~~nitrate~~ reduction rates, environmental variables, *nirS* and archael *amoA* gene and transcript abundance as well as the 20 most abundant archetypes of total and active *nirS* and *amoA* using R. Only significant values ($p<0.05$) are shown. Archetype abundance (nFR) data were square-root transformed and beta-diversity was calculated with the Bray-Curtis coefficient. Alpha diversity of active and total *nirS* and *amoA* communities was estimated by calculating the Shannon diversity index using PRIMER6. Bray-Curtis dissimilarities were used to perform a Mantel test to determine significant differences between active and total communities of *nirS* and *amoA* using R (Version 3.0.2, package "vegan" (Oksanen et al., 2019). Canonical Correspondence Analysis (CCA) (Legendre & Legendre 2012) was used to visualize differences in community composition dependent upon environmental conditions using the software PAST (Hammer et al. 2001). Before CCA analysis, a forward selection (Borcard et al. 1992) of the parameters that described the environmental and biological variables likely to explain the most significant part of the changes in the archetypes was performed.

The make.lefse command in MOTHUR was used to create a linear discriminant analysis (LDA) effect size (LEfSe) (Segata et al. 2011) input file from the MOTHUR shared file. This was followed by a LEfSe (http://huttenhower.sph.harvard.edu/lefse/) to test for discriminatory archetypes between $O_2$ levels. With a normalized relative abundance matrix, LEfSe uses the Kruskal-Wallis rank sum test to detect features with significantly different abundances between assigned archetypes in the different $O_2$ levels and performs an LDA to

estimate the effect size of each feature. A significant alpha of 0.05 and an effect size threshold of 2 were used for all marker genes discussed in this study.

## 3. Results

### 3.1 Hydrographic conditions

The upwelling system off Peru is a hot spot for $N_2O$ emissions (Arévalo-Martínez et al. 2015) with most intense upwelling in austral winter but maximum chlorophyll during December to March (Chavez and Messié, 2009; Messié and Chavez, 2015). The sampling campaign took place during austral fall in the absence of intense upwelling or maximum chlorophyll. The focus of this study was the region close to the coast, which has highly variable $N_2O$ concentration profiles (Kock et al. 2016) and $N_2O$ emissions (Arévalo-Martínez et al. 2015). The Peru Coastal Water (PCW, temperature <19.5°C, salinity 34.9 - 35.1) and the equatorial subsurface waters (ESSW, temperature 8-12°C, salinity 34.7 – 34.9) (Pietri et al. 2013) were the dominant water masses off the Peruvian coast sampled for $N_2O$ production rate measurements (Table 1). At the southern-most transect at 15.5° – 16°S a meso-scale anticyclonic mode water eddy (McGillicuddy et al. 2007), which was about to detach from the coast, was detected from deepening/shoaling of the main/seasonal pycnoclines (Bange et al. 2018, Figure S3~~4~~). Generally, the stations were characterized by a thick anoxic layer (254 m – 427 m) reaching to the seafloor at two shelf stations (894, 883). $NO_2^-$ concentration accumulated only up to 2 µmol $L^{-1}$ in the secondary $NO_2^-$ maximum (SNM) at the northern transect (stations 882, 883), but up to 7.19 µmol $L^{-1}$ along the southern transect (Figure 2, station 907, 912). $N_2O$ concentration profiles showed a high variability with respect to depth and $O_2$ concentrations (Figure 2). The southern transect (station 907,912) showed the lowest $N_2O$ concentrations (5 nmol $L^{-1}$) in the center of the anoxic zones. At the same time, station 912 in the center of the eddy showed highest $N_2O$ concentration with 78.9 nmol $L^{-1}$ at [$O_2$] below detection limit in the upper part of the anoxic zone. Above the ODZ, the maximum $N_2O$ peak ranged from 57.9 – 78.9 nmol $L^{-1}$ and was found at an $O_2$ concentration range from below detection (883, 894, 892, 912) up to 67 µmol $L^{-1}$ (907). Three stations (892, 894 and 904) showed high surface $N_2O$ concentrations of 64 nmol $L^{-1}$.

### 3.2 Depth Distribution of $N_2O$ production rates and total and active nirS and amoA abundance

$N_2O$ production varied with depth and substrate (Figure 3, Table S3). In the oxycline, highest AO (34 ± 0.1 nmol $L^{-1}$ $d^{-1}$ and 35 ± 9.2 nmol $L^{-1}$ $d^{-1}$) coincided with highest $N_2O$ production from AO (0.141 ± 0.003 nmol $L^{-1}$ $d^{-1}$ and 0.159 ± 0.003 nmol $L^{-1}$ $d^{-1}$) at both stations of the northern transect, stations 883 and 882, respectively (Figure 3(I)a, b). $NH_4^+$ oxidation and its $N_2O$ production decreased to zero in the ODZ. The rates of the reductive source pathways for $N_2O$ increased with depth. $N_2O$ production from $NO_2^-$ and $NO_3^-$ displayed similar patterns with highest production at or below the oxic -anoxic interface (Figure 3(II)). $N_2O$ production from $NO_2^-$ showed highest rates of 3.06 ± 1.17 nmol $L^{-1}$ $d^{-1}$ (912) and 2.37 ± 0.54 nmol $L^{-1}$ $d^{-1}$ (906) further south (Figure 3(II) m, q) compared to lower rates at northern stations, where the maximum rate was 0.71 ± 0.38 nmol $L^{-1}$ $d^{-1}$ (Figure 3(II) c, 883). A similar trend was found for $N_2O$ production from $NO_3^-$: lower maximum rates at northern stations with 2.7 ± 0.4 nmol $L^{-1}$ $d^{-1}$ (882) and 5.7 ± 2.8 nmol $L^{-1}$ $d^{-1}$ (883, Figure 3(II) b) and highest rates in southern transects with 7.2 ± 1.64 nmol $L^{-1}$ $d^{-1}$ (((Figure 3(II) l, 904) in transect 3 and up to 118.0 ± 27.8 nmol $L^{-1}$ $d^{-1}$ (Figure 3(II) p, 912) in transect 4. Generally, $N_2O$ production rates from $NO_2^-$ and $NO_3^-$ were 10 to 100-fold higher than from AO.

qPCR analysis detected lowest gene and transcript numbers of archaeal *amoA* and *nirS* in the surface mixed layer (Figure 3(I) k, l, 3(II)r, s). Highest archaeal *amoA* gene and transcript abundance was in the oxycline (1 – 40 µmol $L^{-1}$ $O_2$) with 24,500 ± 340 copies $mL^{-1}$ and 626 ± 29 copies $mL^{-1}$ at station 883 (Figure 3(I)c, d). *amoA* gene and transcript number decreased in the ODZ to 1000 – 6500 gene copies $mL^{-1}$ and 20 - 250 transcript copies $mL^{-1}$. The profiles of *nirS* gene and transcript abundance were similar to each other (Figure 3(II) d, e) with highest abundance in the ODZ up to 1 x $10^6$ copies $mL^{-1}$ and 2.9 x $10^5$ copies $mL^{-1}$, respectively. Denitrifier *nirS* genes and transcripts peaked in the anoxic layer and were significantly correlated with $N_2O$ production from $NO_2^-$ but not from $NO_3^-$. Archaeal *amoA* gene and transcript abundances were significantly correlated with AO and, $N_2O$ production from AO (Figure S5~~3~~). $N_2O$ concentrations did not correlate with any of the measured variables (Figure S5~~3~~).

### 3.3 Influence of $O_2$ concentration on $N_2O$ production

$N_2O$ production along the *in situ* $O_2$ gradient for the substrates $NO_2^-$ and $NO_3^-$ decreased exponentially with increasing $O_2$ concentrations (Figure 4b, c) while for $NH_4^+$, the $N_2O$ production was highest at highest sampled $O_2$ concentration (Figure 4a). At *in situ* $O_2$ levels above 8.4 µmol $L^{-1}$ $N_2O$ production decreased by 100% and 98% from $NO_3^-$ and $NO_2^-$, respectively (Figure 4b, c).

In the manipulated $O_2$ treatments from the oxic - anoxic interface (S11, S19) a unimodal response of $N_2O$ production from $NH_4^+$ and $NO_2^-$ to $O_2$ is apparent (Figure 4d, e). Increasing and decreasing $O_2$ concentrations inhibited $N_2O$ production from $NH_4^+$ and $NO_2^-$ with the highest $N_2O$ production rate between 1.4 - 6 µmol $O_2$ $L^{-1}$. However, this response was only significant in sample S11 (Figure 4d, e). There was no significant response to $O_2$ concentration of $N_2O$ production from $NO_3^-$. $O_2$ did not inhibit $N_2O$ production from $NO_3^-$ up to 23 µmol $L^{-1}$ (Figure 4f).

The proportion of hybrid $N_2O$ produced during AO, i.e., the formation of $N_2O$ from one $^{15}$~~N from the labelled~~ $NH_4^+$ and one $^{14}$~~N from a non – labelled~~ N compound (excluding $NH_4^+$) such as $NO_2^-$, $NH_2OH$ or NO, was consistently between 70 – 85 % across different $O_2$ concentrations for manipulated and natural $O_2$ concentrations (Figure 5a, c). Hybrid formation during $N_2O$ production from $NO_2^-$ varied between 0 and 95% along the natural $O_2$ gradient (Figure 5b). In manipulated $O_2$ treatments hybrid formation from $NO_2^-$ did not change across different $O_2$ treatments but with respect to the original depth, 0% in sample S11 which originated from 145 m of station 892 or 78% in sample S19 from 120m of station 894 (Figure 5d).

Highest $N_2O$ yields during AO (over 1%) occurred between 1.4 and 2 µmol $O_2$ $L^{-1}$, and decreased at both higher and lower $O_2$ concentrations (Figure 6a). However, only the increase in yield from nmol $O_2$ to 1.4 – 2 µmol $L^{-1}$ $O_2$ was significant (t-test, $p<0.05$) and the following decrease in yield was not (t-test, $p>0.05$). In the manipulated $O_2$ treatment of sample S19 (Figure 6c) the same significant pattern was observed, whereas in S11 highest yield was found at 12 µmol $L^{-1}$ $O_2$. $N_2O$ yield during $NO_3^-$ ~~nitrate~~ reduction to $NO_2^-$ decreased to zero at 8.4 µmol $L^{-1}$ $O_2$ along the natural $O_2$ gradient (Figure 6b) while no significant response occurred in the manipulated $O_2$ treatments (Figure 6d). There, $NO_3^-$ ~~nitrate~~ reduction was decreasing with increasing $O_2$ but $N_2O$ production was steady with increasing $O_2$ leading to high yields between 38.8 ± 9 % - 91.2 ± 47 % at 23 µmol $L^{-1}$ $O_2$.

### 3.4 Effect of large particulate organic matter on $N_2O$ production

The autoclaving of the concentrated POM solution liberated $NH_4^+$ from the particles, reducing the N/C ratio of the particles compared to non-autoclaved particles (Table 2). The highest $NH_4^+$ accumulation is found in samples with the largest difference in N/C ratios between autoclaved and non-autoclaved particles (Table 2, 904-20m, 898-100 m). Addition of 0.17 – 1.37 µmol C $L^{-1}$ of autoclaved particles > 50 µm (Table 2) produced a significant increase in $N_2O$ production by up to 5.2- and 4.8-fold in 10 and 7 out of 19 additions for $NO_2^-$ and $NO_3^-$ respectively (Figure 7a, b). There was no linear correlation of the origin (mixed layer depth, oxycline or anoxic zone), the quality (N/C ratio) or the quantity of the organic matter on the magnitude of the increase. Only samples S20 and S17 were not stimulated by particle addition and $N_2O$ production from denitrification did not significantly differ from the control (Figure 7b).

**3.5 Diversity and community composition of total and active nirS and amoA assemblages and its correlation with environmental parameters**

nFR values from functional gene microarrays were used to describe the nitrifier and denitrifier community composition of AOA and *nirS* assemblages, respectively. nFR was averaged from duplicate microarrays, which replicated well ($R^2$ = 0.89 - 0.99). Alpha- diversities of *nirS* and archaeal *amoA* were not statistically different for total and active communities (students t-test, p > 0.05), but were overall lower for RNA (3.2 ± 0.3) than DNA (3.8 ± 0.4) (Table S1). Principle Coordinate Analysis of Bray–Curtis similarity for each probe group on the microarray indicated that the community structure of archaeal *amoA* genes was significantly different from that of archaeal *amoA* transcripts whereas community structure of *nirS* genes and transcripts did not differ significantly (Figure S42). To identify which archetypes were important in explaining differences in community structure of key nitrification and denitrification genes, we identified archetypes that accounted for more than 1% of the total fluorescence for their probe set and that were significantly different with respect to ambient $O_2$ using a lefse analysis (Table S2). Furthermore, we used CCA to test whether the community composition, or even single archetypes, could explain the $N_2O$ production rates.

The nFR distribution showed greater variability in the active (cDNA) AOA community than in the total community (DNA) among depths, stations and $O_2$ concentrations (Figure 8a, b). Archetypes over 1% made up between 76% (DNA) - 83% (cDNA) of the *amoA* assemblage and only 61% (DNA) - 68% (cDNA) of the *nirS* assemblage. The 4 most abundant AOA archetypes AOA55, AOA3, AOA21 and AOA32 made up 20% - 65% of the total and active community (Figure 8a, b). DNA of archetypes AOA55 and AOA79, both related to uncultured AOA in soils, significantly correlated with *in situ* $NH_4^+$ concentrations (Figure S53). DNA and cDNA from AOA3 and AOA83 were significantly enriched in oxic waters and AOA7, closely related with crenarchaeote SCGC AAA288-M23 isolated from station ALOHA near Hawaii (Swan et al. 2011), was significantly enriched in anoxic and hypoxic waters for DNA and cDNA respectively (Table S2). All other archetypes did not vary with $O_2$ levels. DNA of AOA 3, closely related to *Nitrosopelagicus brevis* (CN25), identified as the only archetype to be significantly correlated with $N_2O$ production and yield from AO (Figure S53).

The total and active denitrifier communities were dominated by Nir7, derived from an uncultured clone from the ODZ in the ETSP (Lam et al. 2009), and Nir7 was significantly more enriched in the active community (Figure 8c, d). DNA from ODZ depths of the eddy, S15 (907, 130 m) and S17 (912, 90 m), diverged most obviously from the rest and from each other (Figure 8c, d). Interestingly, these two samples were not divergent among the active *nirS* community (Figure 8c, d; Figure S42). DNA of Nir35, belonging to the Flavobacteriaceae derived from coastal waters of the Arabian Sea (Goréguès et al., 2004), was most abundant (12.3 %) at the eddy edge (S15) as

opposed to the eddy center (S17) where nir167, representing Anammox sequences from Peru, was most abundant (12.0 %). Interestingly, Nir4 and Nir14, among the top 5 abundant archetypes, were significantly enriched in oxic water masses (Table S2). nFR signal of nir166, belonging to Scalindua, and Nir23 were among the top 5 abundant archetypes and significantly enriched in anoxic depths.

CCA is a direct gradient analysis, where the gradient in environmental variables is known a priori and the archetypes are considered to be a response to this gradient. Composition from total and active AOA community did not differ between stations and all samples cluster close together (Figure S64a, b). S18 (912, 5 m) is a surface sample with lowest $NO_3^-$ concentration (8 µmol $L^{-1}$), highest temperature and salinity of the data set and the DNA is positively related with $O_2$ and driven by AOA55, AOA32 and AOA79. RNA of S17 (912, 90 m) clusters with AOA70. AOA55 was abundant and its distribution is driven by $O_2$ and $NH_4^+$ (Figure S53).

CCA clustered the denitrifier community DNA into one main group with a few exceptions (Figure S64 c). Two surface samples (S16, S18) clustered separate and were positively correlated with Nir4 and Nir14 and $O_2$. Two anoxic samples from the eddy core (S17) and eddy edge (S15) clustered separate with S17 being driven by 3 *nirS* archetypes – Nir54, Nir10 and Nir167 and S15 by Nir23, Nir35 and Nir133 (Figure S64 c). Total and active *nirS* community composition did not differ as a function of $O_2$. Although, composition of active and total *nirS* communities were not significantly different, the active community clustered slightly differently. For *nirS* RNA, surface and oxycline samples (S16 and S10) grouped together and were correlated positively with $O_2$, temperature and salinity, whereas the anoxic eddy samples did not differ from the rest (Figure S64d). $N_2O$ production from $NO_2^-$ significantly correlated with *nirS* gene and transcript abundance but both reductive $N_2O$ production pathways were not linked with a single dominant *nirS* archetype (Figure S53)

## 4. Discussion

Most samples originated from Peru Coastal Water (PCW) characterized by supersaturated $N_2O$ concentrations (Kock et al. 2016, Bourbonnais et al. 2017). Only the deepest sample (S1, 882 - 350m) saw the presence of a different water mass, the equatorial subsurface waters. Thus, our findings about regulation of $N_2O$ production at different stations probably apply to the region as a whole. Several studies indicate that water mass hydrography plays an important role in shaping microbial community diversity (Biller et al. 2012, Hamdan et al. 2012) and a coupling of *amoA* alpha diversity to physical conditions such as salinity, temperature and depth has been shown in coastal waters off Chile (Bertagnolli and Ulloa 2017). While salinity, temperature and depth were prominent factors in shaping the community compositions of nitrifiers and denitrifiers (Figure S64), for $N_2O$ production rates correlations with physical and chemical parameters were not consistent. On one hand, oxidative $N_2O$ production from $NH_4^+$ positively correlated with temperature, salinity, oxygen and negatively with depth and $PO_4^{3-}$ concentration., On the other hand, reductive $N_2O$ production from $NO_2^-$ positively correlated with $NH_4^+$ and $NO_2^-$ concentrations, but negatively with $NO_3^-$ concentrations (Figure S53), suggesting when $NO_3^-$ is abundant, denitrifiers are less likely to use $NO_2^-$ for $N_2O$ production during denitrification.. Both oxidative (AO) and reductive ($NO_2^-$ and $NO_3^-$ reduction) N cycling processes produced $N_2O$ with differential effects of $O_2$ on them. Measured $N_2O$ production rates were always highest from $NO_3^-$, followed by $NO_2^-$ and $NH_4^+$, which is consistent with previous studies that showed denitrification as a dominant $N_2O$ source in Peruvian coastal waters harboring an ODZ (Ji et al. 2015a, Casciotti et al. 2018). A low contribution of AO to $N_2O$ production in low $O_2$ waters is in line with a previous study in this area estimating $N_2O$ production based on isotopomer measurements combined with a 3-D Reaction-Advection-Diffusion Box model (Bourbonnais et al. 2017). The low percentage that AO

Formatiert: Tiefgestellt
Formatiert: Hochgestellt
Formatiert: Tiefgestellt
Formatiert: Hochgestellt
Formatiert: Tiefgestellt

contributed to total $N_2O$ production was between 0.5 – 6%, with one exception in the shallowest sample S5 with 30 µmol $L^{-1}$ $O_2$ where AO contributed 86% to total $N_2O$ production. We found strong positive effects of decreasing $O_2$ concentration and increasing particulate matter concentrations on $N_2O$ production in the upper oxycline.

The occurrence of an anticyclonic mode water eddy at 16°S (transect 4, stations 912, 907) at the time of sampling was not unusual, as such eddies have been reported at a similar position (Stramma et al. 2013). High N loss, a large SNM with low $NO_3^-$ concentrations and strong $N_2O$ depletion in the core of ODZ of the eddy result in reduced $N_2O$ inside of this kind of eddies as they age and are advected westward (Cornejo D`Ottone et al. 2016, Arévalo-Martínez et al. 2016). Our study found similar patterns with largest SNM (5.23 µM $NO_2^-$), lowest $NO_3^-$ (14 µmol $L^{-1}$) and $N_2O$ (4 nmol $L^{-1}$) concentrations in the eddy center. For the first time $N_2O$ production rates were measured in an eddy, and the rates of up to 118 ± 2720 nmol $L^{-1}$ $d^{-1}$ are the highest $N_2O$ production rates from denitrification reported in the ETSP. Previously reported maximum rates were up to 86 nmol $L^{-1}$ $d^{-1}$ (Dalsgaard et al. 2012) based on $^{15}N$ tracer incubations. Much smaller maximum rates, ranged from 49 nmol $L^{-1}$ $d^{-1}$ (Bourbonnais et al. 2017) and and 50 nmol $L^{-1}$ $d^{-1}$ (Farìas et al. 2009), were obtained using , both based on a $N_2O$ isotope and isotopomer approaches, which provides a time (weeks- months) and process integrated signals, up to 86 nmol $L^{-1}$ $d^{-1}$ (Dalsgaard et al. 2012) based on $^{15}N$ tracer incubations. Hence, the deviation of maximum rates can be explained by 1) the different approaches and 2) the sampling of the core of the eddy. , both extreme $N_2O$ production at a certain time point and integrated $N_2O$ production over long timescale could be obtained $N_2$ production measurements (from anammox and denitrification) were as not measuredperformed in this study, but should be in future studies to account for potential artefacts by co-occurring $NO_3^-$ reduction processes. Here, so it cannot be determined whether the eddy only stimulated incomplete denitrification to $N_2O$ production but not $N_2$ production from denitrification (i.e. increasing the $N_2O/N_2$ yield) or if the eddy also increased complete denitrification to $N_2$ by this high $N_2O$ production represents a high $N_2O/N_2$ yield or if the $N_2$ production rates were also 10 times compared to stations higher than outside of the eddy. Considering that at some depths only incomplete denitrification (also known as "stop- and go" denitrification) to $N_2O$ is at work, it would not be surprising that $N_2O$ production can reach the same order of magnitude as $N_2$ production from complete denitrification. Aged eddies also show lower $N_2O$ concentration maxima at the upper oxycline (Arévalo-Martínez et al. 2016), which was not the case in this study where a young eddy was just about to detach from the coast. In fact, the eddy stations show the highest $N_2O$ peak in the upper oxycline within this data set. Eddies and their age imprint mesoscale patchiness and heterogeneity in biogeochemical cycling. It appears that young eddies close to the coast with high $N_2O$ concentrations and high $N_2O$ production rates have a great potential for high $N_2O$ emissions compared to aged eddies or waters surrounding eddies.

Formatiert: Hochgestellt
Formatiert: Nicht Hervorheben
Formatiert: Tiefgestellt, Nicht Hervorheben
Formatiert: Nicht Hervorheben
Formatiert: Tiefgestellt, Nicht Hervorheben
Formatiert: Nicht Hervorheben
Formatiert: Tiefgestellt
Formatiert: Tiefgestellt

### 4.1 Effect of $O_2$ on reductive and oxidative $N_2O$ production

The relationship between $O_2$ concentrations and $N_2O$ production by nitrification and denitrification is very complex in ODZs. While poorly constrained, the reported $O_2$ threshold level (1.7 µmol $L^{-1}$ $O_2$) for reductive $N_2O$ production is lower (Dalsgaard et al. 2014) than the reported $O_2$ threshold level (8 µmol $L^{-1}$) for $N_2O$ consumption in the ETSP (Cornejo and Farías 2012). Nevertheless, the suboxic zone between 1 – 8 µmol $L^{-1}$ $O_2$ carries high $N_2O$ concentrations indicating higher $N_2O$ production than consumption. In this study, we focused on this suboxic water masses above the ODZ and determined bulk kinetics of $O_2$ sensitivity in batch experiments, which reflect the metabolism of the microbial community. The effect of $O_2$ on $N_2O$ production differed between natural $O_2$ concentrations with varying communities vs. manipulated $O_2$ concentrations within a community. While

$N_2O$ production from $NO_2^-$ and $NO_3^-$ decreased exponentially along the natural $O_2$ gradient, it did not always decrease for the manipulated $O_2$ treatments. Unchanged $N_2O$ production with higher $O_2$ levels in $NO_3^-$ treatments showed that at least a portion of the community can respond very differently to a sudden increase in $O_2$ than predicted from natural $O_2$ gradients with communities acclimated to a certain $O_2$ concentration. In the ETNP, this pattern has been observed before (Ji et al. 2018a) but the mechanism behind it is unknown. Different responses of $N_2O$ production rates to $O_2$ between *in situ* assemblages and incubat~~ion~~ed samples were not unexpected because different rates at different depths were likely not only due to $O_2$ differences but also other factors such as different organic matter fluxes and different amounts and types of $N_2O$ producers at different depths. In addition, sSampling with Niskin bottles and purging can induce stress responses (Stewart et al. 2012) and ~~change~~shift the richness and structure of the microbial community from the *in situ* community (Torres-Beltran et al. 2019~~), which can be one potential explanation for the different responses between manipulated oxygen and *in situ* oxygen experiments~~). The removal of other gases like $H_2S$ during purging ~~introduces~~is another potential artefact. However, it is unlikely as measurable $H_2S$ concentrations have mostly been found at very shallow coastal stations (< 100 m deep) (Callbeck et al. 2018), ~~which was not the case in~~not the environment of this study. On the contrary, high abundances (up to 12%) of sulfur oxidizing gamma proteobacteria, like SUP05 can be found in eddy-transported offshore waters where they actively contributed to autotrophic denitrification (Calbeck et al. 2018). In this study, ~~it~~we cannot differentiate between autotrophic or organotrophic denitrification, but a contribution of autotrophic denitrification in the eddy center is likely. Off the Chilean coast, active $N_2O$ production by denitrification was found at up to 50 µmol $L^{-1}$ $O_2$ (Farías et al. 2009). These results reinforce prior studies showing that distinct steps of multistep metabolic pathways, such as denitrification, can differ in $O_2$ sensitivity (Dalsgaard et al. 2014, Bristow et al. 2016a, 2016b). In various bacterial strains and natural communities, the $NO_3^-$ reductase enzyme (*Nar*) which catalyzes the first step in denitrification, is reportedly the most $O_2$ tolerant, followed by the more $O_2$ sensitive steps of $NO_2^-$ reduction (*Nir*) and $N_2O$ reduction (Körner und Zumft 1989, McKenney et al. 1994, Kalvelage et al. 2011). The fact~~,~~ that- $N_2O$ production is insensitive to manipulated $O_2$~~we see this pattern only~~ in the $NO_3^-$ treatments and not in the $NO_2^-$ treatments is evidence that it is not due to inhibition of the reduction of $N_2O$ to $N_2$ at higher $O_2$ because then both treatments would look similar. It further indicates that high $N_2O$ production from $NO_3^-$ in high oxygen treatments is unlikely an effect of anoxic micro~~-~~niches. While anoxic micro-niches in batch incubations can never be fully ruled out, there is no reason why they should systematically change $N_2O$ production in $NO_3^-$ from $NO_2^-$ incubations at the same oxygen treatment. We suggest a stimulation of incomplete denitrification, which leads to the accumulation of $N_2O$ in ~~our~~ the serum bottles rather than a stimulation of overall denitrification rates to $N_2$. While $NO_3^-$ ~~nitrate~~ reduction was inhibited by higher $O_2$ concentrations, $N_2O$ production was not, leading to very high yields of $N_2O$ production per $NO_2^-$ produced. We hypothesize that there is a direct channeling of reduced $NO_3^-$ to $N_2O$ without exchange of an internal $NO_2^-$ pool with the surrounding $NO_2^-$. Long turnover times for $NO_2^-$ have been inferred from $\delta^{18}O$ of $NO_2^-$, which was fully equilibrated with water in the offshore waters (Bourbonnais et al. 2015) and more dynamic in the coastal waters (Hu et al. 2016) supporting our hypothesis. If $NO_2^-$ does not exchange, our rate estimates for $NO_3^-$ reduction based on produced $^{15}N\text{-}NO_2^-$ are underestimated resulting in high yields. A low $NO_2^-$ exchange rate has been shown before (Ji et al. 2018b). Based on the assumption that all labelled $N_2O$ from $^{15}NO_3^-$ has gone through the $NO_2^-$ pool, we include the $NO_2^-$ pool into calculating $f_N$~~f~~. In $^{15}NO_3^-$ incubations the enrichment of the substrate pool was low ($f_N$~~f~~ = 0.05 – 0.1) and including $NO_2^-$ resulted in an underestimation of no more than 5 % depending on the *in situ* $NO_2^-$ concentration, and thus does not explain the high rates.

**Formatiert:** Tiefgestellt
**Formatiert:** Tiefgestellt
**Formatiert:** Schriftart: Kursiv
**Formatiert:** Tiefgestellt
**Formatiert:** Tiefgestellt
**Formatiert:** Schriftart: Nicht Fett
**Formatiert:** Schriftart: Nicht Fett
**Formatiert:** Schriftart: Nicht Fett
**Formatiert:** Schriftart: Kursiv
**Formatiert:** Schriftart: Nicht Fett
**Formatiert:** Schriftart: Nicht Fett
**Formatiert:** Schriftart: Nicht Fett
**Formatiert:** Schriftart: Nicht Fett
**Formatiert:** Schriftart: Nicht Fett, Kursiv
**Formatiert:** Schriftart: Nicht Fett
**Formatiert:** Tiefgestellt
**Formatiert:** Tiefgestellt
**Formatiert:** Tiefgestellt
**Formatiert:** Hochgestellt
**Formatiert:** Schriftart: Symbol
**Formatiert:** Hochgestellt
**Formatiert:** Tiefgestellt
**Formatiert:** Hochgestellt
**Formatiert:** Schriftfarbe: Automatisch, Englisch (Großbritannien)

One $N_2O$ producing process not considered in this study is fungal denitrification, but it deserves mentioning because in soils and coastal sediments it contributes substantially to $N_2O$ production (Wankel et al. 2017, Shoun et al. 2012). With $^{15}N$-labelling experiments it is not possible to distinguish between bacterial and fungal denitrification. In ODZs, marine fungal communities show a wide diversity (Jebaraj et al. 2012) and a high adaptive capability is suggested (Richards et al. 2012). Most fungal denitrifiers lack the capability to reduce $N_2O$ to $N_2$, hence all $NO_3^-$ ~~nitrate~~ reduction results in $N_2O$ production (Richards et al. 2012). In a culture study, the fungus, *Fusarium oxysporum,* needed $O_2$ exposure before it started to denitrify (Zhou et al. 2001). To what extent marine fungi play a role in denitrification in open ocean ODZs and their $O_2$ sensitivity remains to be investigated.

$N_2O$ production from $NH_4^+$ did not decrease exponentially with increasing $O_2$ as shown previously for the ETSP (Qin et al. 2017, Ji et al. 2018a, Santoro et al. 2011). $N_2O$ production rather increased with increasing *in situ* oxygen and had an optimum between 1.4 – 6 µmol $O_2$ $L^{-1}$ in manipulated $O_2$ treatments. A similar optimum curve was observed in cultures of the marine AOA *Nitrosopumilus maritimus,* where $N_2O$ production reached maxima at $O_2$ concentrations between 2 - 10 µmol $L^{-1}$ (Hink et al. 2017a). Furthermore, $N_2O$ production by *N. viennensis* and *N. maritimus* was not affected by $O_2$ but instead by the rate of AO (Stieglmeier et al. 2014, Hink et al. 2017a). To find out if this is the case in our study, we plotted AO rate against $N_2O$ production from $NH_4^+$ for natural and manipulated $O_2$ samples (Figure S7~~5~~). The resulting significant linear fit ($R^2 = 0.75$, $p<0.0001$) implies that the rate of AO was the main driver for the intensity of $N_2O$ production from $NH_4^+$ and oxygen had a secondary effect.

Discrepancies in estimates of the $O_2$ sensitivity of $N_2O$ production by nitrification and denitrification are likely due to a combination of taxonomic variation as well as differences in sensitivity among the various enzymes of each pathway.

### 4.2 $N_2O$ yields and hybrid $N_2O$ formation from $NH_4^+$

$N_2O$ yields of AO were 0.15 – 2.07 % ($N_2O$-N mol/ $NO_2^-$-N mol = 1.5 x $10^{-3}$ – 20.7 x $10^{-3}$) which are at the higher end of most marine AOA culture or field studies (Hink et al 2017b, Qin et al. 2017, Santoro et al. 2011, Stieglmeier et al. 2014). Only in 2015 off the coast of Peru a higher maximum yield of 3.14% was reported (Ji et al. 2018a). While high $N_2O$ yields are usually found in low $O_2$ waters (≤6 µmol $L^{-1}$), in this study AO had also high yields at higher oxygen concentrations, 0.9 % at 30 µmol $L^{-1}$ $O_2$ compared to previous studies (0.06% at > 50 µmol $L^{-1}$ Ji et al. 2018a). ~~Not only high $N_2O$ yields in low $O_2$ waters (< 6 µmol $L^{-1}$), but also higher yields at higher $O_2$ concentrations, 0.9 % at 30 µmol $L^{-1}$ $O_2$ compared to 0.06% at > 50 µmol $L^{-1}$ (Ji et al. 2018a) were found~~. In near coastal regions, higher $N_2O$ yield at higher $O_2$ concentrations expands the overall water volume where $N_2O$ production by AO contributes to high $N_2O$ concentration, which is more likely to be emitted to the atmosphere.

Insights into the production mechanism of $N_2O$ is gained from hybrid-$N_2O$ formation based on differentiating between production of single ($^{45}N_2O$) and double ($^{46}N_2O$) - labelled $N_2O$. If the production of $^{45}N_2O$ is higher than what is expected based on the binomial distribution, then an additional source of $^{14}N$ can be assumed. In $^{15}NH_4^+$ incubations, as potential $^{14}N$ substrates (besides $NH_4^+$), $NO_2^-$, $NH_2OH$ and HNO are most likely. Even though, ~~I~~*in situ* $NH_4^+$ is below detection in almost all water depths ($f_N$~~f~~ > 0.9)~~, hence in our incubations this pool is 99% labelled.~~, there remains the potential for $^{15}NH_4^+$ pool dilution by remineralization and DNRA during the incubation. Studies have shown fast turnover for $NH_4^+$, despite low $NH_4^+$ concentrations (e.g.~~f.e.~~ Klawonn et al. 2019). Even if hybrid $N_2O$ production rates are overestimated, it remains the major $N_2O$ production mechanisms ~~of~~from AO in this study.– In future $^{15}N$ -labelling studies, co-occurrence of $NH_4^+$ production by DNRA or

Formatiert: Tiefgestellt
Formatiert: Tiefgestellt
Formatiert: Hochgestellt
Formatiert: Hochgestellt
Formatiert: Tiefgestellt
Formatiert: Hochgestellt

degradation should be measured along with $N_2O$ production to account for pool dilution. ~~As potential $^{14}N$ substrates, $NO_2^-$, $NH_2OH$ and HNO are most likely.~~ Whether hybrid $N_2O$ formation is purely abiotic, a mix of biotic and abiotic or biotic reactions, is debatable (Stieglmeier et al. 2014, Kozlowski et al. 2016, Carini et al. 2018, Lancaster et al. 2018, Stein 2019). Hybrid $N_2O$ production from $NO_2^-$ was variable with depth and oxygen, which can be explained by the different proportions of nitrifier versus denitrifier $NO_2^-$ reduction to $N_2O$. For example, in the interface sample S19 (892, 144 m, 3.69 µmol $L^{-1}$ $NO_2^-$) $N_2O$ production from $NO_2^-$ (0.72 ± 0.19 nmol $L^{-1}$ $d^{-1}$) was 20 times higher than from $NH_4^+$ (0.033 ± 0.0004 nmol $L^{-1}d^{-1}$) and no hybrid $N_2O$ formation from $NO_2^-$ was found (Figure 5d). There, the major $N_2O$ production mechanism seems to be by denitrification rather than nitrification, and even if there was a hybrid production we were not able to detect it within the given error ranges. Hybrid $N_2O$ production from $NH_4^+$ was independent of the rate at which $N_2O$ production took place and independent of the $O_2$ concentration and varied little (70 – 86% of total $N_2O$ production) during AO. Therefore, a purely abiotic reaction outside and without the vicinity of the cell can be excluded because concentrations of potential substrates for abiotic $N_2O$ production like Fe(II), Mn, NO, $NH_2OH$ vary with depth and $O_2$ concentration (Zhu-Barker et al. 2015, Kondo and Moffet 2015, Lutterbeck et al. 2018, Korth et al. 2019). Additionally, at four depths the potential for abiotic $N_2O$ production in $^{15}NO_2^-$ addition experiments showed variations with depth and no significant impact of $HgCl_2$ fixation (Figure S9). Hence, any $^{14}N$ which is integrated into $N_2O$ to produce a hybrid/single labelled $N_2O$ has to be passively or actively taken up by the cell first (Figure 9). There, it reacts with an intermediate product ($^{15}NO$ or $^{15}NH_2OH$) of AO inside the cell. With this set of experiments, it is not possible to disentangle if hybrid production is based on an enzymatic reaction or an abiotic reaction inside the cell. Caranto et al. (2017) showed that the main substrate of $NH_2OH$ oxidation is NO, making NO an obligate intermediate of AO in AOB and suggested the existence of an unknown enzyme that catalyzes NO oxidation to $NO_2^-$ (further details also in Stein 2019). If NO is an obligate intermediate of AO in AOA (Lancaster et al. 2018), a constant rate of spontaneous abiotic or enzymatic $N_2O$ production is very likely, which always depends on the amount of NO produced in the first place. This could explain why we consistently find ~80% hybrid formation at high as well as at low AO rates. Further studies are needed to investigate the full mechanisms.

Formatiert: Tiefgestellt
Formatiert: Hochgestellt
Formatiert: Tiefgestellt
Formatiert: Hochgestellt
Formatiert: Tiefgestellt

### 4.3 Effect of particulate organic matter on $N_2O$ production

A positive stimulation of $N_2O$ production from denitrification by particulate organic matter was found, indicating carbon limitation of denitrification in the ETSP. The experimental POM amendments simulated a low POC export flux and represented a flux that happens over 2 - 15 days, assuming an export flux of 3.8 mmol $m^{-2}$ $d^{-1}$ and that 8% of the total POC pool is >50 µm (Boyd et al. 1999, Martin et al. 1987, Haskell et al. 2015). We are aware that the POM collected by *in situ* pumps is a mix of suspended and sinking particles and hence the flux should be considered a rough estimate. However, the particle size (>50 µm) used in the experiments is indictive of sinking particles. The stimulation of $N_2$ production from denitrification by particulate organic matter has been shown in ODZs before (Ward et al. 2008, Chang et al. 2014), with quantity and quality of organic matter influencing the degree of stimulation (Babbin et al. 2014). In this study, amendments of POM at different degradation stages resulted in variable magnitudes of $N_2O$ production from $NO_2^-$ and $NO_3^-$ with no significant correlations between magnitude of the rates and amount, origin or quality of POM added. The processing of the particles has reduced the original N/C ratios of POM from the mixed layer more than of the POM from the ODZ, resulting in similar N/C ratios of particles from different depths. This could be one possible explanation for a lack of correlation of $N_2O$ production with origin of the POM. Furthermore, $N_2$ production was not quantified and

hence it is not possible to evaluate potential relationships between overall N loss and POM additions or whether the partitioning between $N_2O$ and $N_2$ varied among treatments and depths. $N_2O/N_2$ production ratio can vary from 0 - 100% (Dalsgaard et al. 2014, Bonaglia et al. 2016). A temporary accumulation of $N_2O$ before further reduction to $N_2$ in the incubations can be ruled out as $N_2O$ accumulated linearly over time. The only station, where POM additions did not stimulate $N_2O$ production was in the center of the young eddy (912-S17). There, the highest rates of $N_2O$ production from $NO_3^-$ (118 nmol $L^{-1}$ $d^{-1}$) were found, indicating that denitrification was not carbon limited. This is consistent with previous studies on anti-cyclonic eddies, which have shown high N loss in the core of a young eddy that weakened with aging of the eddy (Stramma et al. 2013, Bourbonnais et al. 2015, Löscher et al. 2016). A direct link between the freshly produced POM fueling N loss on one hand, and decreased N loss with aging due to POM export out of the eddy on the other hand, was proposed (Bourbonnais et al. 2015, Löscher et al. 2016). In this study, the young eddy is a hot spot for $N_2O$ production.

Besides carbon availability as electron donor for denitrification, copper limitation and high $NO_3^-$ availability may play a role. Copper limitation has been argued to lead to $N_2O$ accumulation by inhibiting the copper-dependent $N_2O$ reductase (Granger and Ward 2003, Bonaglia et al. 2016), but it was not a limiting factor for denitrification in the three major ODZs previously (Ward et al. 2008). Water sampling from Niskin bottles in our study was not trace metal clean and could be contaminated with Copper from the sampling system, making a limitation of trace metals in our incubations unlikely. However, OM fueled $N_2O$ production may have become limited by the availability of copper during the incubation.

High $NO_3^-$ availability increases $N_2O$ production from denitrification in salt marshes (Ji et al. 2015b) and in soils (Weier et al. 1993), systems which are generally not carbon limited. Also, at the oxic - anoxic interface of Chesapeake Bay, the ratio of $NO_2^-$ to $NO_3^-$ concentration was identified as a driver for high $N_2O$ production from $NO_3^-$ (Ji et al. 2018b). This study also found higher $N_2O$ production rates from $NO_3^-$ than $NO_2^-$, which linearly correlated with the ratio of $NO_2^-/NO_3^-$ concentrations (Figure S~~8~~6). Intracellularly produced $NO_2^-$ does not seem to exchange with the surrounding pool, but ambient $NO_3^-$ is directly converted to $N_2O$, a process identified as "$NO_2^-$ shunting" in $N_2$ production studies (de Brabandere et al. 2014, Chang et al. 2014). POM as electron donor is an important regulator for reductive $N_2O$ production.

**4.4 Effect of abundance of total and active community composition on $N_2O$ production rates**

The abundances of both *amoA* and *nirS* genes found in the ETSP are similar to those reported in earlier studies in the ETSP (Peng et al. 2013, Ji et al. 2015a, Jayakumar et al. 2013). The *amoA* gene abundances were similar to those reported for the coastal ETSP by Lam et al. (2009), but *nirS* abundances reported here were higher than the *nirS* abundances in that study, probably due to the use of different PCR primers. The community composition of AOA did not significantly differ along the $O_2$ gradient as shown previously (Peng et al. 2013), but a significant correlation between archaeal *amoA* transcript abundance and $N_2O$ production was shown in this study. The combination of qPCR and microarray analysis offered a great advantage to relate the total abundances to the production rates and additionally link particular community components to biogeochemical activities. To determine whether a particular archetype drives the correlation of $N_2O$ production by AO, a Bray-Curtis dissimilarity matrix revealed archetype AOA3 related to *Nitrosopelagicus brevis* (CN25) to be significantly correlated with the $N_2O$ production by AO. This clade is abundant in the surface ocean and typically found in high abundances in the lower euphotic zone (Santoro et al. 2011, 2015). With the demonstration of high abundances of AOA3 coincident with high nitrification rates and high $N_2O$ production rates, we suggest that *Nitrosopelagicus*

*brevis* related AOA likely play an important role in $N_2O$ production in near surface waters in the Eastern Tropical South Pacific.

The lack of significant correlation between community composition or single members of the community and reductive $N_2O$ production is consistent with the fact that *nirS* is not the enzyme directly synthesizing $N_2O$ and *nirS* communities are sources as well as sinks for $N_2O$. Taxonomic analysis of the *nirS* gene and transcripts suggested that there is high taxonomic diversity among the denitrifiers, which is likely linked to a high variability of the total denitrification gene assembly (including *nos*, *nor*, *nir*). In particular the abundance and diversity of nitric oxide reductase (*nor*), the enzyme directly synthesizing $N_2O$, would be of interest, but it is present in nitrifiers and denitrifiers (Casciotti and Ward 2005) and one goal of this study was to differentiate among $N_2O$ produced by nitrifiers and denitrifers. However, *nirS* gene and transcript abundance correlated with $N_2O$ production from $NO_2^-$ making it a possible indicator for one part of reductive $N_2O$ production. It is also worth noting that anammox related *nirS* genes and transcripts (*nirS* 166, 167) contribute up to 12% of the total copy numbers putting a wrinkle on *nirS* abundance as marker gene for denitrifiers only. The subtraction of the anammox related *nirS* genes from total copy numbers did not change the results from Bray-Curtis Analysis. These data indicate that the extent to which gene or transcript abundance patterns or community composition of marker genes of processes can be used as proxies for process rate measurements is variable, likely due to complex factors, including the relative dominance of different community members, the modular nature of denitrification, differences in the level of metabolic regulation (transcriptional, translational, and enzymatic), and the range of environmental conditions being observed.

**4.5 Summary and conclusion**

In this study we used a combined approach of $^{15}N$ tracer techniques and molecular techniques in order to investigate the factors that control $N_2O$ production within the upper oxycline of the ODZ in the ETSP. Our results suggest that denitrification is a major $N_2O$ source along the oxic - anoxic interface of the upper oxycline. Highest $N_2O$ production rates from $NO_2^-$ and $NO_3^-$ were found at or below the oxic-anoxic interface, whereas highest $N_2O$ production from AO was slightly shallower in the oxycline. Overall, *in situ* $O_2$ threshold below 8 µmol $L^{-1}$ favored $NO_3^-$ ~~nitrate~~ and $NO_2^-$ reduction to $N_2O$ and high $N_2O$ yields from AO up to 2.2%. A different pattern was observed for the community response to increasing oxygen, with highest $N_2O$ production from $NH_4^+$ and $NO_2^-$ between 1.4 – 6 µmol $L^{-1}$ $O_2$ and high $N_2O$ production from $NO_3^-$ even at $O_2$ concentrations up to 22 µmol $L^{-1}$. This study highlights the diversity of $N_2O$ production regulation and the need to conduct further experiments where single community members can be better constrained. Our experiments provide the first insights into $N_2O$ regulation by particulate organic matter in the ETSP with particles greatly enhancing $N_2O$ production (up to 5fold). Furthermore, the significant positive correlation between *Nitrosopelagicus brevis* (CN25) and $N_2O$ produced from AO could indicate its importance in $N_2O$ production and points out the great value of combining biogeochemical rate measurements with molecular analysis to investigate multifaceted $N_2O$ cycling. This study shows that short term oxygen increase can lead to high $N_2O$ production even from denitrification and extends the existing $O_2$ thresholds for high reductive $N_2O$ production up to 22 µmol $L^{-1}$ $O_2$. Together with high $N_2O$ yields from AO up to $O_2$ levels of 30 µmol $L^{-1}$, an expansion of low oxygenated waters around ODZs predicted for the future can significantly increase marine $N_2O$ production.

Regardless of which processes are responsible for $N_2O$ production in the ODZ, high $N_2O$ production at the oxic-anoxic interface of the upper oxycline sustains high $N_2O$ concentration peaks with a potential for intense

$N_2O$ emission to the atmosphere during upwelling events. An average total $N_2O$ production rate of 3.1 nmol $N_2O$ $L^{-1}$ $d^{-1}$ in a 50 m thick suboxic layer with 0 – 20 µmol $L^{-1}$ $O_2$ leads to an annual $N_2O$ efflux of 0.5 Tg N $y^{-1}$ in the Peruvian upwelling (2.22 ×$10^5$ $km^2$, Arévalo-Martínez et al. 2015), which is within the estimates based on surface $N_2O$ concentration measurements from 2012-2013 (Arévalo-Martínez et al. 2015, Bourbonnais et al. 2017). The importance of the Peru upwelling system for global $N_2O$ emissions (5 – 22% of global marine $N_2O$ emissions) is directly linked to the extreme $N_2O$ accumulations in coastal waters. Coastal $N_2O$ hotspots are well known (Bakker et al. 2014) and this study shows that they can be explained by considering denitrification as a major $N_2O$ source. While this study does not help to resolve temporal variability, manipulation experiments give valuable insights ~~on~~into the short-term response of $N_2O$ production to oxygen and ~~With~~particles. With the further parametrization of POM export as a driver for $N_2O$ production from denitrification, models may be able to better predict $N_2O$ emissions in highly productive coastal upwelling regions and to evaluate how fluxes might change with changing stratification and deoxygenation.

**Data availability:** The data presented here were archived in the SFB754 database (www.sfb754.de). The $N_2O$ data are also available from the Marine Methane and Nitrous Oxide (MEMENTO) database (https://memento.geomar.de/de/n2o).

**Author contributions**: CF, HWB and BW conceptualized the study. CF and MS performed experiment. CF and ELP analyzed samples. RX and EA collected POM. DLAM sampled and measured $N_2O$ concentrations. AJ performed qPCR. SO supported mass spectrometer analysis. XS supported experimental methods and assisted with data analysis. CF analyzed data and led the writing effort, with substantial contributions from all co-authors.

**Competing interests:** Authors declare no competing interests.

**Acknowledgement:** The work presented here was made possible by the DFG-funded Joint Collaborative Centre SFB754 Phase III (http://www.sfb754.de) and by a fellowship of the German Academic Exchange Service (DAAD) program 'Postdoctoral Researchers International Mobility Experience (PRIME, ID 57350888) awarded to CF. MS was supported by the China Scholarship Council (No. 201406330054). E.L-P had a FPU-PhD fellowship (014/02917) from the Spanish Ministry of Education and a PhD International Mobility scholarship from the Universidad de Granada. CRL was funded by a EU H2020 Marie Curie Individual Fellowship (NITROX, Grant #704272) and by the Villum Foundation (Grant# 16518). EA, HWB and RX were funded by the DFG-funded Joint Collaborative Centre SFB754 program. We thank the captain and crew of R/V Meteor. Moreover, we thank the Peruvian authorities for the permission to work in their territorial waters.

Formatiert: Tiefgestellt

Feldfunktion geändert

Feldfunktion geändert

Feldfunktion geändert

**References**


Anderson, J. H. (1964). The metabolism of hydroxylamine to nitrite by Nitrosomonas. *Biochemistry Journal*, *91*(1948), 8–17. https://doi.org/10.1042/bj0910008

Arévalo-Martínez, D. L., Kock, A., Löscher, C. R., Schmitz, R. A., Bange, H. W., Arevalo-Martínez, D., … Bange, H. W. (2015). Massive nitrous oxide emissions from the tropical South Pacific Ocean. *Nature Geoscience*, *8*(7), 530–533. https://doi.org/10.1038/NGEO2469

Arévalo-Martínez, Damian L., Kock, A., Löscher, C. R., Schmitz, R. A., Stramma, L., & Bange, H. W. (2016). Influence of mesoscale eddies on the distribution of nitrous oxide in the eastern tropical South Pacific. *Biogeosciences*, *13*(4), 1105–1118. https://doi.org/10.5194/bg-13-1105-2016

Babbin, A. R., Bianchi, D., Jayakumar, A., & Ward, B. B. (2015). Rapid nitrous oxide cycling in the suboxic ocean. *Science*, *348*(6239), 1127–1129. https://doi.org/10.1126/science.aaa8380

Babbin, A. R., Keil, R. G., Devol, A. H., & Ward, B. B. (2014). Organic matter stoichiometry, flux, and oxygen control nitrogen loss in the ocean. *Science (New York, N.Y.)*, *344*(6182), 406–408. https://doi.org/10.1126/science.1248364

Bakker, D. C. E., Bange, H. W., Gruber, N., Johannessen, T., Upstill-Goddard, R. C., Borges, A. V., … Santana-Casiano, J. M. (2014). Air-Sea Interactions of Natural Long-Lived Greenhouse Gases ($CO_2$,$N_2O$, $CH_4$) in a Changing Climate. In *Ocean-Atmosphere Interactions of Gases and Particles* (pp. 55–112). https://doi.org/10.1007/978-3-642-25643-1

Bange, H. W. (2008). Gaseous nitrogen compounds (NO, $N_2O$, $N_2$, $NH_3$) in the ocean. In *Nitrogen in the marine environment* (pp. 51–94). Amsterdam: Elsevier.

Battaglia, G., & Joos, F. (2018). Marine N2O Emissions From Nitrification and Denitrification Constrained by Modern Observations and Projected in Multimillennial Global Warming Simulations. *Global Biogeochemical Cycles*, *32*(1), 92–121. https://doi.org/10.1002/2017GB005671

Beman, J. M., Chow, C., King, A. L., Feng, Y., & Fuhrman, J. a. (2011). Global declines in oceanic nitrification rates as a consequence of ocean acidification. *Proceedings of the National Academy of Sciences of the United States of America*, *108*(1), 208–213. https://doi.org/10.1073/pnas.1011053108/-/DCSupplemental.www.pnas.org/cgi/doi/10.1073/pnas.1011053108

Bertagnolli, A. D., & Ulloa, O. (2017). Hydrography shapes community composition and diversity of amoA-containing Thaumarchaeota in the coastal waters off central Chile. *Environmental Microbiology Reports*, *9*(6), 717–728. https://doi.org/10.1111/1758-2229.12579

Biller, S. J., Mosier, A. C., Wells, G. F., & Francis, C. A. (2012). Global Biodiversity of Aquatic Ammonia-Oxidizing Archaea is Partitioned by Habitat. *Frontiers in Microbiology*, *3*, 252. https://doi.org/10.3389/fmicb.2012.00252

Blum, J. M., Su, Q., Ma, Y., Valverde-Pérez, B., Domingo-Félez, C., Jensen, M. M., & Smets, B. F. (2018). The pH dependency of N-converting enzymatic processes, pathways and microbes: effect on net $N_2O$ production. *Environmental Microbiology*, *20*(5), 1623–1640. https://doi.org/10.1111/1462-2920.14063

Bonaglia, S., Klawonn, I., De Brabandere, L., Deutsch, B., Thamdrup, B., & Brüchert, V. (2016). Denitrification and DNRA at the Baltic Sea oxic–anoxic interface: Substrate spectrum and kinetics. *Limnology and Oceanography*, *61*(5), 1900–1915. https://doi.org/10.1002/lno.10343

Borcard, D., Legendre, P., & Drapeau, P. (1992). Partialling out the Spatial Component of Ecological Variation. *Ecology*, *73*(3), 1045–1055. https://doi.org/10.2307/1940179

Bourbonnais, A., Altabet, M. A., Charoenpong, C. N., Larkum, J., Hu, H., Bange, H. W., & Stramma, L. (2015). N-loss isotope effects in the Peru oxygen minimum zone studied using a mesoscale eddy as a natural tracer experiment. *Global Biogeochemical Cycles*, 29, 793-811. https://doi.org/10.1002/2014GB005001

Bourbonnais, A., Letscher, R. T., Bange, H. W., Échevin, V., Larkum, J., Mohn, J., … Altabet, M. A. (2017). $N_2O$ production and consumption from stable isotopic and concentration data in the Peruvian coastal upwelling system. *Global Biogeochemical Cycles*, *31*(4), 678–698. https://doi.org/10.1002/2016GB005567

Bouskill, N. J., Eveillard, D., O'Mullan, G., Jackson, G. A., & Ward, B. B. (2011). Seasonal and annual reoccurrence in betaproteobacterial ammonia-oxidizing bacterial population structure. *Environmental Microbiology*, *13*(4), 872–886. https://doi.org/10.1111/j.1462-2920.2010.02362.x

Boyd, P. W., Sherry, N. D., Berges, J. A., Bishop, J. K. B., Calvert, S. E., Charette, M. A., … Wong, C. S. (1999). Transformations of biogenic particulates from the pelagic to the deep ocean realm. *Deep Sea Research Part II: Topical Studies in Oceanography*, *46*(11–12), 2761–2792. https://doi.org/10.1016/S0967-0645(99)00083-1

Braker, G., Fesefeldt, A., & Witzel, K. P. (1998). Development of PCR primer systems for amplification of nitrite reductase genes (nirK and nirS) to detect denitrifying bacteria in environmental samples. *Applied and Environmental Microbiology*, *64*(10), 3769–3775.

Breider, F., Yoshikawa, C., Makabe, A., Toyoda, S., Wakita, M., Matsui, Y., … Yoshida, N. (2019). Response of N2O production rate to ocean acidification in the western North Pacific. *Nature Climate Change*, *9*(12), 954–958. https://doi.org/10.1038/s41558-019-0605-7

Bristow, L A, Callbeck, C. M., Larsen, M., Altabet, M. A., Dekaezemacker, J., Forth, M., … Canfield, D. E.

(2016a). N2 production rates limited by nitrite availability in the Bay of Bengal oxygen minimum zone. *Nature Geosci*, *advance on*(December). https://doi.org/10.1038/ngeo2847

Bristow, Laura A., Dalsgaard, T., Tiano, L., Mills, D. B., Bertagnolli, A. D., Wright, J. J., … Thamdrup, B. (2016b). Ammonium and nitrite oxidation at nanomolar oxygen concentrations in oxygen minimum zone waters. *Proceedings of the National Academy of Sciences*, *113*(38), 201600359.

Buitenhuis, E. T., Suntharalingam, P., & Le Quéré, C. (2018). Constraints on global oceanic emissions of $N_2O$ from observations and models. *Biogeosciences*, *15*(7), 2161–2175. https://doi.org/10.5194/bg-15-2161-2018

Callbeck, C. M., Lavik, G., Ferdelman, T. G., Fuchs, B., Gruber-Vodicka, H. R., Hach, P. F., … Kuypers, M. M. M. (2018). Oxygen minimum zone cryptic sulfur cycling sustained by offshore transport of key sulfur oxidizing bacteria. *Nature Communications*, *9*(1), 1–11. https://doi.org/10.1038/s41467-018-04041-x

Capone, D. G., & Hutchins, D. A. (2013). Microbial biogeochemistry of coastal upwelling regimes in a changing ocean. *Nature Geoscience*, *6*(9), 711–717. https://doi.org/10.1038/ngeo1916

Caranto, J. D., Lancaster, K. M., Ma, C., Jensen, M. M., Smets, B. F., Thamdrup, B., … Lancaster, K. M. (2017). Nitric oxide is an obligate bacterial nitrification intermediate produced by hydroxylamine oxidoreductase. *Proceedings of the National Academy of Sciences*, *114*(31), 8217–8222. https://doi.org/10.1073/pnas.1704504114

Carini, P., Dupont, C. L., & Santoro, A. E. (2018). Patterns of thaumarchaeal gene expression in culture and diverse marine environments. *Environmental Microbiology*. https://doi.org/10.1111/1462-2920.14107

Carrasco, C., Karstensen, J., & Farias, L. (2017). On the Nitrous Oxide Accumulation in Intermediate Waters of the Eastern South Pacific Ocean. *Frontiers in Marine Science*, *4*, 24. https://doi.org/10.3389/fmars.2017.00024

Casciotti, L., & Ward,B. (2005). Phylogenetic analysis of nitric oxide reductase gene homologues from aerobic ammonia-oxidizing bacteria. *FEMS Microbiology Ecology*, *52*(2), 197–205. http://dx.doi.org/10.1016/j.femsec.2004.11.002

Casciotti, K. L., Forbes, M., Vedamati, J., Peters, B., Martin, T., & Mordy, C. W. (2018). Nitrous oxide cycling in the Eastern Tropical South Pacific as inferred from isotopic and isotopomeric data. *Deep Sea Research Part II: Topical Studies in Oceanography*, (xxxx), 1–13. https://doi.org/10.1016/J.DSR2.2018.07.014

Chang, B. X., Rich, J. R., Jayakumar, A., Naik, H., Pratihary, A., Keil, R. G., … Devol, A. H. (2014). The effect of organic carbon on fixed nitrogen loss in the eastern tropical South Pacific and Arabian Sea oxygen deficient zones. *Limnology and Oceanography*, *59*(4), 1267–1274. https://doi.org/10.4319/lo.2014.59.4.1267

Charpentier, J., Farias, L., Yoshida, N., Boontanon, N., & Raimbault, P. (2007). Nitrous oxide distribution and its origin in the central and eastern South Pacific Subtropical Gyre. *Biogeosciences*, *4*(5), 729–741. https://doi.org/10.5194/bg-4-729-2007

Chavez, F. P., & Messié, M. (2009). A comparison of Eastern Boundary Upwelling Ecosystems. *Progress in Oceanography*, *83*(1–4), 80–96. https://doi.org/10.1016/j.pocean.2009.07.032

Codispoti, L. A. (2010). Interesting Times for Marine N2O. *Science*, *332*, 1339–1340.

Cohen, Y., & Gordon, L. (1978). Nitrous oxide in the oxygen minimum of eastern tropical North Pacific: evidence for its consumption during denitrification and possble mechanisms for its production. *Deep Sea Research*, *25*(1977), 509–524.

Cornejo DOttone, M., Bravo, L., Ramos, M., Pizarro, O., Karstensen, J., Gallegos, M., … Karp-Boss, L. (2016). Biogeochemical characteristics of a long-lived anticyclonic eddy in the eastern South Pacific Ocean. *Biogeosciences*, *13*(10), 2971–2979. https://doi.org/10.5194/bg-13-2971-2016

Crutzen, P. J. (1970). The influence of nitrogen oxides on the atmospheric ozone content. *Quarterly Journal of the Royal Meteorological Society*, *96*(408), 320–325. https://doi.org/10.1002/qj.49709640815

Dalsgaard, T., Stewart, F. J., Thamdrup, B., De Brabandere, L., Revsbech, N. P., Ulloa, O., … Delong, E. F. (2014). Oxygen at nanomolar levels reversibly suppresses process rates and gene expression in anammox and denitrification in the oxygen minimum zone off northern Chile. *MBio*, *5*(6), e01966. https://doi.org/10.1128/mBio.01966-14

Dalsgaard, T., Thamdrup, B., Farías, L., Peter Revsbech, N., & Revsbech, N. P. (2012). Anammox and denitrification in the oxygen minimum zone of the eastern South Pacific. *Limnology and Oceanography*, *57*(5), 1331–1346. https://doi.org/10.4319/lo.2012.57.5.1331

De Brabandere, L., Canfield, D. E., Dalsgaard, T., Friederich, G. E., Revsbech, N. P., Ulloa, O., & Thamdrup, B. (2014). Vertical partitioning of nitrogen-loss processes across the oxic-anoxic interface of an oceanic oxygen minimum zone. *Environmental Microbiology*, *16*(10), 3041–3054. https://doi.org/10.1111/1462-2920.12255

Farías, L., Castro-González, M., Cornejo, M., Charpentier, J. J., Faúndez, J., Boontanon, N., … Yoshida, N. (2009). Denitrification and nitrous oxide cycling within the upper oxycline of the eastern tropical South Pacific oxygen minimum zone. *Limnology and Oceanography*, *54*(1), 132–144. https://doi.org/10.4319/lo.2009.54.1.0132

Frame, C. H., & Casciotti, K. L. (2010). Biogeochemical controls and isotopic signatures of nitrous oxide

Formatiert: Englisch (USA)

Formatiert: Englisch (Großbritannien)

Formatiert: Englisch (Großbritannien)

production by a marine ammonia-oxidizing bacterium. *Biogeosciences*, *7*, 3019–3059. https://doi.org/10.5194/bg-7-2695-2010

Frame, C. H., Lau, E., Nolan, E. J., Goepfert, T. J., & Lehmann, M. F. (2017). Acidification Enhances Hybrid $N_2O$ Production Associated with Aquatic Ammonia-Oxidizing Microorganisms. *Frontiers in Microbiology*, *7*(January), 2104. https://doi.org/10.3389/fmicb.2016.02104

Francis, C. A., Roberts, K. J., Beman, J. M., Santoro, A. E., & Oakley, B. B. (2005). Ubiquity and diversity of ammonia-oxidizing archaea in water columns and sediments of the ocean. *Proceedings of the National Academy of Sciences*, *102*(41), 14683–14688. https://doi.org/10.1073/pnas.0506625102

Ganesh, S., Parris, D. J., Delong, E. F., & Stewart, F. J. (2014). Metagenomic analysis of size-fractionated picoplankton in a marine oxygen minimum zone. *ISME Journal*, *8*(1), 187–211. https://doi.org/10.1038/ismej.2013.144

Goreau, T. J., Kaplan, W. A., Wofsy, S. C., McElroy, M. B., Valois, F. W., & Watson, S. W. (1980). Production of $NO_2^-$ and $N_2O$ by Nitrifying Bacteria at Reduced Concentrations of Oxygen. *Appl. Envir. Microbiol.*, *40*(3), 526–532.

Goréguès, C., Michotey, V., & Bonin, P. (2004). Isolation of hydrocarbonoclastic denitrifying bacteria from berre microbial mats. *Ophelia*, *58*(3), 263–270. https://doi.org/10.1080/00785236.2004.10410234

Granger, J., & Ward, B. B. (2003). Accumulation of nitrogen oxides in copper-limited cultures of denitrifying bacteria. *Limnology and Oceanography*, *48*(1), 313–318. https://doi.org/10.4319/lo.2003.48.1.0313

Hamdan, L. J., Coffin, R. B., Sikaroodi, M., Greinert, J., Treude, T., & Gillevet, P. M. (2012). Ocean currents shape the microbiome of Arctic marine sediments. *The ISME Journal*, *7*(4), 685–696. https://doi.org/10.1038/ismej.2012.143

Hammer, Ø., HARPER, D. A. T., & Ryan, P. D. (2001). PAST: Paleontological statistics software package. *Palaeontologia Electronica*, *4*(1), 1–9. https://doi.org/10.1016/j.bcp.2008.05.025

Haskell, W. Z., Kadko, D., Hammond, D. E., Knapp, A. N., Prokopenko, M. G., Berelson, W. M., & Capone, D. G. (2015). Upwelling velocity and eddy diffusivity from 7Be measurements used to compare vertical nutrient flux to export POC flux in the Eastern Tropical South Pacific. *Marine Chemistry*, *168*, 140–150. https://doi.org/10.1016/J.MARCHEM.2014.10.004

Hink, L., Lycus, P., Gubry-Rangin, C., Frostegård, Å., Nicol, G. W., Prosser, J. I., & Bakken, L. R. (2017)a. Kinetics of $NH_3$-oxidation, NO-turnover, $N_2O$-production and electron flow during oxygen depletion in model bacterial and archaeal ammonia oxidisers. *Environmental Microbiology*, *19*(12), 4882–4896. https://doi.org/10.1111/1462-2920.13914

Hink, L., Nicol, G. W., & Prosser, J. I. (2017)b. Archaea produce lower yields of $N_2O$ than bacteria during aerobic ammonia oxidation in soil. *Environmental Microbiology*, *19*(12), 4829–4837. https://doi.org/10.1111/1462-2920.13282

Holmes, R. M., Aminot, A., Kérouel, R., Hooker, B. A., & Peterson, B. J. (1999). A simple and precise method for measuring ammonium in marine and freshwater ecosystems. *Canadian Journal of Fisheries and Aquatic Sciences*, *56*, 1802–1808.

Hu, H., Bourbonnais, A., Larkum, J., Bange, H. W., & Altabet, M. A. (2016). Nitrogen cycling in shallow low-oxygen coastal waters off Peru from nitrite and nitrate nitrogen and oxygen isotopes. *Biogeosciences*, *13*(5), 1453–1468. https://doi.org/10.5194/bg-13-1453-2016

Hu, Z., Wessels, H. J. C. T., Alen, T., Jetten, M. S. M., & Kartal, B. (2019). Nitric oxide-dependent anaerobic ammonium oxidation. *Nature Communications*, *10*(1244), 1–7. https://doi.org/10.1038/s41467-019-09268-w

Hydes, D., Aoyama, M., Aminot, A., Bakker, K., Becker, S., Coverly, S., … Zhang, J. Z. (2010). Determination of dissolved nutrients (N, P, Si) in seawater with high precision and inter-comparability using gas-segmented continuous flow analysers. *The GO-SHIP Repeat Hydrography Manual IOCCP Report*, *134*(14), 1–87.

IPCC. (2013). *Climate Change 2013: The Physical Science Basis. Contribution of Working Group I to the Fifth Assessment Report of the Intergovernmental Panel on Climate Change*. Cambridge UK and New York, USA: Cambridge University Press. https://doi.org/10.1017/CBO9781107415324.010

Jayakumar, A., Peng, X., & Ward, B. (2013). Community composition of bacteria involved in fixed nitrogen loss in the water column of two major oxygen minimum zones in the ocean. *Aquatic Microbial Ecology*, *70*(3), 245–259. https://doi.org/10.3354/ame01654

Jayakumar, D. A., Naqvi, S. W. A., & Ward, B. B. (2009). Distribution and relative quantification of key genes involved in fixed nitrogen loss from the Arabian Sea oxygen minimum zone. *Indian Ocean Biogeochemcal Processes and Ecological Variability*, 187–203.

Jebaraj, C. S., Forster, D., Kauff, F., & Stoeck, T. (2012). Molecular Diversity of Fungi from Marine Oxygen-Deficient Environments (ODEs) (pp. 189–208). Springer, Berlin, Heidelberg. https://doi.org/10.1007/978-3-642-23342-5_10

Jetten, M. S. M., Ward, B. B., & Jensen, M. M. (2008). The microbial nitrogen cycle. *Environmental Microbiology*, *10*(11), 2903–2909. https://doi.org/10.1111/j.1462-2920.2008.01786.x

Ji, Q., Babbin, A. R., Jayakumar, A., & Ward, B. B. (2015a). Nitrous oxide production by nitrification and

Formatiert: Englisch (Großbritannien)

Formatiert: Englisch (USA)

Formatiert: Deutsch (Schweiz)

denitrification in the Eastern Tropical South Pacific oxygen minimum zone. *Geophysical Research Letters*. https://doi.org/10.1002/2015GL066853

Ji, Q., Babbin, A. R., Peng, X., Bowen, J. L., Ward, B. B., & Ji, Q. (2015b). Nitrogen substrate–dependent nitrous oxide cycling in salt marsh sediments. *Journal of Marine Research*, *7373*, 71–92.

Ji, Q., Buitenhuis, E., Suntharalingam, P., Sarmiento, J. L., & Ward, B. B. (2018). Global nitrous oxide production determined by oxygen sensitivity of nitrification and denitrification. https://doi.org/10.1029/2018GB005887

Ji, Q., Frey, C., Sun, X., Jackson, M., Lee, Y., Jayakumar, A., … Ward, B. B. (2018). Nitrogen and oxygen availabilities control water column nitrous oxide production during seasonal anoxia in the Chesapeake Bay, (March), 6127–6138.

Johnston, H. (1971). Reduction of Stratospheric Ozone by Nitrogen.Oxide Catalysts from Supersonic Transport Exhaust. *Science (New York, N.Y.)*, *173*, 517–522.

Jr., D. J. M., Anderson, L. A., Bates, N. R., Bibby, T., Buesseler, K. O., Carlson, C. A., … Steinberg, D. K. (2007). Eddy / Wind Interactions Stimulate Extraordinary Mid-Ocean Plankton Blooms. *Science*, *316*, 1021–1026. https://doi.org/10.1126/science.1136256

Kalvelage, T., Jensen, M. M., Contreras, S., Revsbech, N. P., Lam, P., Günter, M., … Kuypers, M. M. M. M. (2011). Oxygen sensitivity of anammox and coupled N-cycle processes in oxygen minimum zones. *PLoS ONE*, *6*(12), e29299. https://doi.org/10.1371/journal.pone.0029299

Kalvelage, T., Lavik, G., Jensen, M. M., Revsbech, N. P., Loescher, C., Schunck, H., … Kuypers, M. M. M. (2015). Aerobic Microbial Respiration In Oceanic Oxygen Minimum Zones. *Plos One*, *10*(7). https://doi.org/e013352610.1371/journal.pone.0133526

Kartal, B., Kuypers, M. M. M., Lavik, G., Schalk, J., Op den Camp, H. J. M., Jetten, M. S. M., & Strous, M. (2007). Anammox bacteria disguised as denitrifiers: nitrate reduction to dinitrogen gas via nitrite and ammonium. *Environmental Microbiology*, *9*(3), 635–642. https://doi.org/10.1111/j.1462-2920.2006.01183.x

Klawonn, I., Bonaglia, S., Whitehouse, M. J., Littmann, S., Tienken, D., Kuypers, M. M. M., … Ploug, H. (2019). Untangling hidden nutrient dynamics: rapid ammonium cycling and single-cell ammonium assimilation in marine plankton communities. *The ISME Journal*. https://doi.org/10.1038/s41396-019-0386-z

Kock, A., Arévalo-Martínez, D. L., Löscher, C. R., & Bange, H. W. (2016). Extreme $N_2O$ accumulation in the coastal oxygen minimum zone off Peru. *Biogeosciences*, *13*(3), 827–840. https://doi.org/10.5194/bg-13-827-2016

Kondo, Y., & Moffett, J. W. (2015). Iron redox cycling and subsurface offshore transport in the eastern tropical South Pacific oxygen minimum zone. *Marine Chemistry*, *168*, 95–103. https://doi.org/10.1016/J.MARCHEM.2014.11.007

Körner, H., & Zumft, W. G. (1989). Expression of denitrification enzymes in response to the dissolved oxygen level and respiratory substrate in continuous culture of Pseudomonas stutzeri. *Applied and Environmental Microbiology*, *55*(7), 1670–1676.

Korth, F., Kock, A., Arévalo-Martínez, D. L., & Bange, H. W. (2019). Hydroxylamine as a Potential Indicator of Nitrification in the Open Ocean. *Geophysical Research Letters*, *46*(4), 2158–2166. https://doi.org/10.1029/2018GL080466

Kozlowski, J. A., Stieglmeier, M., Schleper, C., Klotz, M. G., & Stein, L. Y. (2016). Pathways and key intermediates required for obligate aerobic ammonia-dependent chemolithotrophy in bacteria and Thaumarchaeota. *The ISME Journal*, *10*(8), 1–10. https://doi.org/10.1038/ismej.2016.2

Lam, Lavik, G., Jensen, M. M., Vossenberg, J. van de, Schmid, M., Woebken, D., … Kuypers, M. M. M. (2009). Revising the nitrogen cycle in the Peruvian oxygen minimum zone. *Proceedings of the National Academy of Sciences*, *106*(12), 4752–4757.

Lancaster, K. M., Caranto, J. D., Majer, S. H., & Smith, M. A. (2018). Alternative Bioenergy : Updates to and Challenges in Nitrification Metalloenzymology. *Joule*, *2*(3), 421–441. https://doi.org/10.1016/j.joule.2018.01.018

Landolfi, A., Somes, C. J., Koeve, W., Zamora, L. M., & Oschlies, A. (2017). Oceanic nitrogen cycling and $N_2O$ flux perturbations in the Anthropocene. *Global Biogeochemical Cycles*, *31*(8), 1236–1255. https://doi.org/10.1002/2017GB005633

Larsen, M., Lehner, P., Borisov, S. M., Klimant, I., Fischer, J. P., Stewart, F. J., … Glud, R. N. (2016). In situ quantification of ultra-low $O_2$ concentrations in oxygen minimum zones: Application of novel optodes. *Limnology and Oceanography: Methods*, *14*(12), 784–800. https://doi.org/10.1002/lom3.10126

Legendre, P., & Legendre, L. (2012). *Numerical ecology*. New York, NY, USA: Elsevier.

Liu, Z., Stewart, G., Kirk Cochran, J., Lee, C., Armstrong, R. A., Hirschberg, D. J., … Miquel, J.-C. (2005). Why do POC concentrations measured using Niskin bottle collections sometimes differ from those using in-situ pumps? *Deep Sea Research Part I: Oceanographic Research Papers*, *52*(7), 1324–1344. https://doi.org/10.1016/J.DSR.2005.02.005

Löscher, C. R., Kock, A., Könneke, M., LaRoche, J., Bange, H. W., & Schmitz, R. A. (2012). Production of

Formatiert: Englisch (USA)

Formatiert: Englisch (Großbritannien)

Formatiert: Englisch (Großbritannien)

oceanic nitrous oxide by ammonia-oxidizing archaea. *Biogeosciences*, *9*(7), 2419–2429. https://doi.org/10.5194/bg-9-2419-2012

Löscher, Carolin R., Bange, H. W., Schmitz, R. A., Callbeck, C. M., Engel, A., Hauss, H., … Wagner, H. (2016). Water column biogeochemistry of oxygen minimum zones in the eastern tropical North Atlantic and eastern tropical South Pacific oceans. *Biogeosciences*, *13*(12), 3585–3606. https://doi.org/10.5194/bg-13-3585-2016

Lutterbeck, H. E., Arévalo-Martínez, D. L., Löscher, C. R., & Bange, H. W. (2018). Nitric oxide (NO) in the oxygen minimum zone off Peru. *Deep Sea Research Part II: Topical Studies in Oceanography*, (xxxx), 0–1. https://doi.org/10.1016/j.dsr2.2017.12.023

Martin, J. H., Knauer, G. A., Karl, D. M., & Broenkow, W. W. (1987). VERTEX: carbon cycling in the northeast Pacific. *Deep Sea Research Part A. Oceanographic Research Papers*, *34*(2), 267–285. https://doi.org/10.1016/0198-0149(87)90086-0

Martinez-Rey, J., Bopp, L., Gehlen, M., Tagliabue, A., & Gruber, N. (2015). Projections of oceanic $N_2O$ emissions in the 21st century using the IPSL Earth system model. *Biogeosciences*, *12*(13), 4133–4148. https://doi.org/10.5194/bg-12-4133-2015

McIlvin, M. R., & Altabet, M. A. (2005). Chemical Conversion of Nitrate and Nitrite to Nitrous Oxide for Nitrogen and Oxygen Isotopic Analysis in Freshwater and Seawater. *Analytical Chemistry*, *77*(17), 5589–5595.

McKenney, D. J., Drury, C. F., Findlay, W. I., Mutus, B., McDonnell, T., & Gajda, C. (1994). Kinetics of denitrification by Pseudomonas fluorescens: Oxygen effects. *Soil Biology and Biochemistry*, *26*(7), 901–908.

Messié, M., & Chavez, F. P. (2015). Seasonal regulation of primary production in eastern boundary upwelling systems. *Progress in Oceanography*, *134*, 1–18. https://doi.org/10.1016/j.pocean.2014.10.011

Mincer, T. J., Church, M. J., Taylor, L. T., Preston, C., Karl, D. M., & DeLong, E. F. (2007). Quantitative distribution of presumptive archaeal and bacterial nitrifiers in Monterey Bay and the North Pacific Subtropical Gyre. *Environmental Microbiology*, *9*(5), 1162–1175. https://doi.org/10.1111/j.1462-2920.2007.01239.x

Murdock, S. A., & Juniper, S. K. (2017). Capturing Compositional Variation in Denitrifying Communities: a Multiple- Primer Approach That Includes Epsilonproteobacteria. *Applied and Environmental Microbiology*, *83*(6), 1–16.

Newell, S. E., Babbin, A. R., Jayakumar, A., & Ward, B. B. (2011). Ammonia oxidation rates and nitrification in the Arabian Sea. *Global Biogeochemical Cycles*, *25*(4), 1–10. https://doi.org/10.1029/2010gb003940

Nicholls, J. C., Davies, C. A., & Trimmer, M. (2007). High-resolution profiles and nitrogen isotope tracing reveal a dominant source of nitrous oxide and multiple pathways of nitrogen gas formation in the central Arabian Sea. *Limnology and Oceanography*, *52*(1), 156–168. https://doi.org/10.4319/lo.2007.52.1.0156

Oksanen, J., Blanchet, F. G., Friendly, M., Kindt, R., Legendre, P., Mcglinn, D., … Maintainer, H. W. (2019). Package "vegan" Title Community Ecology Package. *Community Ecology Package*, *2*(9), 1–297.

Peng, X., Jayakumar, A., & Ward, B. B. (2013). Community composition of ammonia-oxidizing archaea from surface and anoxic depths of oceanic oxygen minimum zones. *Frontiers in Microbiology*, *4*(JUL), 1–12. https://doi.org/10.3389/fmicb.2013.00177

Pietri, A., Testor, P., Echevin, V., Chaigneau, A., Mortier, L., Eldin, G., … Grados, C. (2013). Finescale Vertical Structure of the Upwelling System off Southern Peru as Observed from Glider Data. *Journal of Physical Oceanography*, *43*(3), 631–646. https://doi.org/10.1175/JPO-D-12-035.1

Qin, W., Meinhardt, K. A., Moffett, J. W., Devol, A. H., Armbrust, E. V., Ingalls, A. E., & Stahl, D. A. (2017). Influence of Oxygen Availability on the Activities of Ammonia-oxidizing Archaea. *Environmental Microbiology Reports*. https://doi.org/10.1111/1758-2229.12525

Ravishankara, A. R., Daniel, J. S., & Portmann, R. W. (2009). Nitrous oxide ($N_2O$): the dominant ozone-depleting substance emitted in the 21st century. *Science (New York, N.Y.)*, *326*(5949), 123–125. https://doi.org/10.1126/science.1176985

Richards, T. A., Jones, M. D. M., Leonard, G., & Bass, D. (2012). Marine Fungi: Their Ecology and Molecular Diversity. *Annual Review of Marine Science*, *4*(1), 495–522. https://doi.org/10.1146/annurev-marine-120710-100802

Ryabenko, E., Kock, a., Bange, H. W., Altabet, M. a., & Wallace, D. W. R. (2011). Contrasting biogeochemistry of nitrogen in the Atlantic and Pacific oxygen minimum zones. *Biogeosciences Discussions*, *8*(4), 8001–8039. https://doi.org/10.5194/bgd-8-8001-2011

Santoro, A. E., Buchwald, C., McIlvin, M. R., & Casciotti, K. L. (2011). Isotopic Signature of $N_2O$ Produced by Marine Ammonia-Oxidizing Archaea. *Science*, *333*, 1282–1285. https://doi.org/10.1126/science.1208239

Santoro, A. E., & Casciotti, K. L. (2011). Enrichment and characterization of ammonia-oxidizing archaea from the open ocean: phylogeny, physiology and stable isotope fractionation. *The ISME Journal*, *5*(11), 1796–1808. https://doi.org/10.1038/ismej.2011.58

Santoro, A. E., Casciotti, K. L., & Francis, C. A. (2010). Activity, abundance and diversity of nitrifying archaea

Formatiert: Englisch (USA)

Formatiert: Schriftart: (Standard) Calibri

and bacteria in the central California Current. *Environmental Microbiology*, *12*(7), 1989–2006. https://doi.org/10.1111/j.1462-2920.2010.02205.x

Santoro, A. E., Dupont, C. L., Richter, R. A., Craig, M. T., Carini, P., McIlvin, M. R., … Saito, M. A. (2015). Genomic and proteomic characterization of "Candidatus Nitrosopelagicus brevis": An ammonia-oxidizing archaeon from the open ocean. *Proceedings of the National Academy of Sciences*, *112*(4), 1173–1178. https://doi.org/10.1073/PNAS.1416223112

Schmidtko, S., Stramma, L., & Visbeck, M. (2017). Decline in global oceanic oxygen content during the past five decades. *Nature*, *542*(7641), 335–339. https://doi.org/10.1038/nature21399

Schunck, H., Lavik, G., Desai, D. K., Großkopf, T., Kalvelage, T., Löscher, C. R., … Laroche, J. (2013). Giant hydrogen sulfide plume in the oxygen minimum zone off Peru supports chemolithoautotrophy. *PloS One*, *8*(8), e68661. https://doi.org/10.1371/journal.pone.0068661

Segata, N., Izard, J., Waldron, L., Gevers, D., Miropolsky, L., Garrett, W. S., & Huttenhower, C. (2011). Metagenomic biomarker discovery and explanation. *Genome Biology*, *12*(6), R60. https://doi.org/10.1186/gb-2011-12-6-r60

Shoun, H., Fushinobu, S., Jiang, L., Kim, S. W., & Wakagi, T. (2012). Fungal denitrification and nitric oxide reductase cytochrome P450nor. *Philosophical Transactions of the Royal Society B: Biological Sciences*, *367*(1593), 1186–1194. https://doi.org/10.1098/rstb.2011.0335

Sigman, D. M., Casciotti, K. L., Andreani, M., Barford, C., Galanter, M., & Böhlke, J. K. (2001). A Bacterial Method for the Nitrogen Isotopic Analysis of Nitrate in Seawater and Freshwater. *Analytical Chemistry*, *73*, 4145–4153.

Stein, L. Y. (2019). Insights into the physiology of ammonia-oxidizing microorganisms. *Current Opinion in Chemical Biology*, *49*, 9–15. https://doi.org/10.1016/J.CBPA.2018.09.003

Stewart, F. J., Ulloa, O., & Delong, E. F. (2011). Microbial metatranscriptomics in a permanent marine oxygen minimum zone. *Environmental Microbiology*, *14*(1), 23–40. https://doi.org/10.1111/j.1462-2920.2010.02400.x

Stewart, F. J., Dalsgaard, T., Young, C. R., Thamdrup, B., Revsbech, N. P., Ulloa, O., … Delong, E. F. (2012). Experimental incubations elicit profound changes in community transcription in OMZ bacterioplankton. *PloS One*, *7*(5), e37118. https://doi.org/10.1371/journal.pone.0037118

Stieglmeier, M., Mooshammer, M., Kitzler, B., Wanek, W., Zechmeister-Boltenstern, S., Richter, A., & Schleper, C. (2014). Aerobic nitrous oxide production through N-nitrosating hybrid formation in ammonia-oxidizing archaea. *The ISME Journal*, *8*(5), 1135–1146. https://doi.org/10.1038/ismej.2013.220

Stramma, L., Bange, H. W., Czeschel, R., Lorenzo, A., & Frank, M. (2013). On the role of mesoscale eddies for the biological productivity and biogeochemistry in the eastern tropical Pacific Ocean off Peru. *Biogeosciences*, *10*(11), 7293–7306. https://doi.org/10.5194/bg-10-7293-2013

Stramma, Lothar, Johnson, G. C., Sprintall, J., & Mohrholz, V. (2008). Expanding Oxygen-Minimum Zones in the Tropical Oceans. *Science*, *320*, 655–659.

Sun, X., Ji, Q., Jayakumar, A., & Ward, B. B. (2017). Dependence of nitrite oxidation on nitrite and oxygen in low-oxygen seawater. *Geophysical Research Letters*, *44*(15), 7883–7891. https://doi.org/10.1002/2017GL074355

Swan, B. K., Martinez-Garcia, M., Preston, C. M., Sczyrba, A., Woyke, T., Lamy, D., … Stepanauskas, R. (2011). Potential for chemolithoautotrophy among ubiquitous bacteria lineages in the dark ocean. *Science*, *333*(6047), 1296–1300. https://doi.org/10.1126/science.1203690

Thamdrup, B., & Dalsgaard, T. (2002). Production of $N_2$ through Anaerobic Ammonium Oxidation Coupled to Nitrate Reduction in Marine Sediments. *Applied and Environmental Microbiology*, *68*(3), 1312–1318. https://doi.org/10.1128/aem.68.3.1312-1318.2002

Thomsen, J. K., Geest, T., & Cox, R. P. (1994). Mass Spectrometric Studies of the Effect of pH on the Accumulation of Intermediates in Denitrification by Paracoccus denitrificans. *Applied and Environmental Microbiology*, *60*(2), 536–541.

Tiano, L., Garcia-Robledo, E., Dalsgaard, T., Devol, A. H., Ward, B. B., Ulloa, O., … Peter Revsbech, N. (2014). Oxygen distribution and aerobic respiration in the north and south eastern tropical Pacific oxygen minimum zones. *Deep-Sea Research Part I: Oceanographic Research Papers*, *94*, 173–183. https://doi.org/10.1016/j.dsr.2014.10.001

Torres-Beltrán, M., Mueller, A., Scofield, M., Pachiadaki, M. G., Taylor, C., Tyshchenko, K., … Hallam, S. J. (2019). Sampling and processing methods impact microbial community structure and potential activity in a seasonally anoxic fjord: Saanich inlet, British Columbia. *Frontiers in Marine Science*, *6*(MAR), 1–16. https://doi.org/10.3389/fmars.2019.00132

Trimmer, M., Chronopoulou, P.-M., Maanoja, S. T., Upstill-Goddard, R. C., Kitidis, V., & Purdy, K. J. (2016). Nitrous oxide as a function of oxygen and archaeal gene abundance in the North Pacific. *Nature Communications*, *7*, 13451. https://doi.org/10.1038/ncomms13451

Vajrala, N., Martens-Habbena, W., Sayavedra-Soto, L. A., Schauer, A., Bottomley, P. J., Stahl, D. A., & Arp, D. J. (2013). Hydroxylamine as an intermediate in ammonia oxidation by globally abundant marine archaea. *Proceedings of the National Academy of Sciences*, *110*(3), 1006–1011.

Formatiert: Deutsch (Schweiz)

Formatiert: Englisch (Großbritannien)

Formatiert: Englisch (Großbritannien)

Formatiert: Deutsch (Schweiz)

https://doi.org/10.1073/pnas.1214272110
Van Der Star, W. R. L., Van De Graaf, M. J., Kartal, B., Picioreanu, C., Jetten, M. S. M., & Van Loosdrecht, M. C. M. (2008). Response of anaerobic ammonium-oxidizing bacteria to hydroxylamine. *Applied and Environmental Microbiology*, *74*(14), 4417–4426. https://doi.org/10.1128/AEM.00042-08
Wankel, S. D., Ziebis, W., Buchwald, C., Charoenpong, C., De Beer, Di., Dentinger, J., … Zengler, K. (2017). Evidence for fungal and chemodenitrification based $N_2O$ flux from nitrogen impacted coastal sediments. *Nature Communications*, *8*, 1–11. https://doi.org/10.1038/ncomms15595
Ward, B. B., Tuit, C. B., Jayakumar, A., Rich, J. J., Moffett, J., & Naqvi, S. W. a. (2008). Organic carbon, and not copper, controls denitrification in oxygen minimum zones of the ocean. *Deep-Sea Research Part I: Oceanographic Research Papers*, *55*(12), 1672–1683. https://doi.org/10.1016/j.dsr.2008.07.005
Weier, K. L., Doran, J. W., Power, J. F., & Walters, D. T. (1993). Denitrification and the Dinitrogen/Nitrous Oxide Ratio as Affected by Soil Water, Available Carbon, and Nitrate. *Soil Science Society of America Journal*, *57*(1), 66. https://doi.org/10.2136/sssaj1993.03615995005700010013x
Weigand, M. A., Foriel, J., Barnett, B., Oleynik, S., & Sigman, D. M. (2016). Updates to instrumentation and protocols for isotopic analysis of nitrate by the denitrifier method. *Rapid Communications in Mass Spectrometry*, *30*(12), 1365–1383. https://doi.org/10.1002/rcm.7570
Wright, J. J., Konwar, K. M., & Hallam, S. J. (2012). Microbial ecology of expanding oxygen minimum zones. *Nature Reviews Microbiology*, *10*(6), 381–394. https://doi.org/10.1038/nrmicro2778
Wuchter, C., Abbas, B., Coolen, M. J. L., Herfort, L., van Bleijswijk, J., Timmers, P., … Sinninghe Damsté, J. S. (2006). Archaeal nitrification in the ocean. *Proceedings of the National Academy of Sciences of the United States of America*, *103*(33), 12317–12322. https://doi.org/10.1073/pnas.0600756103
Yang, S., Gruber, N., Long, M. C., & Vogt, M. (2017). High ENSO driven variability of denitrification and suboxia in the Eastern Pacific Ocean. *Global Biogeochemical Cycles* 31(10) 1470-1487. https://doi.org/10.1002/2016GB005596
Yoshida, N. (1988). $^{15}N$-depleted $N_2O$ as a product of nitrification. *Nature*, *335*(6190), 528–529. https://doi.org/10.1038/335528a0
Zhou, Z., Takaya, N., Sakairi, M. A. C., & Shoun, H. (2001). Oxygen requirement for denitrification by the fungus Fusarium oxysporum. *Archives of Microbiology*, *175*(1), 19–25. https://doi.org/10.1007/s002030000231
Zhu-Barker, X., Cavazos, A. R., Ostrom, N. E., Horwath, W. R., & Glass, J. B. (2015). The importance of abiotic reactions for nitrous oxide production. *Biogeochemistry*, *126*(3), 251–267. https://doi.org/10.1007/s10533-015-0166-4
Zumft, W. G. (1997). Cell biology and molecular basis of denitrification. *Microbiology and Molecular Biology Reviews*, *61*(4), 533–616.

**Formatiert:** Englisch (Großbritannien)

**Tables**

**Table 1:** Overview of characteristics of samples. bd - below detection limit of Winkler method and seabird sensor (2 µmol $L^{-1}$), x - analysis includes qPCR and microarray with qPCR products, x* - only qPCR, no microarray

| *ID* | *Stat #* | *Coordinates/ position* | *bottom depth (m)* | *sampling depth (m)* | *water column feature* | *Tem. (°C)* | *Sal.* | *$O_2$ (µM) seabird* | *NO3- (µM)* | *NO2- (µM)* | *NH4+ (µM)* | *$^{15}N$ incubation* | *Tracer added* | *nirS* | *amoA* |
|---|---|---|---|---|---|---|---|---|---|---|---|---|---|---|---|
| S2 | 882 | 10.95W 78.56N | 1075 | 352 | anoxic core | 11.4 | 34.82 | bd | 32.51 | 0.68 | 0.01 | depth profile | $NH_4^+$, $NO_2^-$, $NO_3^-$ | x | x |
| S1 | 882 | | 1075 | 299 | below interface | 12.1 | 34.86 | bd | 30.21 | 0.52 | 0.00 | depth profile | $NH_4^+$, $NO_2^-$, $NO_3^-$ | x | x |
| S3 | 882 | | 1075 | 259 | oxic-anoxic interface | 13.0 | 34.92 | bd | 29.39 | 1.63 | 0.01 | depth profile | $NH_4^+$, $NO_2^-$, $NO_3^-$ | x | x |
| S4 | 882 | | 1075 | 219 | above interface | 13.7 | 34.96 | 6.06 | 31.65 | 0.13 | 0.01 | depth profile | $NH_4^+$, $NO_2^-$, $NO_3^-$ | x | x |
| S5 | 882 | | 1075 | 74 | oxycline | 15.4 | 35.05 | 15.04 | 30.00 | 0.02 | 0.00 | depth profile | $NH_4^+$, $NO_2^-$, $NO_3^-$ | x | x |
| S6 | 883 | 10.78W 78.27N | 305 | 305 | anoxic core | 12.2 | 34.87 | bd | 27.27 | 1.72 | 0 | depth profile | $NH_4^+$, $NO_2^-$, $NO_3^-$ | x | x |
| S7 | 883 | | 305 | 268 | below interface | 12.8 | 34.91 | bd | 26.61 | 2.05 | 0 | depth profile | $NH_4^+$, $NO_2^-$, $NO_3^-$ | x | x |
| S8 | 883 | | 305 | 250 | oxic-anoxic interface | 13.1 | 34.92 | bd | 28.06 | 1.66 | 0 | depth profile | $NH_4^+$, $NO_2^-$, $NO_3^-$ | x | x |
| S9 | 883 | | 305 | 189 | above interface | 13.8 | 34.97 | bd | 30.47 | 0.00 | 0 | depth profile | $NH_4^+$, $NO_2^-$, $NO_3^-$ | x | x |
| S10 | 883 | | 305 | 28 | oxycline | 16.4 | 35.09 | 30.06 | 26.81 | 0.04 | 0 | depth profile | $NH_4^+$, $NO_2^-$, $NO_3^-$ | x | x |
| S19 | 892 | 12.41W 77.81N / | 1099 | 144 | below oxic-anoxic interface | 13.51 | 34.91 | bd | 19.01 | 3.69 | 0.13 | $O_2$ manipulation | $NH_4^+$, $NO_2^-$, $NO_3^-$ | x | x |
| S11 | 894 | 12.32W 77.62N/ | 502 | 120 | oxic-anoxic interface | 14.21 | 34.98 | bd | 28.92 | 0.01 | 0.00 | $O_2$ manipulation | $NH_4^+$, $NO_2^-$, $NO_3^-$ | x | x |
| S12 | 904 | 13.99W 76.66N | 560 | 179 | below interface | 13.46 | 34.94 | bd | 25.54 | 1.25 | 0.00 | POM addition (from 898) | $NO_2^-$, $NO_3^-$ | x | x* |
| S13 | 904 | | 560 | 124 | oxic-anoxic interface | 14.40 | 35.00 | bd | 27.57 | 0.09 | 0.00 | POM addition (from 898) | $NO_2^-$, $NO_3^-$ | x | x* |
| S14 | 906 | 14.28W 77.17N | 4761 | 149 | below interface | 13.70 | 34.96 | bd | 25.80 | 0.90 | 0.04 | POM addition (from 904) | $NO_2^-$, $NO_3^-$ | x | x* |
| S20 | 906 | | 4761 | 92 | oxic-anoxic interface | 14.50 | 35.00 | bd | 20.03 | 3.87 | 0.33 | POM addition (from 904) | $NO_2^-$, $NO_3^-$ | x | x* |
| S15 | 907 | 15.43W 75.43N | 800 | 130 | below interface | 14.21 | 34.98 | bd | 14.63 | 5.23 | 0.03 | POM addition (from 904) | $NO_2^-$, $NO_3^-$ | x | x |
| S16 | 907 | | 800 | 9.9 | surface | 17.82 | 35.13 | 208.3 | 16.09 | 0.99 | 0.16 | POM addition (from 904) | $NO_2^-$, $NO_3^-$ | x | x |
| S17 | 912 | 15.86W 76.11N | 3680 | 90 | below interface | 15.09 | 35.03 | bd | 19.38 | 2.85 | 0.03 | POM addition (from 906) | $NO_2^-$, $NO_3^-$ | x | x |
| S18 | 912 | | 3680 | 5 | surface | 18.05 | 35.18 | 206.0 | 8.31 | 0.47 | 0.12 | POM addition (from 906) | $NO_2^-$, $NO_3^-$ | x | x |
| S21 | 917 | 14.78W 78.04N/ | 4128 | 140 | Interface | 13.1 | 34.86 | bd | 17.3 | 3.9 | 0.0 | POM addition (from 906) | $NO_2^-$, $NO_3^-$ | x | x* |

**Table 2**: Quality (N/C), quantity (Addition µmol $L^{-1}$) and origin (station and depth) of added, autoclaved and non-autoclaved particulate organic matter (POM) and increase in $NH_4^+$ concentration after autoclaving.

| POM | Feature | Station | Depth (m) | Addition (µmol $L^{-1}$) | N/C of autoclaved POM | N/C of non-autoclaved POM | $NH_4^+$ (µM) after autoclaving |
|---|---|---|---|---|---|---|---|
| POM 1 | mixed layer depth | 898 | 60 | 0.55 | 0.10 | 0.15 | 0.7 |
| | | 904 | 20 | 0.17 | 0.09 | 0.17 | 1.56 |
| | | 906 | 50 | 0.48 | 0.07 | 0.11 | 0.57 |
| POM 2 | oxycline | 898 | 100 | 1.37 | 0.06 | 0.13 | 0.85 |
| | | 904 | 50 | 0.38 | 0.09 | 0.12 | 0.46 |
| | | 906 | 100 | 0.44 | 0.08 | 0.10 | 0.55 |
| POM 3 | anoxic zone | 898 | 300 | 0.43 | 0.09 | 0.10 | 0.15 |
| | | 904 | 150 | 0.19 | 0.10 | 0.10 | 0.20 |

1170

**Figure Legends:**

**Figure 1**: Study area with the distribution of near-surface chlorophyll concentrations (monthly averaged for June 2017) from MODIS satellite obtained from the NASA Ocean Color Web site at 4-km resolution. Study site showing transect and station numbers, in the Eastern Tropical South Pacific during cruise M138.

**Figure 2:** Depth profiles of $O_2$, nutrients and $N_2O$ in the upper 400 m for all stations. Panel numbers 1 - 4) refer to the transect numbers.

**Figure 3:** (I) Profiles of AO, (a, e, I), $N_2O$ production rates from $NH_4^+$ (b, f, j), archaeal *amoA* gene (c, g, k) and transcript copy numbers $mL^{-1}$ (d, h, l). (II) Profiles of $NO_3^-$ ~~nitrate~~ reduction rates (a, f, k, o), $N_2O$ production rates from $NO_3^-$ (b, g, l, p) and $NO_2^-$ (c, h, m, q) and *nirS* gene (d, I, n, r) and transcript copy numbers $mL^{-1}$ (e, j, m, s). In (I) and (II), the panel numbers 1 – 4 correspond to transect numbers. Negative values on the y-axis represent shallower, oxic depths and the positive values represent deeper, anoxic depth (0 = interface). Shaded area indicates the anoxic zone. Note different scale for $N_2O$ production rates.

**Figure 4**: $O_2$ dependence of $N_2O$ production rates from $NH_4^+$ (a, d), $NO_2^-$ (b, e) and $NO_3^-$ (c, f). Upper panel (a-c) is $N_2O$ production along natural $O_2$ gradient from all stations. Figure 4 (b, c) are additionally zoomed ~~up~~in to oxygen concentrations below 5µmol $L^{-1}$. Lower panel (d-f) is $N_2O$ production in manipulated $O_2$ experiments with water from oxic - anoxic interface from slope station 892 (S11, 0 µmol $L^{-1}$ $O_2$, 145m) and shelf station 894 (S19, 0 µmol $L^{-1}$, 120 m). Note different scale for $N_2O$ production rates from $NH_4^+$. Vertical error bars represent ± Standard error (n = 5 per time course). Horizontal error bars represent ± Standard error of measured $O_2$ over the time of incubations (n = 6).

**Formatiert:** Hochgestellt

**Figure 5**: $O_2$ dependency of hybrid $N_2O$ formation from $NH_4^+$ (a, c) and $NO_2^-$ (b ,d) along the natural $O_2$ gradient (a, b) and for the $O_2$ manipulations (c, d) from sample S11 (0 µmol $L^{-1}$ $O_2$, 145m) and S19 (894, 0 µmol $L^{-1}$, 120 m)

**Figure 6**: Yields (%) of $N_2O$ production during $NH_4^+$ oxidation (a, c) and during $NO_3^-$ ~~nitrate~~ reduction (b, d) along the natural $O_2$ gradient (a, b) and for the $O_2$ manipulations (c, d) from sample S11 (892, 0 µmol $L^{-1}$ $O_2$, 145m) and S19 (894, 0 µmol $L^{-1}$, 120 m). Error bars present ± SD calculated as error propagation.

**Figure 7**: Bar plots of $N_2O$ production after additions of autoclaved suspended and sinking particles >50 µm (See Table 2). POM1 = mixed layer depth, POM2 = oxycline, POM3 = ODZ. Error Bars represent ± SE of linear regression. * indicates significant difference to control rate ($p < 0.05$)

**Figure 8:** Stacked bar plot of community composition of AOA *amoA* archetypes (a, b) and *nirS* archetypes (c, d). Only archetypes over 1% contribution are shown. (a, c) total community composition (DNA). (b, d) active community composition (cDNA).

**Figure 9**: Scheme illustrating the possible reactions for hybrid $N_2O$ formation. The ellipse represents an AOA cell.

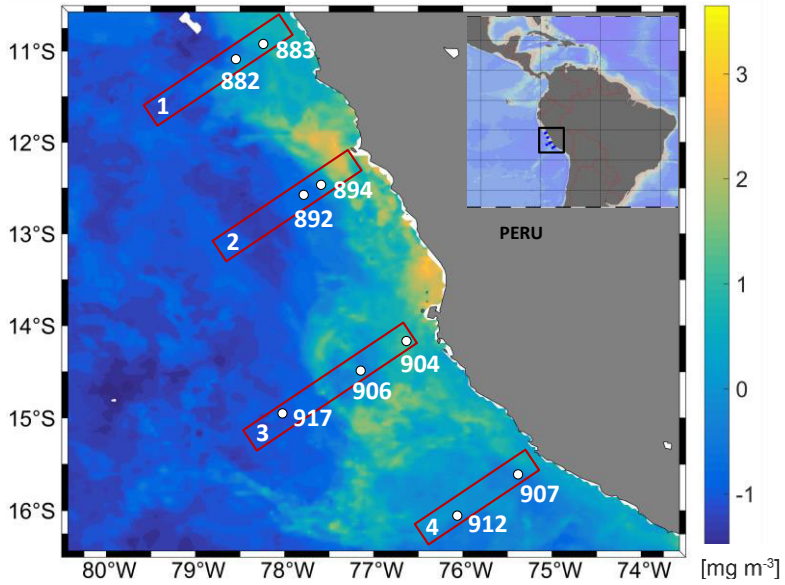
11°S
12°S
13°S
14°S
15°S
16°S
80°W
79°W
78°W
77°W
76°W
75°W
74°W
883
882
1
894
892
2
904
906
917
3
907
912
4
PERU
3
2
1
0
-1
[mg m-3]

**Figure 1**

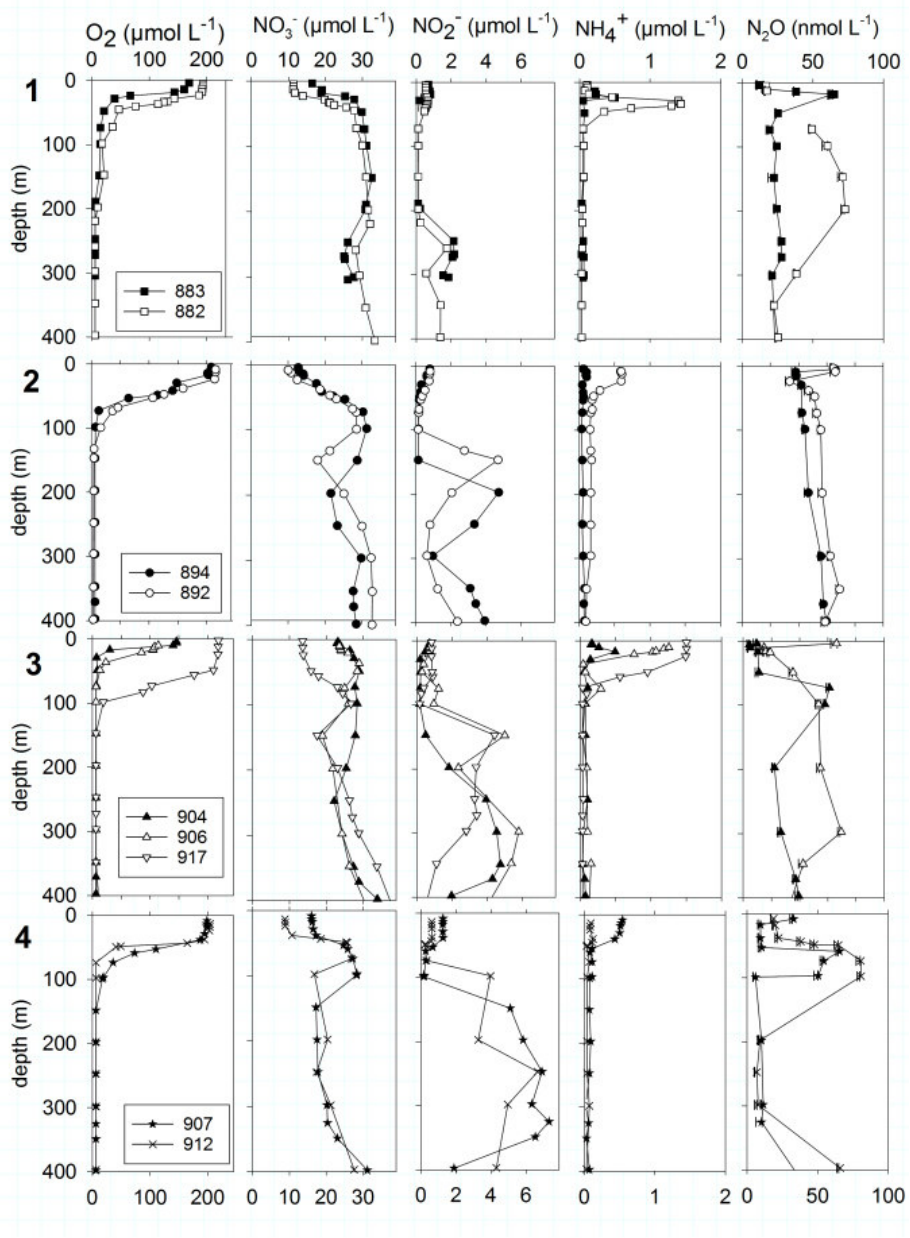


1210

**Figure 2**

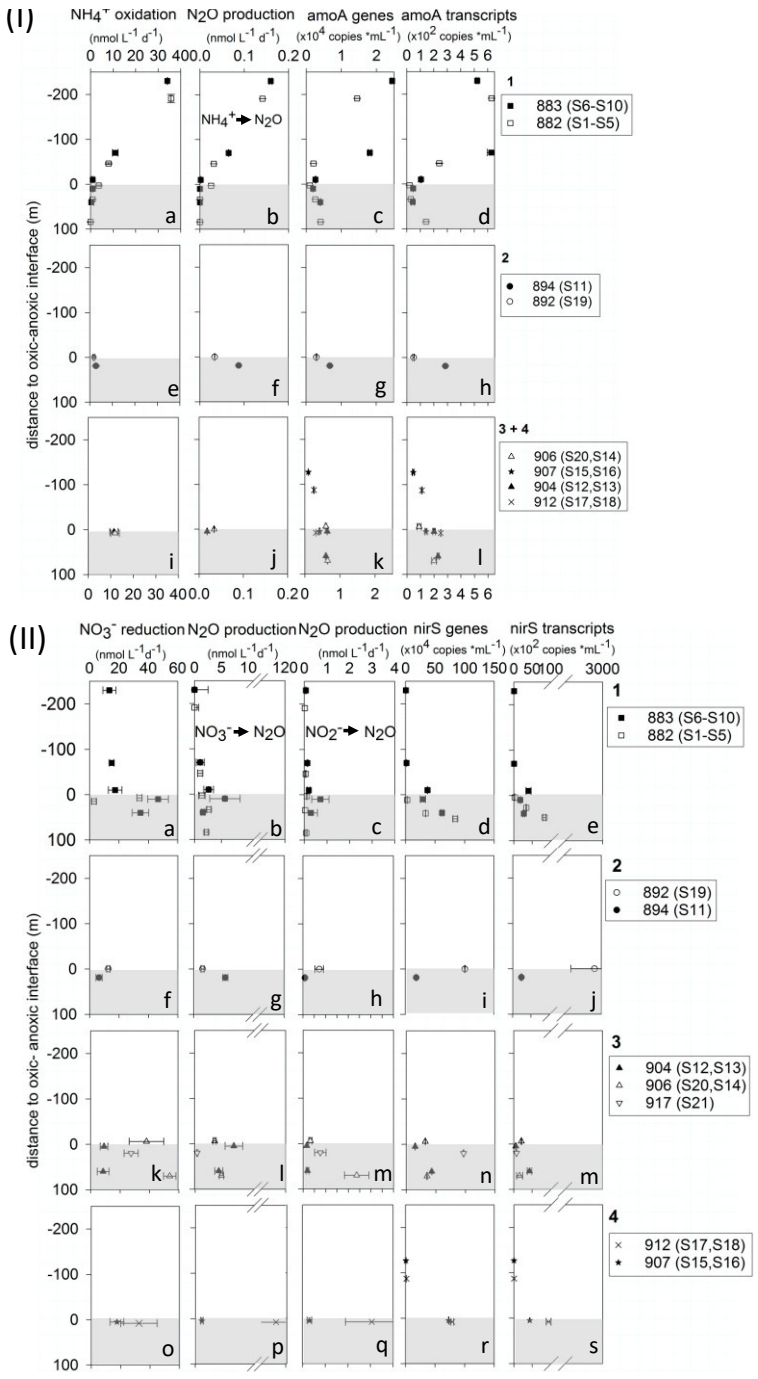
(I)
NH4+ oxidation
N2O production
amoA genes
amoA transcripts
(nmol L-1 d-1)
(nmol L-1 d-1)
(x10^4 copies *mL-1)
(x10^2 copies *mL-1)
0 10 20 30 40
0.0 0.1 0.2
0 1 2
0 1 2 3 4 5 6
NH4+ → N2O
distance to oxic-anoxic interface (m)
-200
-100
0
100
a
b
c
d
e
f
g
h
i
j
k
l
1
883 (S6-S10)
882 (S1-S5)
2
894 (S11)
892 (S19)
3 + 4
906 (S20,S14)
907 (S15,S16)
904 (S12,S13)
912 (S17,S18)
(II)
NO3- reduction
N2O production
N2O production
nirS genes
nirS transcripts
(nmol L-1 d-1)
(nmol L-1 d-1)
(nmol L-1 d-1)
(x10^4 copies *mL-1)
(x10^2 copies *mL-1)
0 20 40 60
0 5 10 120
0 1 2 3 40
0 50 100 150
0 50 100 3000
NO3- → N2O
NO2- → N2O
distance to oxic- anoxic interface (m)
-200
-100
0
100
a
b
c
d
e
f
g
h
i
j
k
l
m
n
m
o
p
q
r
s
1
883 (S6-S10)
882 (S1-S5)
2
892 (S19)
894 (S11)
3
904 (S12,S13)
906 (S20,S14)
917 (S21)
4
912 (S17,S18)
907 (S15,S16)

**Figure 3**

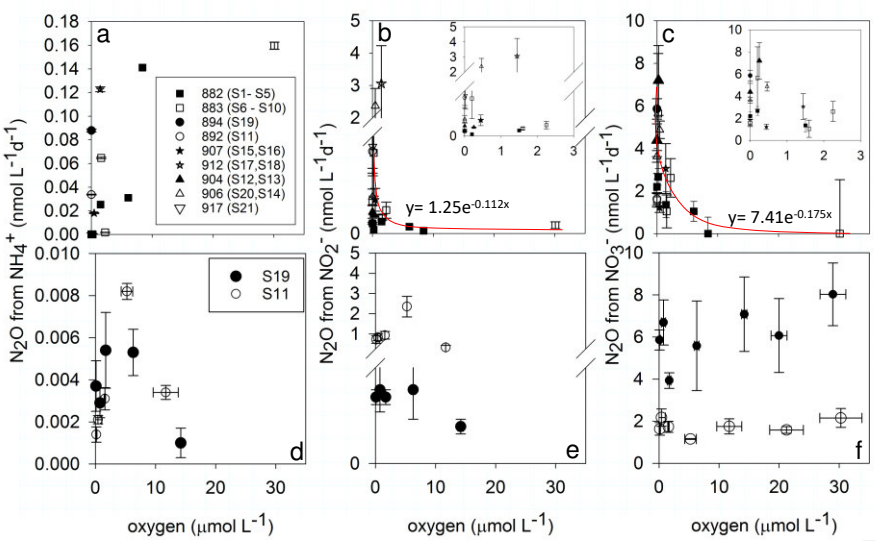


1215 **Figure 4**

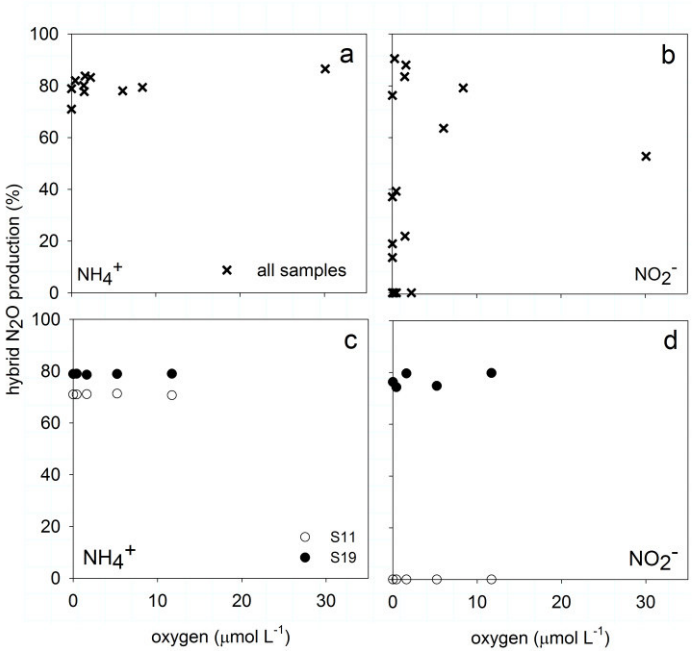
a
b
c
d
all samples
S11
S19
hybrid N2O production (%)
oxygen (µmol L-1)
oxygen (µmol L-1)

**Figure 5**

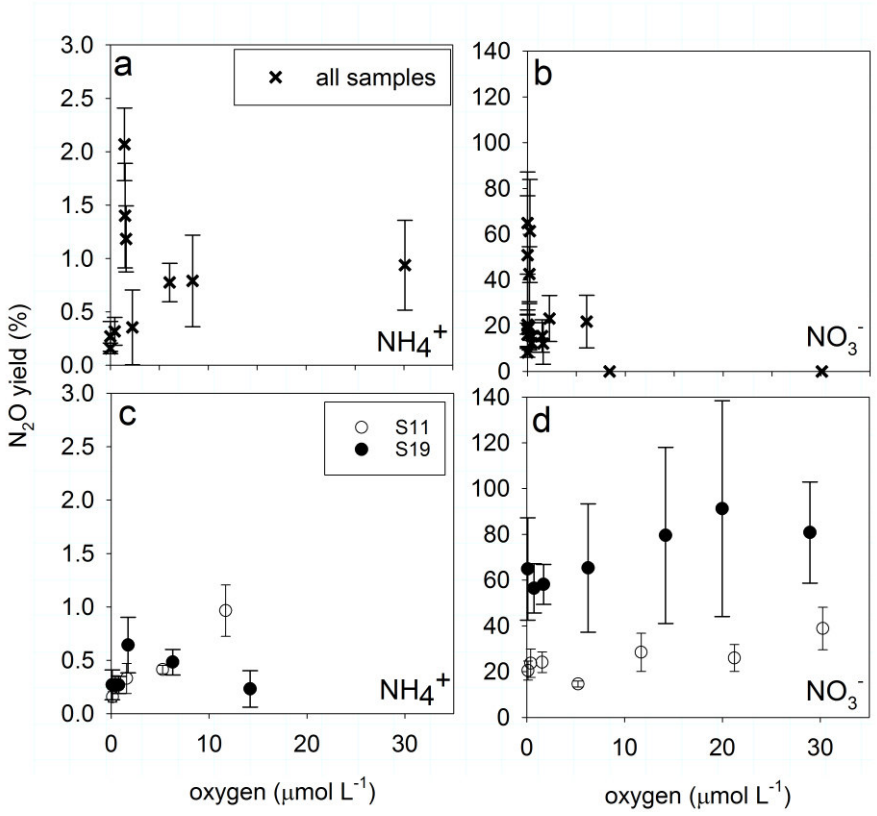


1220

**Figure 6**

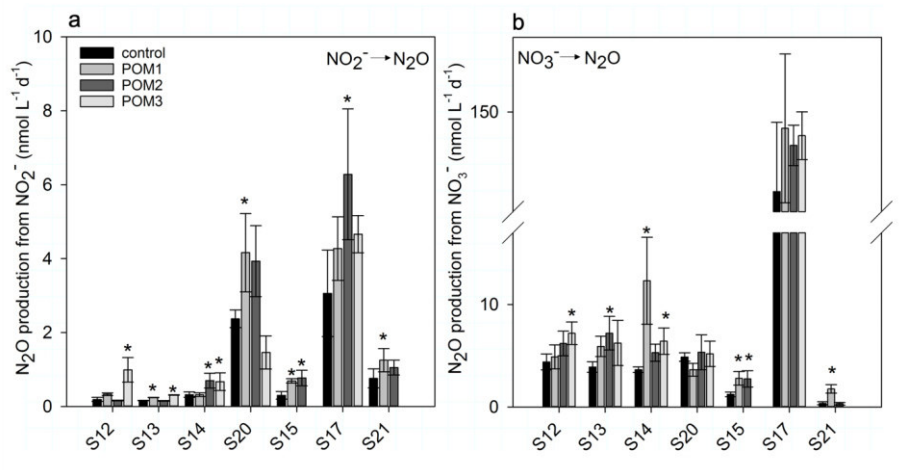


1225

**Figure 7**

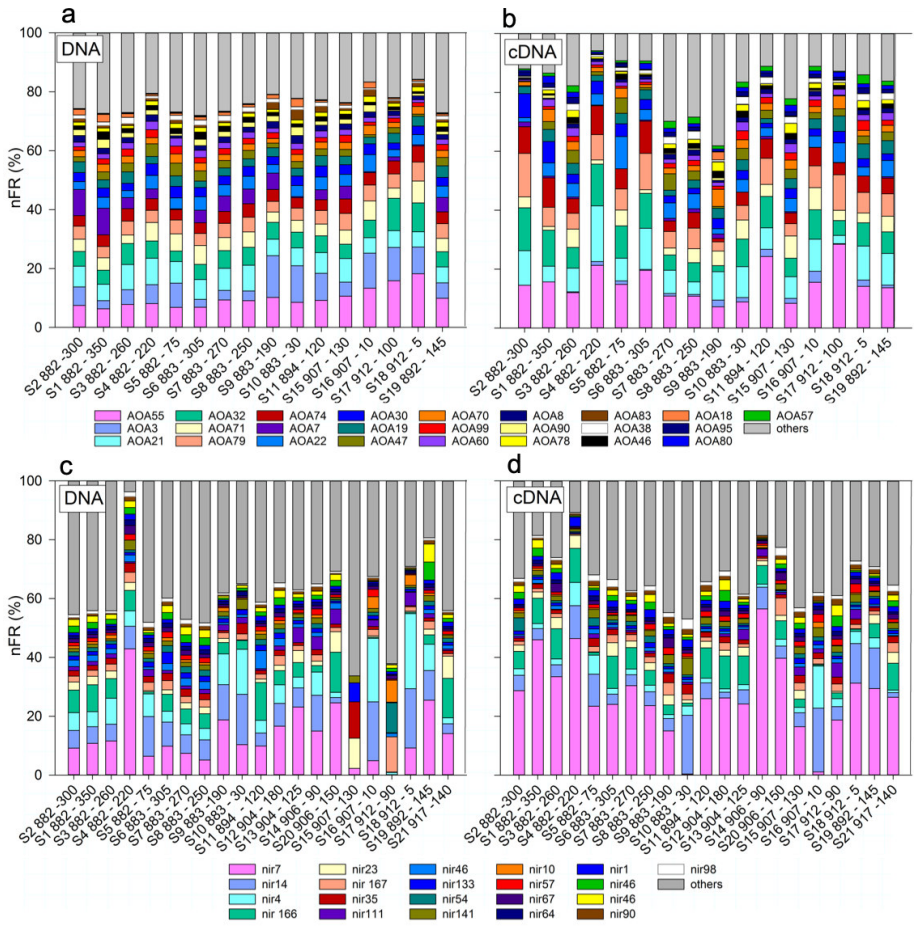


**Figure 8**

1230

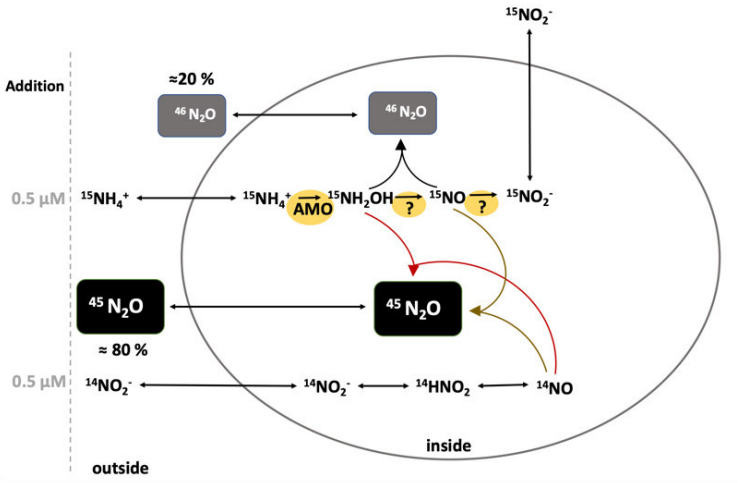


**Figure 9**

1235

**Supplements**

# Regulation of nitrous oxide production in low oxygen waters off the coast of Peru

Claudia Frey[1,2,*], Hermann W. Bange[2], Eric P. Achterberg[3], Amal Jayakumar[1], Carolin R. Löscher[4], Damian L. Arévalo-Martínez[2], Elizabeth León-Palmero[5], Mingshuang Sun[2], Xin Sun[1], Ruifang C. Xie[3], Sergey Oleynik[1], Bess B. Ward[1]

**Table S1:** Average alpha diversities of total and active archaeal *amoA* and *nirS* communities.

| | ***nirS*** | ***amoA*** |
|---|---|---|
| **DNA** | 3.8 ± 0.4 | 3.6 ± 0.1 |
| **cDNA** | 3.4 ± 0.5 | 3.2 ± 0.3 |

**Table S2:** Overview of abundant archetypes (> 1%) that are significantly enriched in respective $O_2$ levels (Lefse analysis). $O_2$ levels were split in 3 categories: anoxic (<1 µmol $L^{-1}$ $O_2$, Seabird $O_2$ and Winkler titration detection limits), hypoxic (1 – 10 µmol $L^{-1}$ $O_2$), oxic (> 10 µmol $L^{-1}$ $O_2$).

| *amoA* | **archetype** | **anoxic** | **hypoxic** | **oxic** | *nirS* | **archetype** | **anoxic** | **hypoxic** | **oxic** |
|---|---|---|---|---|---|---|---|---|---|
| DNA | AOA3 | | | x | DNA | nir4 | | | x |
| | AOA7 | x | | | | nir14 | | | x |
| | AOA78 | | | x | | nir23 | x | | |
| | AOA83 | | | x | | nir46 | x | | |
| | | | | | | nir166 | x | | |
| cDNA | AOA3 | | | x | cDNA | nir4 | | | x |
| | AOA7 | | x | | | nir14 | | | x |
| | AOA83 | | | x | | nir23 | x | | |
| | | | | | | nir141 | | | x |
| | | | | | | nir166 | x | | |

**Table S3:** All samples with rates, standard errors, fraction label ($f_N$), yields, copy numbers $mL^{-1}$ of *nirS* and *amoA* genes and transcripts.

| sample ID | station | depth (m) | oxygen (µM) | f NH4+ | f NO2- | f NO3- | NO pro (nM/d) NH4+ | SE | Hybrid free NH4+ (nM/d) | SE | NH4 ex (nM/d) | SE | N2O yield (%) NH4+ | SE | NO pro (nM/d) NO2- | SE | %Hybrid f ree NO2- | SE | NO pro (nM/d) NO3- | SE | NO3-reduction (nM/d) | SE | N2O yield (%) NO3- | STD | nirS gene copy number*mL-1 | STD | nirS transcript copy number*mL-1 | STD | amoA gene copy number*mL-1 | STD | amoA transcript copy number *mL-1 | STD |
|---|---|---|---|---|---|---|---|---|---|---|---|---|---|---|---|---|---|---|---|---|---|---|---|---|---|---|---|---|---|---|---|
| 51 | 882 | 298 | 0.2 | 0.98 | 0.45 | 0.058 | 0.0 | 0.002 | - | 0.89 | 0.22 | nd | 0.00 | 0.04 | 0.000 | 2.67 | 0.39 | 7.20 | 1.7 | 42.53 | 0.28 | 41291940 | 1879.7 | 270713 | 135.7 | 2548.1 | 17.3 | 3065 | 13.2 |
| 52 | 882 | 352.6 | bd | 0.97 | 0.39 | 0.035 | 0.0 | 0.001 | - | 0.00 | 0.24 | nd | 0.00 | 0.09 | 0.03 | 18.98 | 2.20 | 0.35 | 19.42 | 8.3 | 18.49 | 0.45 | 3629049 | 4880.8 | 382.9 | 493.27 | 259.3 | 1414 | 10.4 |
| 53 | 882 | 258.7 | 1.5 | 0.99 | 0.22 | 0.059 | 0.0253 | 0.000 | 77.8 | 3.62 | 1.21 | 1.40 | 0.49 | 0.11 | 0.02 | 21.9 | 1.96 | 0.61 | 14.8 | 1.5 | 15.45 | 0.46 | 1162755 | 3188.8 | 424.9 | 17.4 | 974.8 | 97.2 | 2026 | 0.8 |
| 54 | 882 | 218.9 | 6.06 | 0.97 | 0.77 | 0.056 | 0.0310 | 0.000 | 78.1 | 8.00 | 1.69 | 0.78 | 0.18 | 0.06 | 0.01 | 63.6 | 1.05 | 0.47 | 7.53 | 2.1 | 21.76 | 0.53 | 8205.52 | 10680.0 | 823.8 | 45.9 | 2018.8 | 187.6 | 2403.9 | 41.4 |
| 55 | 882 | 73.9 | 8.4 | 0.98 | 0.95 | 0.059 | 0.1451 | 0.003 | 79.4 | 35.71 | 9.07 | 0.79 | 0.43 | 0.02 | 0.00 | 79.2 | 0.00 | 0.78 | 5.90 | 2.4 | 0.00 | 0.00 | 1997.17 | 1455.5 | 54.8 | 22.1 | 1446.28 | 656.3 | 628.4 | 10.0 |
| 56 | 883 | 304.1 | bd | 0.99 | 0.21 | 0.064 | 0.0 | 0.001 | - | 0.33 | 0.99 | nd | 0.00 | 0.29 | 0.29 | 37.16 | 1.57 | 0.32 | 34.67 | 5.99 | 8.30 | 0.26 | 618285.8 | 19727.5 | 2716.5 | 247.3 | 4050.4 | 999 | 44.0 | 10.8 |
| 57 | 883 | 268.1 | 0.2 | 0.99 | 0.18 | 0.065 | 0.0 | 0.001 | - | 0.98 | 0.30 | nd | 0.00 | 0.71 | 0.38 | 5.65 | 2.82 | 46.65 | 6.97 | 19.49 | 0.52 | 2939037 | 6312.4 | 1749.2 | 198.9 | 1920.1 | 218 | 473.1 | 0.2 |
| 58 | 883 | 249.4 | 2.25 | 0.99 | 0.21 | 0.062 | 0.007 | 0.000 | 83.3 | 0.95 | 0.45 | 0.35 | 0.35 | 0.20 | 0.07 | 0.00 | 2.62 | 0.90 | 17.44 | 4.61 | 23.11 | 0.43 | 3724795 | 1698.1 | 4006.6 | 690.7 | 2901.8 | 1240 | 1654.8 | 3.1 |
| 59 | 883 | 189 | 1.6 | 0.99 | 0.99 | 0.058 | 0.0647 | 0.001 | 83.8 | 10.94 | 1.27 | 1.18 | 0.31 | 0.14 | 0.02 | 88.04 | 1.05 | 0.77 | 15.08 | 1.61 | 12.20 | 0.75 | 1689.2 | 539.0 | 48.9 | 0.7 | 1811.5 | 432.2 | 624.2 | 29.8 |
| 510 | 883 | 28 | 30.1 | 0.99 | 0.91 | 0.065 | 0.1996 | 0.003 | 86.6 | 34.07 | 0.11 | 0.94 | 0.42 | 0.07 | 0.03 | 52.79 | 0.00 | 2.53 | 13.49 | 4.44 | 0.00 | 0.00 | 6311.1 | 86.6 | 42.1 | 5.0 | 2451.8 | 188.5 | 521.7 | 8.3 |
| 511 | 884 | 118.9 | bd | 0.98 | 0.96 | 0.060 | 0.0873 | 0.001 | 78.9 | 2.71 | 1.01 | 0.27 | 0.14 | 0.09 | 0.01 | 76.3 | 5.86 | 0.48 | 6.4 | 2.1 | 64.86 | 0.34 | 1850119 | 846.8 | 2421.5 | 154.4 | 6850.4 | 15.4 | 2848 | 7.4 |
| 512 | 904 | 179.4 | bd | nd | 0.26 | 0.070 | nd | nd | nd | nd | nd | nd | nd | 0.19 | 0.06 | 0.00 | 4.39 | 0.77 | 8.47 | 4.05 | 50.90 | 0.55 | 4250235 | 19445 | 4347.9 | 612.0 | 6000.2 | 108.9 | 2315 | 8.5 |
| 513 | 904 | 134.0 | 0.25 | nd | 0.82 | 0.060 | nd | nd | nd | nd | nd | nd | nd | 0.16 | 0.00 | 90.52 | 7.20 | 1.64 | 9.06 | 2.62 | 61.40 | 0.37 | 1538816 | 2896.0 | 562.2 | 74.1 | 9435.6 | 146 | 1982 | 10.3 |
| 514 | 906 | 147.1 | bd | nd | 0.33 | 0.070 | nd | nd | nd | nd | nd | nd | nd | 0.32 | 0.07 | 13.67 | 3.63 | 0.28 | 38.0 | 11.7 | 16.05 | 0.32 | 3189771 | 14520 | 2104.1 | 67.1 | 6031.7 | 1356 | 887 | 14.2 |
| 515 | 907 | 130 | 0.44 | 0.97 | 0.25 | 0.130 | 0.0180 | 0.000 | 81.0 | 11.38 | 1.80 | 0.32 | 0.13 | 0.30 | 0.10 | 39.3 | 1.23 | 0.23 | 17.51 | 4.66 | 12.96 | 0.32 | 7290154 | 3136.3 | 4274.9 | 0.0 | 4212.9 | 145.4 | 1405 | 8.6 |
| 516 | 907 | 9.2 | 209.3 | nd | nd | nd | nd | nd | nd | nd | nd | nd | nd | nd | nd | nd | nd | nd | nd | nd | nd | nd | 625154 | 795.7 | 14.8 | 4.4 | 994.1 | 6.8 | 45.9 | 5.9 |
| 517 | 912 | 89.8 | 1.44 | 0.97 | 0.38 | 0.090 | 0.1227 | 0.002 | 80.2 | 11.86 | 1.90 | 2.07 | 0.34 | 3.06 | 1.17 | 83.55 | 118.00 | 27.80 | 31.50 | 13.38 | 87.8 | 39.3 | 7830921 | 25186.2 | 5472.8 | 647.3 | 3077.8 | 7.0 | 2416 | 5.0 |
| 518 | 912 | 4.7 | 2045 | nd | nd | nd | nd | nd | nd | nd | nd | nd | nd | nd | nd | nd | nd | nd | nd | nd | nd | nd | 1923111 | 5198.0 | 443 | 10.8 | 2588.8 | 192.7 | 1157 | 2.8 |
| 519 | 882 | 143.7 | bd | 0.76 | 0.11 | 0.090 | 0.0337 | 0.000 | 71.0 | 1.79 | 0.356 | 0.16 | 0.05 | 0.72 | 0.19 | 1.63 | 0.90 | 12.69 | 1.12 | 20.47 | 0.20 | 1010946.4 | 4608.8 | 2810.15 | 3179.2 | 2916.5 | 1193.9 | 4938 | 5.8 |
| 520 | 906 | 92.2 | 0.46 | nd | 0.11 | 0.080 | nd | nd | nd | nd | nd | nd | nd | 2.37 | 0.54 | 0.00 | 4.88 | 0.41 | 53.8 | 4.2 | 15.34 | 0.11 | 3513148 | 9639.0 | 1956.3 | 835.7 | 6526.0 | 99.3 | 2634 | 18.5 |
| 521 | 907 | 139.2 | bd | nd | 0.1 | 0.100 | nd | nd | nd | nd | nd | nd | nd | 0.76 | 0.25 | 0.0 | 0.36 | 0.13 | 27.5 | 4.8 | 2.63 | 0.35 | 9070240 | 8836.2 | 7316 | 80.2 | 2723.7 | 0.0 | 717 | 0.7 |
| Average | | | | | | 0.049 | | | 80.1 | 8.8 | | 0.8 | | 0.5 | | 31.0 | 8.7 | | 20.4 | | 26.0 | | | | | | | | | | |
| STD | | | | | | 0.007 | | | 4.2 | 11.9 | | 0.3 | | 0.8 | | 39.4 | 2.2 | | 14.4 | | 29.2 | | | | | | | | | | |

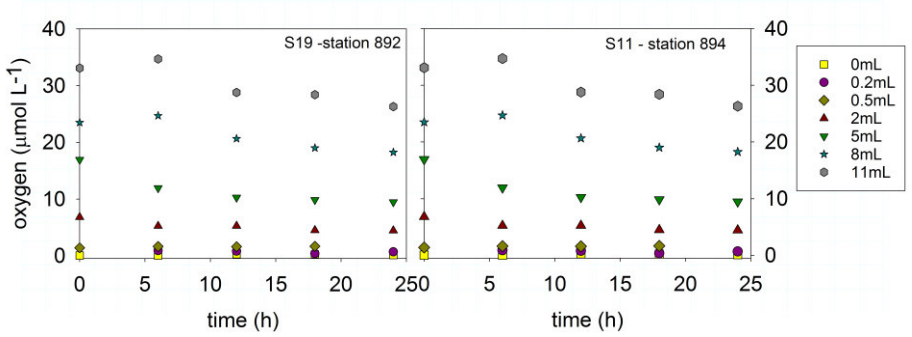


Figure S1: Dissolved oxygen concentrations inside the serum bottles during the 24h incubations ofthe oxygen manipulation experiments at station 892 and 894. No tracer was added to ~~the~~ these bottles. Only the $^{15}NO_3^-$ incubations received 8mL and 11mL additions of saturated site water.

**Formatiert:** Hochgestellt

**Formatiert:** Tiefgestellt

**Formatiert:** Hochgestellt

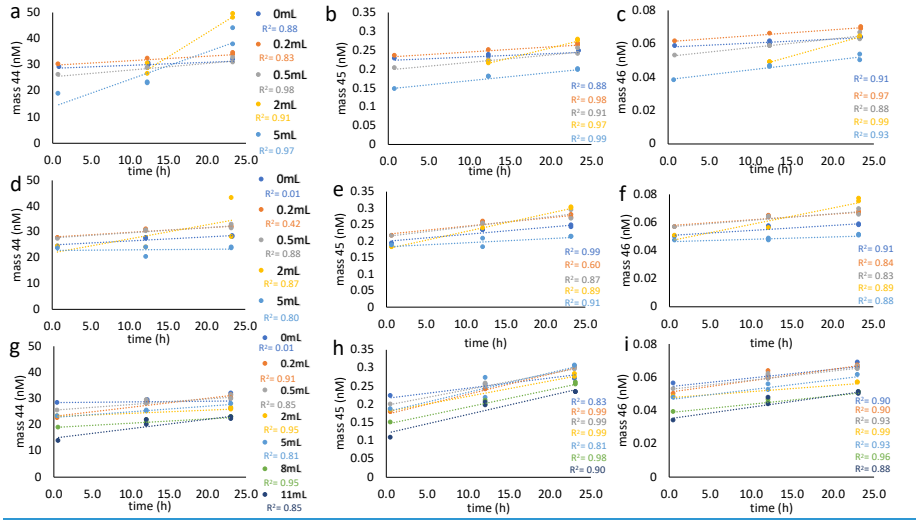


Figure S2: Examples of the production of mass 44 (a,b,c), 45 (d,e,f),and 46 (g,h,i) over 24hfrom the oxygen manipulation experiment performed at station 892, sample S11. $R^2$of the linear regression ~~are~~is given for each treatment and mass. Treatments in center and right panels are same as labeled in the left panel.

**Formatiert:** Hochgestellt

**Formatiert:** Links, Abstand Vor: 0 Pt., Nach: 0 Pt., Zeilenabstand: einfach

**Formatiert:** Schriftart: (Standard) +Textkörper (Calibri), 11 Pt., Nicht Fett

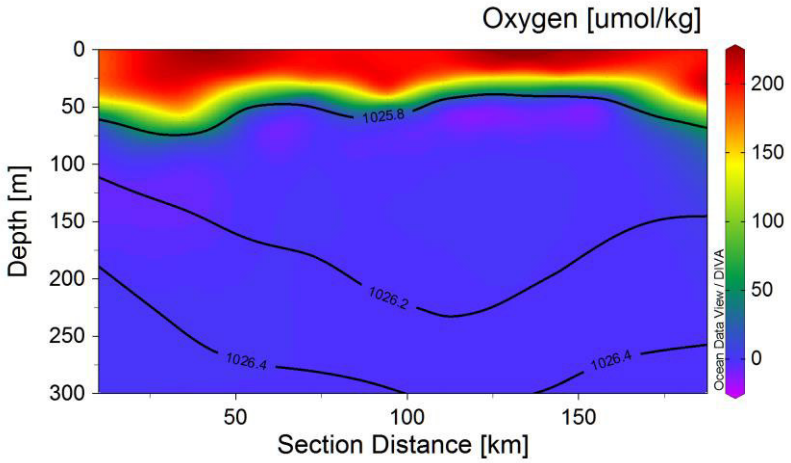


**Figure S3~~1~~:** Oxygen and density contours plot from CTD data across the eddy transect 4.

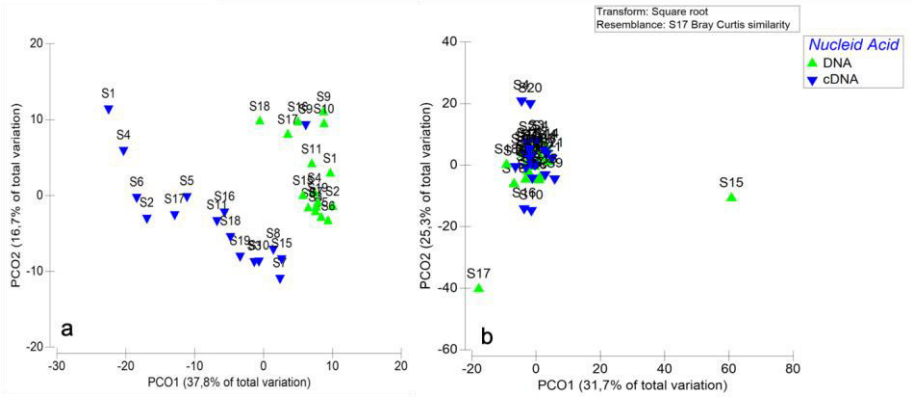


**Figure S42**: Principle component analysis of amoA DNA and cDNA (a) and *nirS* DNA and cDNA (b).

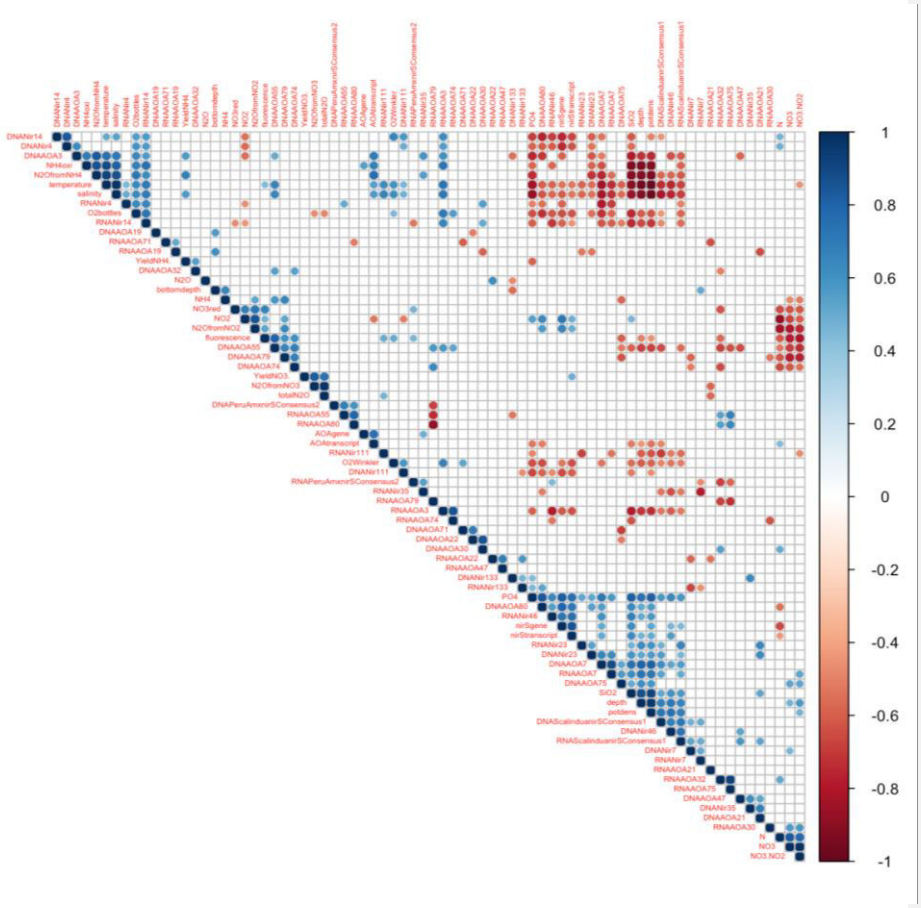


**Figure S53:** Heat map of significant positive (blue) or negative (red) correlations ($p<0.05$) based on a Spearman Rank correlation analysis.

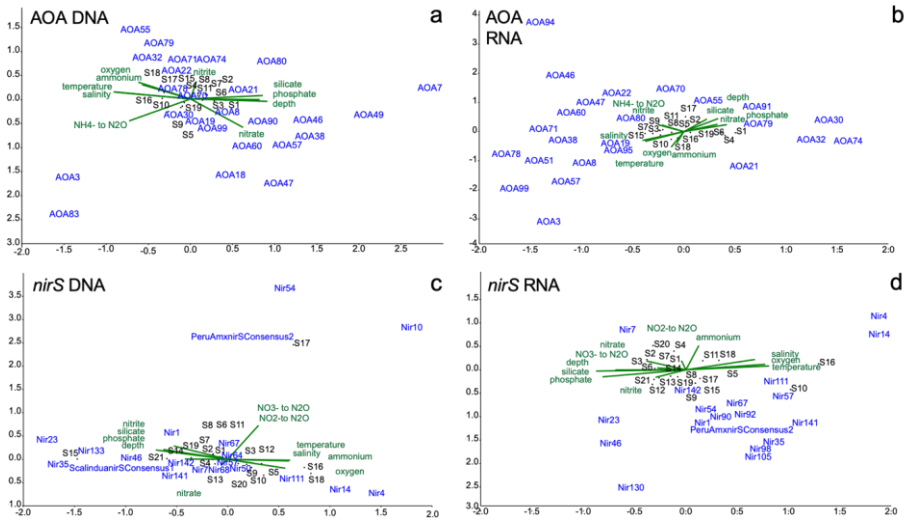


**Figure S64:**Triplot of Canonical Correspondence Analysis showing the archetype composition as a response to the environmental parameters. Upper panel ~~shows~~ *amoA*archetypes(a,b) and lower panel *nirS* archetypes (c,d). On the right is the DNA (a,c) and on the left is the cDNA (b,d).

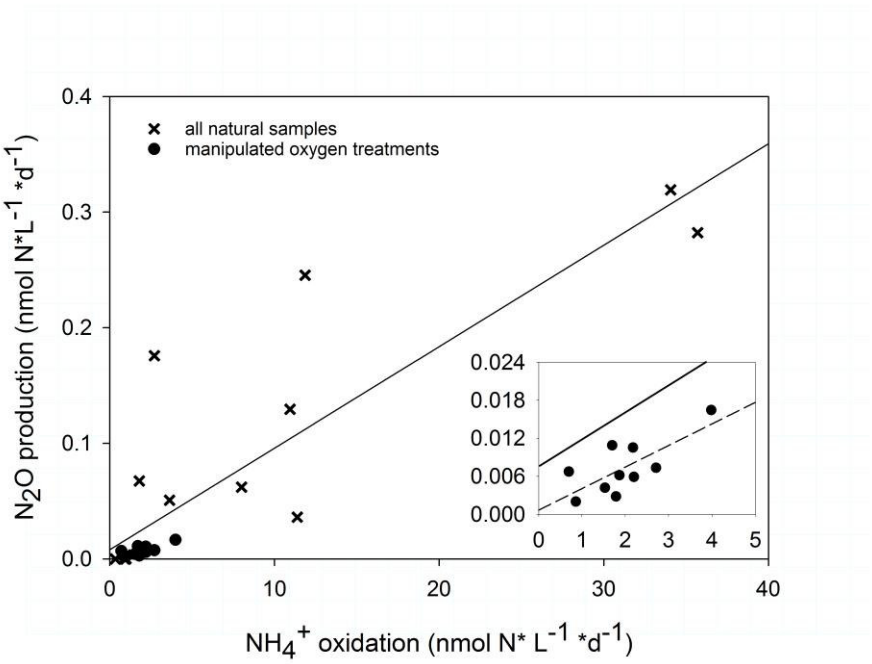


**Figure S~~7~~5:** Scatter plot of AO versus $N_2O$ production from $NH_4^+$with linear fit through all data (~~with~~ y = 0.0088 x + 0.0080 $R^2$= 0.75, p<0.0001). Z~~z~~oom ~~up~~ inshows manipulated treatments with small AO rates and ~~l~~Linear fit through ~~all data with y = 0.0088 x + 0.0080 $R^2$= 0.75, p<0.0001~~treatments ~~with~~ (y = 0.0034x + 0.0007, $R^2$= 0.73, p<0.0001).

**Formatiert:** Schriftart: 10 Pt.

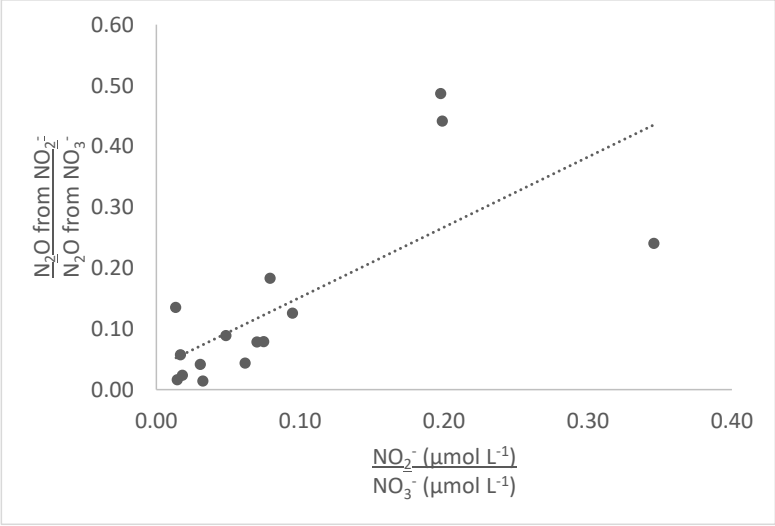


**Figure S86:** Scatter plot of the ratio of $N_2O$ production rates from $NO_2^-$ and that from $NO_3^-$ plotted against ratio of $NO_2^-$ and $NO_3^-$ concentrations. Linear fit ~~with~~ (y = 12.153267 x +- 0.0365254 $R^2$= 0.6286, p<0.0001).

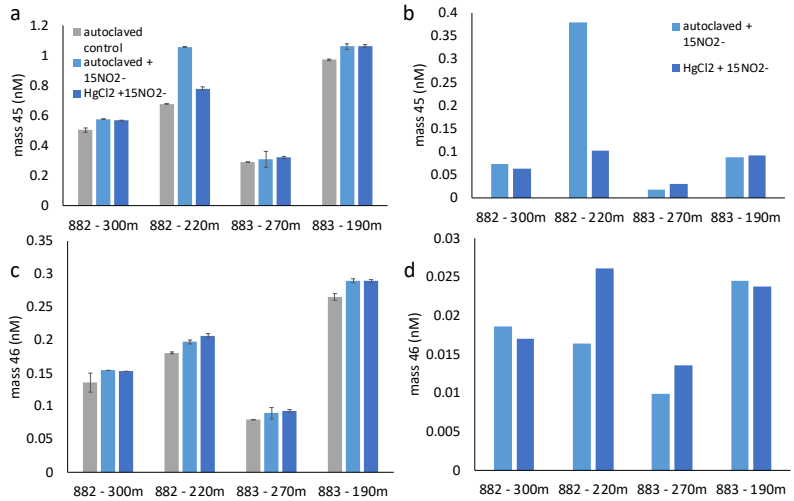


Figure S9: Abiotic $N_2O$ Production of mass 45 (a) and mass 46 (c)from $^{15}NO_2^-$ for 4 depths. The control did not receive tracer addition. The bottles incubated for 65 - 80 days from simultaneous tracer and $HgCl_2$ addition or autoclaving until the measurement in the lab. Figure b) and d) show offset between control and the treatments. Error bars are from duplicates. There is little abiotic production from both masses, between 0.018 – 0.37 for mass 45 and 0.009 – 0.026 for mass 46. There was no significant difference between addition of $HgCl_2$ and autoclaving to stop biological activity. Only at station 882, depth 220m mass 45 and 46 responded very differently.

**Formatiert:** Schriftart: (Standard) Arial, 10 Pt., Fett

**Formatiert:** Schriftart: (Standard) Times New Roman, 10 Pt.

**Formatiert:** Schriftart: (Standard) Times New Roman, 10 Pt., Tiefgestellt

**Formatiert:** Schriftart: (Standard) Times New Roman, 10 Pt.

**Formatiert:** Schriftart: (Standard) Times New Roman, 10 Pt., Hochgestellt

**Formatiert:** Schriftart: (Standard) Times New Roman, 10 Pt.

**Formatiert:** Schriftart: (Standard) Times New Roman, 10 Pt., Tiefgestellt

**Formatiert:** Schriftart: (Standard) Times New Roman, 10 Pt., Hochgestellt

**Formatiert:** Schriftart: (Standard) Times New Roman, 10 Pt.

**Formatiert:** Tiefgestellt

**Formatiert:** Schriftart: (Standard) Times New Roman, 10 Pt.

**Formatiert:** Schriftart: (Standard) Times New Roman, 10 Pt., Tiefgestellt

**Formatiert:** Schriftart: (Standard) Times New Roman, 10 Pt.

**Formatiert:** Englisch (USA)

**Interactive comment "Regulation of nitrous oxide production in low oxygen waters off the coast of Peru"**

Response to Referee #1:

We are grateful to the reviewer for the positive feedback and constructive suggestions which greatly helped us in preparing a revised manuscript.
We addressed the specific suggestions below (our replies in bold).

Abstract: Another important finding is that hybrid $N_2O$ formation represented 70-86% of the $N_2O$ production during ammonium oxidation, regardless of the ammonium oxidation rate or $O_2$ concentrations. One sentence about this should be added to the abstract.

**We added: "Hybrid $N_2O$ formation (i.e. $N_2O$ getting one N atom from $NH_4^+$ and the other from other substrates such as $NO_2^-$) was the dominant species, comprising 70 – 86 % of total produced $N_2O$ from $NH_4^+$, regardless of the ammonium oxidation rate or $O_2$ concentrations."**

Introduction Lines 70-75: The distinction between hybrid $N_2O$ production by ammonia oxidizing archaea and chemodenitrification (e.g. nitrite reduction coupled to iron II oxidation) should be better made. Hybrid $N_2O$ formation (mediated by AOA) has been observed in the ODZ water-column, but not chemodenitrification (also referred to as abiotic $N_2O$ production; Wankel et al., 2017), likely due to substrate limitation (Fe, Mn).

**In line 74, we added: Abiotic $N_2O$ production, also known as chemodenitrification, from intermediates like $NH_2OH$, NO or $NO_2^-$ can occur under acidic conditions (Frame et al. 2017), or in the presence of reduced metals like Fe or Mn and catalyzing surfaces (Zhu-Barker et al. 2015, Wankel et al. 2017), but the evidence of abiotic $N_2O$ production (chemodenitrification) in ODZs is still lacking.**

line 78: Correct nitrifier-denitrifiaction for denitrification.

**We added (line 80) denitrification, but did not replace nitrifier-denitrification because this is what the paragraph is about.**

Lines 79-81: It should be noted that Frame and Casciotti (2010) only observed higher yields at decreasing $O_2$ concentrations for high starting cell densities. At lower cell densities (closer to values found in ODZs), the impact of decreasing $O_2$ on $N_2O$ yield was much lower than observed in other studies.

**We re-wrote the sentence as follow (line 83-87): Overall, the yield of $N_2O$ per $NO_2^-$ generated from AO is lower in AOA then AOB (Hink et al. 2017, 2018) but it should be noted that the degree to which $N_2O$ yield increases with decreasing $O_2$ concentrations is variable with cell densities in cultures or field sites, (Cohen & Gordon 1978; Yoshida 1988; Goreau et al. 1980; Frame & Casciotti 2010, Santoro et al. 2011, Löscher et al. 2012, Ji et al. 2015a, 2018a).**

Lines 102-104: Charpentier et al (2007) also suggested that nitrifier-denitrification is enhanced by high concentration of organic particles, which creates high $NO_2^-$ and low-$O_2$ microenvironments.

**We added a sentence in line 81-83. "It has also been suggested that high concentration of organic particles create high $NO_2^-$ and low-$O_2$ microenvironments enhancing nitrifier-denitrification (Charpentier et al. 2007)."**

Lines 113-114: It would also be relevant to look at *nor* genes which are encoding nitric oxide reductase.

**The reviewer is correct, but the goal here was to distinguish between nitrifiers and denitrifiers and for that the *nor* gene is not ideal as it is present in both. Furthermore, in Fuchsmann et al. (2017) (doi10.3389/fmicb.2017.02384) the canonical forms of the gene *norB* and *qnorB* were very low abundant, suggesting that there might be other genes encoding enzymes mediating NO reduction to $N_2O$.**

Materials and methods:
Line 136: It is not clear why a 3 mL He helium headspace is created before incubating, since it will impact in-situ $O_2$ concentrations.

**The headspace was added for several reasons: 1) to avoid diffusion of oxygen from the septum into the liquid directly, headspace provided an additional barrier, 2) to be able to purge the serum bottles and 3) to avoid artificial differences by different treatments, all bottles received a headspace. We added (line 148 – 150): "He purging removed dissolved oxygen contamination which is likely introduced during sampling and the headspace prevents direct oxygen leakage from the rubber seals (DeBrabandere et al. 2012)."**

Line136-137: I assume purging is done to avoid $O_2$ contamination? What is the $O_2$ threshold defining anoxia here? One potential problem with purging is that it also removes other gases (e.g., $H_2S$) involved in autotrophic denitrification (for instance, see Callbeck *et al*., 2018).

**Yes, purging was done to decrease oxygen contamination during sampling. We rewrote the sentence as such (line 147-148): A 3 mL helium (He) headspace was created and samples from anoxic ($O_2$ < below detection) water depths were He purged for 15min. We also added line 148 – 150, as written as answer to your previous comment. The point of H2S removal during purging is added into the discussion section line 511- 521: "In addition, sampling with Niskin bottles and purging can induce stress responses (Stewart et al. 2012) and shift the richness and structure of the microbial community from the *in situ* community (Torres-Beltran et al. 2019), which can be one potential explanation for the different responses between manipulated $O_2$ and *in situ* $O_2$ experiments. The removal of other gases like $H_2S$ during purging introduces another potential artefact. However, this is unlikely because measurable $H_2S$ concentrations have mostly been found at very shallow coastal stations (< 100 m deep) (Callbeck et al. 2018), which have not been sampled in this study. On the contrary, high abundances (up to 12 %) of sulfur oxidizing gamma proteobacteria, like SUP05 can be found in eddy-transported offshore waters where they**

**actively contributed to autotrophic denitrification (Callbeck et al. 2018). This study cannot differentiate between autotrophic or organotrophic denitrification, but a contribution of autotrophic denitrification in the eddy center is likely."**

Lines 150-153: How did $O_2$ vary during the incubations? These data should perhaps be included as part of the supplementary materials.

**The oxygen concentrations stayed constant in the low oxygen treatments, while it decreased in higher oxic treatments. That explains the higher standard deviation in higher treatments. Oxygen concentrations over time are added to the supplements Figure S1.**

Line 153: Explain the rationale for using particles >50 μm.

**It is the fraction that is sinking. This is stated in line 607-608: "However, the particle size (>50 μm) used in the experiments is indictive of sinking particles."**

Lines 192-219: Plots showing increase in $^{15}N$ labeled products over time should be included in the supplementary materials. Were the relationships always linear?

**Linear relationships were used to calculate the slopes and only significant slopes were included as written in line 233-235. We added example time plots from the oxygen manipulation experiments into the supplements. See Figure S2.**

Lines 228-229: These nirS primers exclude epsilon-proteobacteria (Murdock, et al., 2017). Epsilon proteobacteria are often the dominant portion of autotrophic sulfur oxidizers in sulfidic waters (e.g., Grote et al., 2008), thus this aspect should be discussed.

**We added a statement in the methods that we are aware that epsilon-proteobacteria are not captured with the Primer we used. Line 260 - 263: "The *nirS* Primers are not specific for epsilon-proteobacteria (Murdock et al. 2017), but in previous metagenomes from the ETSP epsilon-proteobacteria where below 3-4% or not found, except in very sulfidic, coastal stations (Stewart et al. 2011, Wright et al. 2012, Ganesh et al. 2012, Schunck et al. 2013, Kavelage et al. 2015)."**

Line 256: Add accession number.

**Added. GEO Accession No GSE142806**

**Results:**

Lines 282-283: Could a contour plot of chlorophyll concentration added to the supplementary material for reference?

**We added surface Chlorophyll data to the station map. See Figure 1.**

Lines 334-335: This result is a bit puzzling as previous studies (e.g., Dalsgaard et al., 2014), observed fifty percent inhibition of N2O production by denitrification at about 300nM O2. These observations are also unlike results from their *in situ* O2 gradient experiment.

**This is not contradictory to Dalsgaard et al. 2014. They were in depths with high NO2- concentration indicative for the core of the anoxic zone, whereas this study took place at the upper part of the anoxic zone and in the oxycline.**

Lines 349-350: It is also surprising to observe the highest yield for $N_2O$ production at highest $O_2$ concentrations, for which $N_2O$ production should be inhibited (Dalsgaard et al., 2014).

**This is not to be confused with the N2O yield/N2. The yields are for NO3- and not like in Dalsgaard with 15NO2- which apparently makes a large difference as we can show in this study!!!**

**Discussion:**

Lines 421-426: Some of these are likely causal relationships.

**Yes, absolutely.**

Lines 425-426: This suggest that when $NO_3^-$ is abundant, denitrifying bacteria are less likely to use $NO_2^-$ (either from their internal pool or outside the cell) for $N_2O$ production during denitrification.

**This comment is added to the text line 460 - 461.**

Line 441: What is the detection limit for [$N_2O$]?

**The detection limits is 2nM. We added that information into the method section 2.1. line 137.**

Lines 441-444: Bourbonnais et al. (2017) used biogeochemical tracers ($N_2O$ concentrations and isotopes) that integrates over longer timescales compared to $^{15}N$-labeled incubations, which are more like taking a snapshot in time. Therefore, discrepancies between $N_2O$ production rate is expected and should be discussed in this context.

**We rewrote that section: "Previously reported maximum rates were up to 86 nmol $L^{-1}$ $d^{-1}$ (Dalsgaard et al. 2012) based on $^{15}N$ tracer incubations. Much smaller maximum rates, 49 nmol $L^{-1}$ $d^{-1}$ (Bourbonnais et al. 2017) and 50 nmol $L^{-1}$ $d^{-1}$ (Farìas et al. 2009), were obtained using $N_2O$ isotope and isotopomer approaches which provide time and process integrated signals. Hence, the deviation of maximum rates can be explained by 1) the different approaches and 2) the sampling of the core of the eddy.** "

Line 451: Cite Fassbender et al. (2018) that discusses impacts of eddies on biogeochemical processes at different scales.

**We did not add Fassbender here, because the recommended paper does not contain information on impact of eddy age on the N2O distribution, which is the point we are trying to make here.**

Lines 443: The error on this higher rate estimate seems rather large (in Figure 3, p).

**We added the exact rate with the standard deviation.**

Lines 458-460: This part is confusing. The $O_2$ threshold for reductive $N_2O$ production should be higher than for $N_2O$ consumption, not the converse. In other words, nitric oxide reductase should be more $O_2$ tolerant than nitrous oxide reductase (Dalsgaard et al., 2014). Otherwise, $N_2O$ would not accumulate.

**This is exactly my point. There is a discrepancy between the thresholds in rates we find and the N2O concentration maxima we measure between 1 – 8uM O2. If N2O production is so sensitive from denitrification then where is all the N2O coming from? Just NH4+ oxidation is unlikely based on the N2O production rates we find from NH4+ oxidation. There might be a higher threshold for N2O production from denitrification?**

Lines 445-446: I do not understand this statement.

**We did not measure N2 production rates, so we cannot say anything about the N2O/N2 yield during denitrification. This yield is subject to changes and not constant, Because of that, we have no chance to make an estimate on the N2 production rate. Maybe in the Eddy incomplete denitrification to N2O was favored and that is what we measured or complete denitrification was fueled and this is what we measured. We rephrased the sentence (line 481- 485) to "$N_2$ production measurements were not performed in this study, so it cannot be determined whether the eddy only stimulated $N_2O$ production but not $N_2$ production from denitrification (i.e. increasing the $N_2O/N_2$ yield) or if the eddy also increased complete denitrification to $N_2$ by 10 times compared to stations outside of the eddy. "**

Lines 479-481: This hypothesis is also supported by a rather long turnover time for $NO_2^-$ as inferred from the $\delta^{18}O$ of $NO_2^-$, which is generally fully equilibrated with water in offshore waters (Bourbonnais et al., 2015). This is not the case in coastal waters, where $NO_2^-$ seems to be more dynamic (see and cite Hu et al., 2016).

**We added this statement into the manuscript as follow (line 532 – 534): "Long turnover times for $NO_2^-$ have been inferred from $d^{18}O$ of $NO_2^-$, which was fully equilibrated with water in the offshore waters (Bourbonnais et al. 2015) and more dynamic in the coastal waters (Hu et al. 2016) supporting our hypothesis. "**

Lines 495-496: How can these contrasting results be reconciled?

**We attribute this to the intensity of the ammonium oxidation rate which exerts a first order control on the N2O production rate. Meaning if the NH4+ oxidation rates would exponential decrease with O2 concentration then we would find that relationship in the N2O production rates. We discuss this further down in line 554 – 556.**

Lines 522-524: If hybrid $N_2O$ formation during AOA is purely (or even partly) abiotic, then measured rates would be overestimated as $HgCl_2$ would not stop $N_2O$ production at the end of the incubations. For how long were these samples stored before being measured? This point should be better discussed.

**The samples were stored between 2 – 5 month. Abiotic N2O production would take place and continue until we measure the samples, indeed. But it also goes on in all samples raising the N2O baseline (in mass 44,45,46) for all and not just in specific ones. This impact will likely vary with depth, but then all the timepoints are affected by the same abiotic production. The rates are calculated from the increase over time making them independent of the baseline. We added a figure to the supplements S9, where results for abiotic production from 15NO2- tracer are shown from 4 depths from 2 stations. The addition of 15NO2- tracer results in little abiotic production; 0.018 – 0.37 nM 45N2O and 0.009 – 0.026 nM 46N2O up to the point of mass spec analysis, but independent HgCl2 addition. We added this point into the discussion line 281. However, we did not test abiotic N2O from NH4+ tracer, hence this can not be fully ruled out. We added that point in line 588-590: "Additionally, at four depths the potential for abiotic $N_2O$ production in $^{15}NO_2^-$ addition experiments showed variations with depth and no significant impact of HgCl2 fixation (Figure S9)."**

Lines 565-566: What was the chlorophyll concentration in the center of the eddy?

**Low, below 1mg/m3. We added a map with surface Chlorophyll, see Figure 1.**

Lines 641-643: $N_2O$ emission to the atmosphere are possible only if the water is upwelled.

**We rephrased the sentence to (line 698): "Regardless of which processes are responsible for $N_2O$ production in the ODZ, high $N_2O$ production at the oxic-anoxic interface of the upper oxycline sustains high $N_2O$ concentration peaks with a potential for intense $N_2O$ emission to the atmosphere during upwelling events."**

Lines 649-652: Temporal variability is particularly not well captured in observational studies.

**We added a sentence to pick up on that comment (line 705 – 706): "While this study does not help to resolve temporal variability, manipulation experiments give valuable insights on the short-term response of $N_2O$ production to oxygen and particles. "**

Figure legends:
Rename Figure 7: $N_2O$ production after additions of...

**The figure was renamed accordingly.**

Figures 2 and 3 are too small. Legend (station #) is almost impossible to read.

**The figure Legend and axis label were adjusted.**

Figure 5: Samples impacted by denitrification should be more clearly indicated (by a circle or rectangle and in the Figure legend) in Figure 5b.

**In all samples in Figure 5b, $N_2O$ production from 15NO3- was found. If that is what the reviewer means. There was no adjustment done to the figure.**

Supplements:
Figures S1: I recommend expanding the scale at lower $O_2$ concentrations since this is the focus of the paper.

**We did not expand the scale here as the focus is the shallowing of the oxycline in the center of the eddy , which is nicely visible in this figure.**

Figure S5: Add linear regression and r-square for natural samples in the zoom up plot.

**Linear regressions and equations were added to the Figure S7.**

Figure S6: Since there are only a few data points for $[NO_2^-]/[NO_3^-]$ higher than 0.10, I don't think the outlier (light gray dot) can be removed. There is much more scatter in Figure 5 in Ji et al. (2018) for the same relationship.

**The point was included into the regression.**

Response to Referee #2:
We thank to reviewer for the positive feedback and valuable suggestions which greatly improved the quality of the manuscript.
We addressed the specific suggestions below (our replies in bold).

*General comments:*

Check nitrite/NO ¯ throughout manuscript 2

**We checked for consistency and changed all nitrites to $NO_2^-$.**

You note differences in process rates and between the communities exposed *in situ* to O2 gradients and in the O2 manipulation experiments (e.g. Line 463-4). I think at least some discussion is needed as to the potential effects of purging the samples with gas as described in refs below (e.g. Dalsgaard et al, deBrabandere et al, Holtappels et al, Stewart et al.)

**We added a sentence to the method section, line 148-151: "He purging removed dissolved oxygen contamination which is likely introduced during sampling and the headspace prevents possible oxygen leakage from the rubber seals (DeBrabandere et al. 2012)" and in line 158/159: "Total incubation times were adjusted to prevent bottle effects, which become significant after 20 h based on respiration rate measurements (Tiano et al. 2014). "**

**Furthermore, we added a part in the discussion line 508-521. "Different responses of $N_2O$ production rates to $O_2$ between *in situ* assemblages and incubation were not unexpected because different rates at different depths were likely not only due to $O_2$ differences but also other factors such as different organic matter fluxes and different amounts and types of $N_2O$ producers at different depths. In addition, sampling with Niskin bottles and purging can induce stress responses (Stewart et al. 2012) and shift the richness and structure of the microbial community from the *in situ* community (Torres-Beltran et al. 2019), which can be one potential explanation for the different responses between manipulated oxygen and *in situ* oxygen experiments. The removal of other gases like $H_2S$ during purging introduces another potential artefact. However, it is unlikely as measurable $H_2S$ concentrations have mostly been found at very shallow coastal stations (< 100 m deep) (Callbeck et al. 2018), which was not the case in this study. On the contrary, high abundances (up to 12%) of sulfur oxidizing gamma proteobacteria, like SUP05 can be found in eddy-transported offshore waters where they actively contributed to autotrophic denitrification (Calbeck et al. 2018). In this study, it cannot differentiate between autotrophic or organotrophic denitrification, but a contribution of autotrophic denitrification in the eddy center is likely."**

Can you be sure that there is no DNRA occurring in your experiments – in particular given the Lam et al. 2009 'Revising the N cycle...' paper also off the Peruvian coast. The presence of DNRA would complicate your isotope pairing experiments with 15NO3- and 15NO2- by transferring 15N into the NH4+ pool and you would get 'hybrid'N2O' of 15nh4+ and 15no2- forming 46N2O and be wrongly assigned. DNRA would also potentially dilute your 15NH4+ pool with 14N from background NO3- and alter the assumed 99% labelling in these experiments. I realise the contribution of AO to N2O production is small relative to denit, but the artefacts of DNRA on the rates/data should be discussed as it could lead to some N2O from AO being 'hidden'.

**The reviewer raises a very important point and no, we cannot be sure that the occurrence of DNRA is impacting our results. We added this consideration to the manuscript in line 216 - 232. "Nevertheless, this assumption brings some initial considerations which need to be accounted for. There is a potential for overestimating hybrid $N_2O$ production in $^{15}NO_2^-$ incubations by 5% in samples with high $NO_3^-$ reduction rates. But in incubations from anoxic depths with high $NO_3^-$ reduction rates, no hybrid $N_2O$ production is found at all. For example, accounting for a decrease in $f_N$ of the $NO_3^-$ pool by active $NO_2^-$ oxidation, the process with highest rates (Sun et al. 2017), had an effect of only ± 0.2 % on the final rate estimate. The presence of DNRA complicates $^{15}N$-labelling incubations because it can change f in all three tracer experiments. In the vicinity of DNRA in $^{15}NO_3^-$ incubations, $^{15}NO_2^-$ and $^{15}NH_4^+$ can be produced from $^{15}NO_3^-$ which can contribute to $^{46}N_2O$ production by AO. Even when a maximum DNRA rate (20 nM $d^{-1}$ in Lam et al. 2009) is assumed to produce 0.02 nM $^{15}NH_4^+$ in 24 h with all of it being oxidized to $N_2O$ (max. $N_2O$ production from AO 0.16 nM $d^{-1}$, this study), its contribution to $^{46}N_2O$ production is likely minor and within the standard error of $N_2O$ production rates from $NO_3^-$. Hence an overestimation of the $N_2O$ production rates is unlikely. The same applies in incubations with $^{15}N$-$NO_2^-$ when DNRA produces $^{15}NH_4^+$, additional $^{46}N_2O$ can be produced with a hybrid mechanism by AO not accounted for in the present rate calculations. In $^{15}NO_2^-$ incubations with high starting f (>0.7) the production of $^{14}NO_2^-$ by $NO_3^-$ reduction (which decreases f) leads to an underestimation by max. 9%, whereas in incubations with a low f (<0.3) the effect is less with max. 3 % underestimation of $N_2O$ production rates. In $^{15}NH_4^+$ incubations (f >0.9), max. DNRA rate would lead to an underestimation of 3.5 %. "**

**Specific comments:**

Section 2.1: As with other papers with many sites, sampling points and manipulation experiments a written methods text quickly becomes very complicated with different additions, concentrations, replicates, time points etc. I think as a result of the text being quite confusing some information has been missed/is unclear. Adding a table of experiments, stations, variables, sampling routine (e.g. time points), number of replicates, other factors (e.g. whether O2 was measured in vials) would be informative/helpful to readers who are interested in comparing/replicating experiments.

**It is correct, that such set ups can get confusing very quickly, but in table 1 stations, depths, measured variables and the kind of experiment performed are given. However, we added one column with the kind of tracer addition we did. The replicates and time points did not vary between experiments and hence is only stated in the test. We only measured oxygen in one bottle with each incubation per depth or treatment, which was also consistent and written in the text line 168/169.**

Also Section 2.1: Missing info on NO3- and NO2- analyses (e.g. shown in Fig 2).

**The measurement of nitrite and nitrate concentrations is given in line 130-132.**

Line 145 (O2 manipulation experiments): Why was such a 'coarse' O2 range used compared to previous studies which use O2 manipulations generally below 1-2µM (e.g. Dalsgaard et al 2014, Bristow et al 2016)?

**In Bristow et al. 2016 a and b the maximal oxygen concentration in their manipulation experiments was 10uM and 20uM dissolved oxygen, so we are not quite sure what the referee means. Dalsgaard et al 2014 performed a really nice microcosm experiment, where oxygen concentrations were monitored online in the flask they subsampled. In our case, each time point was a separate bottle making it impossible to use such an approach. For the experimental design in this study, it was important to choose oxygen levels where we can be sure that oxygen concentrations are different enough from each other that we can differentiate the two treatments (f.e. 100nM and 200nM would be tricky to tell apart with our standard deviations of 180nM and 240nM over 24h). We added a plot of oxygen over time into the supplements Figure S1.**

Line 145 (O2 manipulation experiments): This is a bit confusing: '...headspace volume was adjusted depending on the amount of site water added...'. Do you mean that after the addition of different oxygenated water volumes you also wanted to end up with a 3mL headspace as in the 'natural gradient' O2 experiment? Please rephrase and explain more clearly.

**Yes, that is exactly what we were trying to do. The sentence was rephrased (line 163 – 164) to "For the $O_2$ manipulation experiments, all serum bottles were He purged and after the addition of different amounts of air saturated site water a final headspace volume of 3 mL was achieved."**

Line 153 (OM experiments): So only total N2O was measured in the OM experiments? Or were 15N substrates also added. Unclear as it is written now.

**$^{15}$N substrates were also added in the organic matter addition experiments. We changed the text to : "For all experiments,.." in line 151 and adjusted line 174 as followed: "200µL of POC solution were added to each serum bottle before $^{15}N\text{-}NO_3^-$ or $^{14}N\text{-}NO_2^-$ tracer injection."**

Line 166: Do you mean 'Ascarite' instead of Ascarid?

**Yes, we mean "Ascarite" and it was changed.**

Line 186-8: Rephrase to: 'If more single labelled N2O is produced than expected (...), a hyrid formation of one nitrogen atom from nh4+ and one from no2- (...) is assumed to be taking place se found in archaeal ammonia oxidizers'

**The sentence was rephrased as recommended.**

Line 191: What about 45N2O formed from dilution from background 14NO3- and 14NO2- in samples? Then you will get 45N2O from 15NOx + 14NOx ... You note earlier (ca Line 140) that there is likely substantial 14NO3- (at least in some samples/depths) which will be reduced to 14NO2- and dilute your 15NO2- pool. Perhaps there is something I have missed in the text but this doesn't make sense to assume all 45N2O in incubations with 15NO2, especially in anoxic/low O2 manipulations where NOx can be respired.

**Indeed, there is a potential for overestimating hybrid N2O production in 15NO2- incubations by 5% in samples with high NO3- reduction rates. But in incubations from anoxic depths with high NO3- reduction rates, no hybrid N2O production is found at**

**all. We added all potential problems which come with the assumption of a costant f into that section, starting line 217.**

Section 3.3: Could the % inhibition of processes be plotted to help comparison to other relevant studies on O2 manipulation on AO/no2- ox/denit (e.g. Kalvelage et al 2011, Dalsgaard et al 2014, Bristow et al 2016). I think at least some short discussion is warranted in relation to O2 effects on processes in these previous papers.

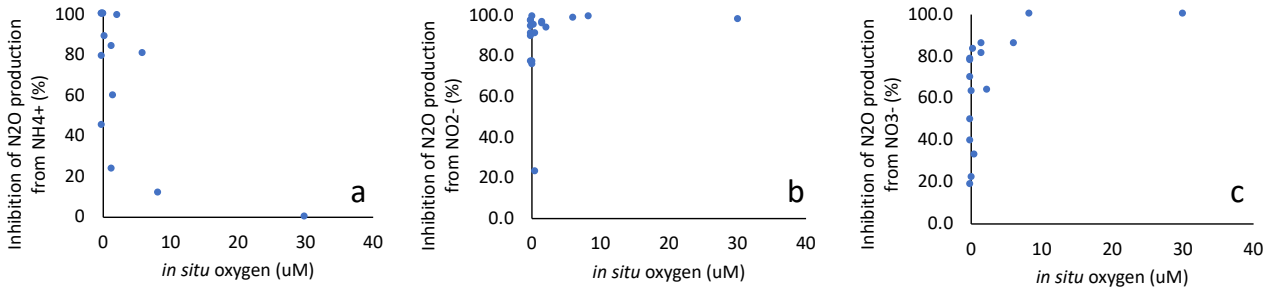


**We added the inhibition curves along the natural O2 gradient here, but we stay with the same figures in the main text as we want to show absolute rates. Section 3.3 is a results section, so we do not refer to papers there. However, in the discussion part 4.1 we cited Kalvelage et al. 2011 (line 525) and Dalsgaard et al. 2014 (line 522). Bristow et al. 2016 is added to the section 4.1. Out of these papers, only Dalsgaard et al. 2014 measured N2O production, hence the focus in the discussion is on their paper.**

Section 3.4: This is a little confusing, additional 14NH4+ was also added along with the POC to experiments? Or was the POC filtered/rinsed after autoclaving?

**The particles were in 0.2um filtered low nutrient seawater and during autoclaving some nitrogen from the particles was liberated into that solution. By adding 200uL of that concentrated POM solution with max. 1.56µM of NH4+ means we added minor amounts of NH4+ into our incubation bottles (0.3nM NH4+), which is neglectable form that perspective. It may be more important with respect to the change in N/C ratios. We adjusted the text, which reads now (line 386 – 389): "The autoclaving of the concentrated POM solution liberated $NH_4^+$ from the particles, reducing the N/C ratio of the particles compared to non-autoclaved particles (Table 2). The highest $NH_4^+$ accumulation is found in samples with the largest difference in N/C ratios between autoclaved and non-autoclaved particles (Table 2, 904-20m, 898-100 m)."**

Line 466: In relation to the 'Unchanged N2O production with higher O2 levels in NO3- treatments...' sentence: Can anoxic niches be ruled out in these experiments? You do note the sampling being during low upwelling and chl period but the settling of small particulates during experiments may create anoxic/low O2 zones to sustain anaerobic processes.

**Anoxic micro niches can never be fully ruled out, if not investigated. The Chlorophyll concentrations were in deed low for an upwelling area, max 5mg/m3, but on average 1mg/m3 and less. Figure 1, map of the study site was adjusted with Chlorophyll concentrations. The treatment was identical between depth profile samples and manipulation samples, so if the particles settle, they would settle in all of the bottles and create microniches in the samples from the depth profile as well. There is no**

**plausible explanation why more anoxic micro niches should be in the oxygen manipulations compared to the others.**

Sentence line 470-472 Bristow et al 2016 should also be a ref here in relation to kinetics of multi-step processes

**Bristow et al. 2016a and b were added.**

Line 477: How can you be sure none of the N2O was consumed without further measurements (e.g. 15N-N2)? Production may just be much faster than consumption.

**We are not able to say anything about N2 production, we can only assume. We added sufficient amounts of 44N2O carrier prior to the incubation to trap 15N-labelled N2O. If N2O reduction is taking place at high rates, we would see a decrease in the N2O pool over time. A plot with the mass 44, 45 and 46 over time was added to the supplements (Figure S2).**

Line 512-515: Confusing sentences, consider rephrasing.

**Sentence was rephrased (line 565 – 567): " While high $N_2O$ yields are usually found in low $O_2$ waters (<6 µmol $L^{-1}$), in this study AO had also high yields at higher oxygen concentrations, 0.9 % at 30 µmol $L^{-1}$ $O_2$ compared to previous studies (0.06% at > 50 µmol $L^{-1}$ Ji et al. 2018a)."**

Line 521: This is a bit of an oversimplification - because something is below detection doesn't necessarily mean nothing is happening, more likely a tight coupling between consumption and production (e.g. see Figure 4 in Klawonn et al 2019 and Figure 3 in Olofsson et al 2019 references). Could there be a dilution of your 15NH4+ pool to consider due to rapid cryptic cycling on shorter scales than your experiments? Ideally 15NH4+ and total NH4+ would be followed through the time series to check for dilution effects. Both show very rapid NH4+ turnover (within ~5h) in oligotrophic waters

**The 15NH4+ substrate was not measured on the GC-IRMS because high $^{15}N$ label/ almost pure tracer is always problematic to analyze. We added the possibility of an overestimation of hybrid production to the method section line 217 and rephrased the wording here to (line 573-575) "Even though, *in situ* $NH_4^+$ is below detection in almost all water depths (f > 0.9), there remains the potential for $^{15}NH_4^+$ pool dilution by remineralization and DNRA during during the incubation. Despite below detection limit studies have shown fast turnover for $NH_4^+$ (Klawonn et al. 2019)."**

Line 532: If measured, the accumulation and consumption of intermediates (e.g. NO2-) could also be used to imply biotic vs abiotic mechanisms (e.g. Betlach and Tiedje 1981 reference).

**We measured NO2- concentrations and isotopic composition in the 15NH4+ treatments, but not other intermediates like NH2OH or NO. The change in concentration was below our detection limit 50nM. Abiotic N2O production was seen in the 15NO2- treatments in the anoxic depth. A supplementary figure was added Figure S9.**

Line 560-3: Could a 15N recovery/inventory be calculated for the experiments (e.g. 15N recovery from initial substrate, measured intermediates and 15N-N2O?) This could help infer a % N2O production from denitrification which is important for putting the N2O production from denit in context – i.e. how do variations in O2 impact the proportion of N2O produced by denit relative to N2?

**The reviewers make a good point, having both the N2 and N2O production from the same flask at low rates would be very nice. We do not think that there is a way we can come to a N2O /N2 yield without measuring $N_2$. The biological variations in the NO3- pool were so big that the little change in 15NO3- was too small to be detected. Therefore, the yield of N2O/NO2- was calculated.**

Fig 4 b, c & Fig 6 b: consider zoomed-in insert of x-axis (e.g. similar to Fig S5)

**Zoom ups are added into the figures.**

Figure S5: Seems to be two different slopes here from manipulated vs natural O2 gradients – could also be discussed in relation to purging artefacts.

**Both slopes are indicated in figure S7 now. Yes, this could be a purging artefact, but the scatter at the lower range is very high.**

Response to second round of Referee #2 suggestions:

Dear Referee,
we appreciate your additional suggestions to our first response and integrated them into our current manuscript. We outlined our point to point reply below (in bold).

General comments:
Thanks, I realise it will be a small % but important to acknowledge. It would also be good to add a sentence in the discussion to suggest that DNRA(& anammox) are measured in addition in future work to rule out potential artefacts – there are now several (sediment) papers on the artefacts of the coocurrence of NO3- reducing processes on the IPT assumptions.

**We added the importance of measuring N2 production in future studies in the discussion:**
**Line 574: "In future $^{15}N$ -labelling studies, DNRA should be measured to rule out potential pool dilution by the co-occurrence of $NH_4^+$ production. "**
**Line 482- 485: "$N_2$ production measurements (from anammox and denitrification) were not performed in this study, but should be carried out in future studies to account for potential artefacts by co-occurring $NO_3^-$ reduction processes."**

I think you just need to change "In the vicinity of DNRA in 15NO3- incubations..." to "In relation to DNRA in 15NO3- incubations..."

**We rephrased the whole sentence in the results section to: "In $^{15}NO_3^-$ incubations, active DNRA produces $^{15}NO_2^-$ and $^{15}NH_4^+$ from $^{15}NO_3^-$ which can contribute to $^{46}N_2O$ production by AO."**

I meant that in Bristow et al. and Dalsgaard et al that a lot of their measurements are concentratedbelow 1-2 uM oxygen and fewer concentrations in the 'higher' 10-20uM range... i.e. focusing on theconcentrations where the inhibition/regulation really 'happens'. But I understand the reasons youdescribe above given the standard deviations of O2 measurements and without more sensitive sensorsit would be difficult to designate concentrations, I agree. I appreciate that Dalsgaard et al do have anice reactor/microcosm set up which I realise is very specialised for precisely these experiments and with larger volumes than the serum vials – also that it is a lot of work with these types of experiments. I think it would still be good to add a sentence/statement as to why 'your' oxygen concentrations werechosen (e.g. given the reasons above, SD in measurements etc) if possible.

**We think that the standard deviations of the different oxygen levels explain why we did not resolve the lower end better and did not add anything there. However, we agree with the referee that it does not become clear why a larger range was applied for the 15NO3- treatments, so we explained that better:**
**Line 167-169: "For the $^{15}N$-$NO_3^-$ incubations two more $O_2$ treatments with 21.5 ± 2.8 and 30.2 ± 3.35 µM $O_2$ were carried out to extend the range of a previous study in which $N_2O$ production from $^{15}NO_3^-$ did not decrease up to $O_2$ concentration of 7 µM (Ji et al. 2018)."**

But if there is the same amount of particles in all vials/O2 manipulations then there is potential for some anoxic processes to be 'unaffected' by O2 additions - with some changes in anoxic microsite volume with O2 diffusion into particles. I realise this is hard to rule out – especially as you collect small particles from the water column to use, indicating that they are there. I think it would be important to write something shortly about why you consider it unlikely that any (significant) anoxic niches occur.

**We do not consider it unlikely that anoxic niches occur, but we do think that anoxic niches do not explain the large difference in response of N2O production at high oxygen levels in the depth profiles (no to little N2O production) compared to the manipulated oxygen treatments (very high N2O production), because the potential for anaerobic microsites is given in all incubations. We added the potential for anaerobic processes inside microniches in line 530 – 534: „ It further indicates that high $N_2O$ production from $NO_3^-$ in high oxygen treatments is unlikely an effect of anoxic micro niches. While anoxic micro niches in batch incubations can never be fully ruled out, there is no reason why they should systematically change N2O production in $NO_3^-$ from $NO_2^-$ incubations at the same oxygen treatment. "**

Shortly suggest/indicate benefits of also measuring other end products (e.g. 15N-N2 and maybe also 15NH4+ from DNRA) in the text (i.e. how does the 'efficiency' of denit change with changing O2)

**We added the advantage of measuring several potential end products in line 574 about DNRA and in line 482- 485 about anammox and denitrification (see first comment). The advantage of having production rates of N2O and N2 together is already discussed starting in line 485, and also starting in line 532, where we highlight the value of having the N2O yields. The different responses/efficiency of denitrification to oxygen is extensively discussed in lines 523 onwards.**

Some kind of 'conclusion' is needed at the end of the last sentence in relation to your study. Papers referring to 'cryptic' biogeochemical cycling in ODZ waters would also be nice to include in relating to 'hidden' processes.

**As suggested, we added a conclusion to in line 581: "Even if hybrid $N_2O$ production rates are overestimated, it remains the major $N_2O$ production mechanisms of AO in this study."**

**In this paragraph we want to explain the occurrence of hybrid N2O formation rather than hidden process – so we did not add papers on cryptic cycling there.**